NASA CR-159788
TRW ER-8101

TUNGSTEN WIRE/FeCrAly MATRIX TURBINE BLADE FABRICATION STUDY

FINAL REPORT

Prepared For

NATIONAL AERONAUTICS and SPACE ADMINISTRATION
NASA LEWIS RESEARCH CENTER

Contract NAS3-20391

D.W. PETRASEK, Project Manager

1. Report No.	2. Government Accession No.	3. Recipient's Catalog No.
NASA CR-159788		

4. Title and Subtitle	5. Report Date
Tungsten Wire/FeCrAlY Matrix Turbine Blade Fabrication Study	December 1979
	6. Performing Organization Code
7. Author(s)	8. Performing Organization Report No.
P. Melnyk and J. N. Fleck	ER-8101
	10. Work Unit No.
9. Performing Organization Name and Address	11. Contract or Grant No.
TRW Inc. 23555 Euclid Avenue Cleveland, Ohio 44117	NAS 3-20391
	13. Type of Report and Period Covered
12. Sponsoring Agency Name and Address	Contractor Report.
National Aeronautics and Space Administration Washington, D. C. 20546	14. Sponsoring Agency Code

15. Supplementary Notes

Project Manager, D. W. Petrasek

NASA Lewis Research Center, Cleveland, Ohio 44135

16. Abstract

The objective of this program was to establish a viable FRS monotape technology base and then apply same to the fabrication of a complex, advanced turbine blade. All elements of monotape fabrication were addressed. A new process for incorporation of the matrix, including bi-alloy matrices, was developed. Bonding, cleaning, cutting, sizing, and forming parameters were established.

These monotapes were then used to fabricate a 48-ply solid JT9D-7F 1st stage turbine blade. Core technology was then developed and first a 12-ply and then a 7-ply shell hollow airfoil was fabricated. As the fabrication technology advanced, additional airfoils incorporated further elements of sophistication, by introducing in sequence bonded root blocks, cross-plying, bi-metallic matrix, tip cap, trailing edge slots, and impingement inserts.

17. Key Words (Suggested by Author(s))	18. Distribution Statement
Composites Tungsten Fiber Iron Base Superalloy Fabrication Turbine Blade Monotapes Impingement Inserts Forming Bi-Metallic Tooling	Unclassified - Unlimited

19. Security Classif. (of this report)	20. Security Classif. (of this page)	21. No. of Pages	22. Price*
Unclassified	Unclassified	85	

N80-29331 #

ER-8101

CR-159788

TUNGSTEN WIRE/FeCrAlY MATRIX TURBINE BLADE FABRICATION STUDY

By

P. Melnyk

J. N. Fleck

TRW EQUIPMENT

Prepared For

National Aeronautics and Space Administration
NASA Lewis Research Center

Contract NAS 3-20391

D. W. Petrasek, Project Manager

TABLE OF CONTENTS

		Page
FOREWORD		viii
ABSTRACT		ix
1.0	INTRODUCTION	1
2.0	PROGRAM PLAN	2
3.0	PROCEDURES AND RESULTS	4
3.1	Materials	4
3.2	Blade Selection and Design Analysis (Task I)	5
3.3	Monotape Fabrication and Evaluation (Task II)	8
3.3.1	Matrix Material Preparation	8
3.3.2	Fiber Preparation	9
3.3.3	Monotape Assembly	9
3.3.4	Monotape Consolidation & Bonding	12
3.3.5	Monotape Evaluation	15
3.3.6	Chemical Milling and Cleaning	18
3.3.7	Monotape Cutting	18
3.3.8	Monotape-to-Monotape Bonding	19
3.4	Blade Fabrication Development (Task III)	23
3.4.1	Tooling Development	23
3.4.2	Ply Development	30
3.4.3	Ply Cutting and Assembly	32
3.4.4	Consolidation and Bonding	34
3.4.5	Forming	36
3.4.6	Core Technology	36
3.4.7	Impingement Inserts	43
3.4.8	Root Attachment	43

(contd)

TABLE OF CONTENTS, contd.

		Page
3.5	Blade Demonstration	48
3.5.1	Iteration 1, Solid Airfoil #1 (Unidirectional)	48
3.5.1.1	Monotape Fabrication	48
3.5.1.2	Monotape Forming	48
3.5.1.3	Monotape Cleaning & Sizing	50
3.5.1.4	Blade Assembly & Bonding	50
3.5.1.5	Evaluation	50
3.5.2	Iteration 2, Solid Airfoil #2 (Unidirectional)	53
3.5.2.1	Monotape Fabrication	53
3.5.2.2	Monotape Forming	53
3.5.2.3	Monotape Cleaning	53
3.5.2.4	Ply Cutting	53
3.5.2.5	Blade Assembly	55
3.5.2.6	Blade Bonding	55
3.5.2.7	Blade Evaluation	55
3.5.3	Iteration 3, Solid Airfoil #3 (Cross-Plied)	60
3.5.4	Iteration 4, Solid Airfoil #4 (Enclosed Leading and Trailing Edges)	62
3.5.4.1	Fabrication	62
3.5.4.2	Conclusions - Solid Airfoils	62
3.5.5	Iteration 5, Hollow Airfoil #1	62
3.5.5.1	Core Fabrication	62
3.5.5.2	Ply Preparation and Blade Assembly	65
3.5.5.3	Blade Bonding	65
3.5.5.4	Blade Evaluation	65
3.5.5.5	Core Leaching	69
3.5.6	Iteration 6, Hollow Airfoil #2	69
3.5.7	Iterations 7 & 8, Dummy Airfoils	69
3.5.8	Iteration 9, Hollow Airfoil #2	74
3.5.9	Iteration 10, Hollow Airfoil #4 (T.E. Slots)	74
3.5.10	Iteration 11, Bimetallic Hollow Airfoil #1	74
3.5.11	Iteration 12, Bimetallic Hollow Airfoil #2	78
3.5.12	Iteration 13, Hollow, Bimetallic, Wrap-around Blade with Arc Root	78

(contd)

TABLE OF CONTENTS, contd

		Page
4.0	SUMMARY AND CONCLUSIONS	84
5.0	RECOMMENDATIONS	86
6.0	REFERENCES	87

LIST OF FIGURES

		Page No.
2-1	Program Plan	3
3-1	Three Views of JT9D-7F First Stage Turbine Blade	6
3-2	Reinforcement Pattern for Demonstration Blade	7
3-3	Filament Winding Machine and Several Fiber Mats	10
3-4	Elements of a "green" FeCrAlY-Tungsten wire monotape prepared by the spray method, including two pieces of powder sprayed steel substrate (side) and tungsten wire mat (center)	11
3-5	Mo/TZM Bonding Die Assembly Used in Fabrication of Monotapes	13
3-6	Vacuum Hot Press Used for FRS Specimens	14
3-7	Microstructure of FeCrAlY-Tungsten wire monotapes in the as-polished condition fabricated by the powder spray (A) and the rolled powder cloth (B) methods	16
3-8	Microstructure of FeCrAlY-Tungsten wire monotapes after acid etching showing relative cleanliness of matrix and thickness uniformity of monotapes fabricated by the spray (A) and the rolled powder cloth (B) methods	17
3-9	Laser Cutting Trials on W/FeCrAlY Monotape	20
3-10	Laser Cut W Mat	21
3-11	Schematic of Tensile-Shear Specimen	22
3-12	Bonding Die Assembly Used in the Diffusion Bonding of the JT9D-79 First Stage FRS Airfoil	26
3-13	Blade Twist Considerations in Selecting a Bonding Plane	27
3-14	JT9D-7F First Stage Blade	28
3-15	Overall Appearance of the JT9D-7F, Mo/TZM Airfoil Bonding Die Inserts (Left) and Steel Airfoil Assembly Fixture (Right) After EDM Cutting of Airfoil Cavities	29
3-16	Typical Section Through Airfoil	31
3-17	A Photograph of Ply Trim Templates for JT9D-7F Airfoil	33
3-18	JT9D-7F Airfoil Assembly Fixture Showing the Location and the Length of Actual Airfoil (Top) and Finished Mo/TZM Airfoil Bonding Die Inserts (Bottom)	35
3-19	Overall Appearance of the Trial JT9D-7F Airfoil After Blending of Leading and Trailing Edges	37
3-20	Forming Dies for Wrap-Around Trials	38

LIST OF FIGURES (continued)

		Page No.
3-21	Forming Dies Installed in 4-Column Die Nest for Alignment	39
3-22	First Forming Operation on 5-Ply Panel	40
3-23	Second Forming Operation	40
3-24	Second Form after Removal of Steel Back-up Material	41
3-25	Leading Edge of Wrap-Around Panel after Etching to Expose Fibers	42
3-26	Overall Appearance of the Solid Root Blocks Fabricated by the Computer Programmed Wire EDM Method	45
3-27	Punch and Die for Laminated Root Trials	46
3-28	Typical Laminated Root Specimen	47
3-29	Tungsten-1% ThO_2-Wire/FeCrAlY Matrix Monotape Formed to the JT9D-7F Airfoil Configuration	49
3-30	Overall Appearance of the Solid FRS Blade No. 1 in the As-pressed Condition	51
3-31	Photomacrograph of a cross-section of the solid FRS Blade No. 1 illustrating good bond and the absence of the center cushion ply and the level of uniformity in monotape thickness and fiber distribution	52
3-32	Overall Appearance of a Formed and Manually Cut Monotape Ply	54
3-33	Assembled Blade in the Assembly Fixture after Bolting of Blade Ply Ends	56
3-34	Appearance of the solid FRS Blade No. 2 after finishing of the leading and trailing edges and the removal of metallography samples from the root and tip ends	57
3-35	Photomacrograph of the solid FRS Blade No. 2 cross section at the root end illustrating good bond and the uniformity of wire distribution in the monotapes	58
3-36	Photomacrograph of the solid FRS Blade No. 2 cross section at the tip end illustrating good matrix bond and the uniformity of ply thickness and wire distribution in the monotapes	59
3-37	Solid, Cross-Plies FRS Airfoil with Brazed Root Blocks	61
3-38	Special Monotape Configurations	63
3-39	Solid FRS Airfoil with Diffusion-Bonded Root Blocks	64
3-40	Typical As-pressed Steel Core	66
3-41	Photomacrograph of a cross section of a simple hollow FRS blade prior to leaching of the steel core	67

LIST OF FIGURES (continued)

		Page No.
3-42	Photomacrograph of a cross section of a simple hollow FRS blade after core removal	68
3-43	Photomicrographs of the shell in the simple FRS hollow blade illustrating good matrix bond, uniformity of wire distribution and cladding of the shell surfaces	70
3-44	Photomicrographs of a section of the shell of the hollow FRS blade illustrating the high level of matrix cleanliness and the absence of matrix-wire reaction in the monotapes produced by the powder spray method	71
3-45	Assembly without Use of Bolts	72
3-46	Second Hollow Airfoil	73
3-47	Relative Location of the Trailing Edge Slots	75
3-48	Tooling Concept for Trailing Edge Slots	76
3-49	First Hollow Airfoil with Trailing Edge Slot	77
3-50	Bi-Alloy Monotape	79
3-51	First Hollow, Bimetallic Airfoil	80
3-52	Second Bi-Alloy Hollow Airfoil	81
3-53	Schematic of Hollow FRS Blade with Impingement Insert, Tip Cap, and Arc-Root	82

LIST OF TABLES

		Page No.
3-I	Materials Summary	4
3-II	Chemical Analyses of FeCrAlY Powder	4
3-III	Summary of 538°C (1000°F) Tensile Shear Test Results . . .	24

FOREWORD

The work described in this report was performed in the Materials Technology Laboratory of TRW Inc. under the sponsorship of the National Aeronautics and Space Administration, Contract NAS 3-20391. The program was assigned to the Materials Development Department, managed by Dr. I. J. Toth. Mr. Paul Melnyk was the program manager. Major contributions were also made by the following:

Mr. F. Weiss, Fabrication
Mr. D. Cvelbar, "
Mr. W. Boback, "
Mr. D. Engeman, Metallography

The NASA Technical Manager was Mr. D. W. Petrasek.

The TRW Engineering Report Number is ER-8101.

Prepared by P. Melnyk

P. Melnyk
Program Manager

Approved by J. N. Fleck

J. N. Fleck
Section Manager

and I. J. Toth

I. J. Toth
Department Manager

ABSTRACT

The objective of this program was to establish a viable FRS monotape technology base and then apply same to the fabrication of a complex, advanced turbine blade. All elements of monotape fabrication were addressed. A new process for incorporation of the matrix, including bi-alloy matrices, was developed. Bonding, cleaning, cutting, sizing, and forming parameters were established.

These monotapes were then used to fabricate a 48-ply solid JT9D-7F 1st stage turbine blade. Core technology was then developed and first a 12-ply and then a 7-ply shell hollow airfoil was fabricated. As the fabrication technology advanced, additional airfoils incorporated further elements of sophistication, by introducing in sequence bonded root blocks, cross-plying, bi-metallic matrix, tip cap, trailing edge slots, and impingement inserts.

1.0 INTRODUCTION

Improvement of aircraft gas turbine engine performance and durability would be greatly facilitated by the development of higher strength turbine blade materials. Current blade materials (nickel and cobalt base superalloys) are already being used at 0.8 of their homologous melting points; therefore, substantial improvement of these materials seems unlikely. Fortunately, refractory fiber reinforced superalloy composites may provide the needed strength improvements.

Combinations of refractory-metal fibers and superalloys in the form of composites have been made by NASA and others and have shown promise from stress-rupture and impact data that have been generated. For example, programs have been conducted at NASA-Lewis Research Center (1-4) which have demonstrated that composites could be produced having superior stress-rupture properties compared to conventional superalloys at temperatures of 1093° and 1204°C (2000° and 2200°F). Additionally, it was shown that, by careful fabrication techniques and selection of compatible matrix alloys, tungsten fiber/nickel alloy composites could be produced having adequate impact properties for turbine blade or vane applications.

A NASA-sponsored program at TRW (5) resulted in the development of a diffusion bonding process for the fabrication of tungsten fiber/nickel alloy composite monotapes. The use of pre-consolidated monotapes to fabricate more complex shapes was also demonstrated.

A turbine blade material needs a combination of properties in addition to strength and impact resistance. Among these are oxidation resistance, thermal fatigue resistance, and mechanical fatigue resistance.

Investigations concerned with the response of tungsten fiber/superalloy composites to thermal cycling were conducted in NASA-sponsored programs at TRW (6,7). The results obtained in these investigations indicated that thermal cycling can cause a number of effects in reinforced tungsten/superalloy composites which include: dimensional instability, warpage, delamination, matrix debonding and matrix microcracking. The results also indicated that these effects may be controlled by proper selection of matrix strength, matrix ductility and the amount and distribution of fiber reinforcement. In addition, various combinations of fiber and matrix materials were fabricated and evaluated for the purpose of selecting a specific combination that affords the best compromise in overall properties required for a turbine blade application. The tungsten fiber/FeCrAlY matrix composite system afforded the best compromise in overall properties required for a turbine blade application of the matrix composite systems investigated.

The tungsten-1% ThO_2-wire/FeCrAlY-matrix composite system has demonstrated a high potential for providing an advanced turbine blade material capable of a 55° to 110°C (100° to 200°F) use temperature increase over first generation directionally solidified eutectics (8-10). Stress-rupture lives of over 300 hours at 1149°C (2100°F) and 241 MPa (35 ksi) and over 1000 hours at 1093°C (2000°F) and 276 MPa (40 ksi) were obtained with specimens containing 40 to 45 volume percent fiber. No damage was sustained by specimens thermally cycled between room temperature and 1204°C (2200°F) for 1000 cycles. A reduction in fiber diameter of less than 10% occurred due to interaction with the matrix when specimens were exposed at 1093°C (2000°F) for 1000 hours.

The current program was intended to further develop the tungsten-1% ThO_2-wire/FeCrAlY-matrix composite system for ultimate turbine blade applications by investigating hollow turbine blade fabrication methods. The program goal was to determine the feasibility of fabricating an actual blade, which was representative of a current high performance part, with the capability of meeting or exceeding the current life cycle requirements.

2.0 PROGRAM PLAN

The planned program was to consist of five tasks, as shown in Figure 2-1. The objectives of Task I were to select a representative advanced turbine blade. A design analysis was to be performed by NASA; the results of this analysis would be integrated into the fabrication development.

In Task II, the goals were to optimize fabrication parameters for W-1ThO_2/Fe25Cr-4Al-1Y monotapes. Cutting techniques for monotapes would be evaluated. Cleaning techniques to promote optimum bonding between monotapes would also be established.

All elements of blade fabrication feasibility were to be addressed in Task III. This included ply development, based upon NASA's design analysis, and techniques for cutting these plies. Methods of ply assembly were to be evaluated, and bonding parameters studied. There can be no exposed fibers on the blade, so cladding procedures would be needed; this would ultimately require tip protection, as well. Root attachment methods were to be addressed. The target airfoil would be hollow; therefore, core technology was to be established. Any required finishing operations would also be assessed.

All of these elements would be combined in Task IV to fabricate a demonstration hollow FRS turbine blade.

Task V consisted of the contract's report requirements.

Figure 2-1. Program Plan

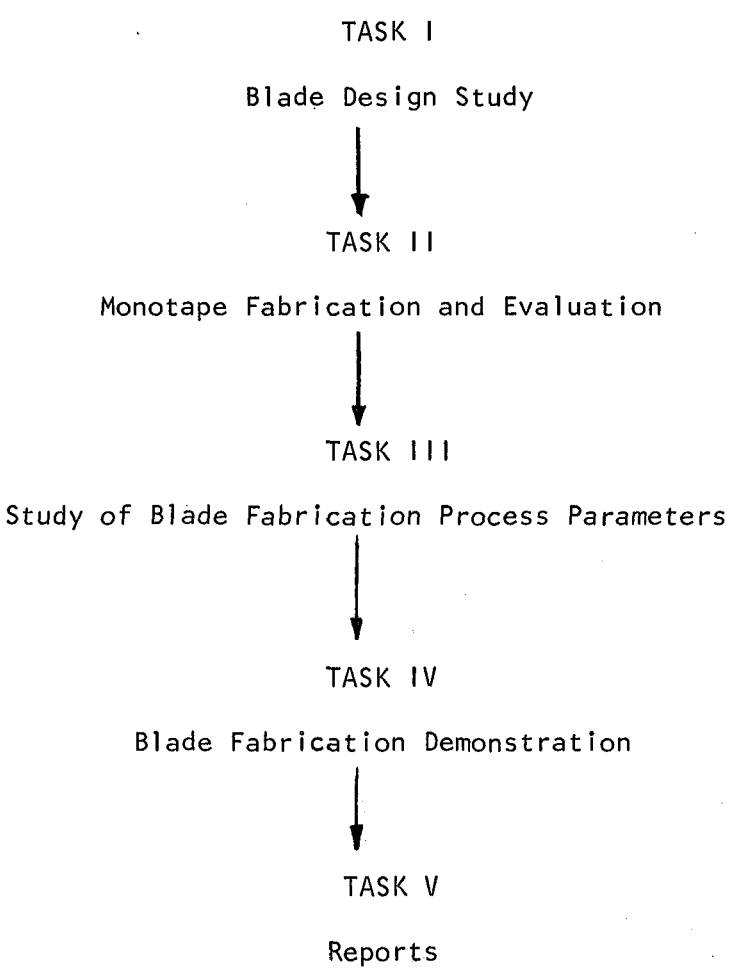

3.0 PROCEDURES AND RESULTS

The developments effected during this program were the culmination of a number of iterations, some of which were performed during the technology tasks and others during the course of the blade demonstrations. The descriptions which follow are essentially a chronological presentation of activities. When further work on a given element of the process was perfomed later in the program, it will be so noted.

3.1 Materials

The major materials required for this program are summarized in Table 3-I. The FeCrAlY powder was supplied in three size ranges, viz. -20 by +100, -100 by +500, and -500 mesh. Chemical analyses were performed on samples from each size range. Results are given in Table 3-II.

TABLE 3-I. Materials Summary

Material	Use	Condition	Vendor
FeCrAlY	Matrix	Powder	Special Metals
W-1ThO_2	Fiber	0.1 and 0.2 mm (0.004 and 0.008 in.) Cleaned & Straightened Wire	GTE-Sylvania
TZM	Dies	Billet Stock	AMAX Specialty Metals

TABLE 3-II. Chemical Analyses of FeCrAlY Powder

	Element - Weight %				
Sample	Fe	Cr	Al	Y	O
Specification	Bal.	20-25	4.5-5.5	0.5-1.0	0.02 Max.
-20 + 100 Mesh	"	22.71	4.52	ND	0.012
-100 + 500 Mesh	"	22.61	4.72	ND	0.022
-500 Mesh	"	22.61	4.64	ND	0.059

ND - Not Determined.

The chromium and aluminum levels met specifications for all particle size ranges, but as might be anticipated, the total oxygen level was higher in the case of the -500 mesh material. The finer particle size ranges are required to make thin powder cloth such as the 0.05mm (0.002 inch) thick material needed for 50-70 volume fraction monotapes with 0.1mm (0.004 inch) fibers.

3.2 Blade Selection and Design Analysis (Task I)

At a meeting between TRW and NASA, the first stage JT9D-7F turbine blade shown in Figure 3-1 was selected as the configuration to be developed under this contract. The rationalization and reasoning for selecting this particular blade are given in reference 10. Dimensional data for the JT9D blade were provided to NASA for their use in establishing the blade geometry, ply configuration, fiber content, etc. that made up the TFRS blade design. The blade design parameters supplied to TRW by NASA for use in the fabrication study are as follows:

A. Composite Blade Dimensions

1. Airfoil per JT9D external dimensions.
2. Airfoil extended from root into bottom of base.
3. Base dimensions and platform per JT9D external dimensions except for additional material at leading and trailing edges needed to enclose airfoil.
4. Exact base geometry variations from JT9D to be determined by TRW--subject to NASA approval.

B. Volume Fraction Reinforcement Along Blade Span

1. 40 volume percent and 70 volume percent plies shall be used to build up the hollow, cross plied airfoil as schematically illustrated in Figure 3-2.
2. TRW shall determine the exact ply dimensions required to meet practical fabrication requirements--subject to NASA approval.
3. 40 volume percent cross plies material will be formed around the leading edge.

C. Reinforcing Fiber Diameter - 0.1mm (0.004 inch)

D. Internal Cooling Channel Dimensions

1. The internal passage dimensions shall be a RESULT for the most part. They shall be those resulting from the need to fit the JT9D external geometry with the ply layup and the exact ply dimensions determined by TRW.
2. Fins and braces may be incorporated into the core.

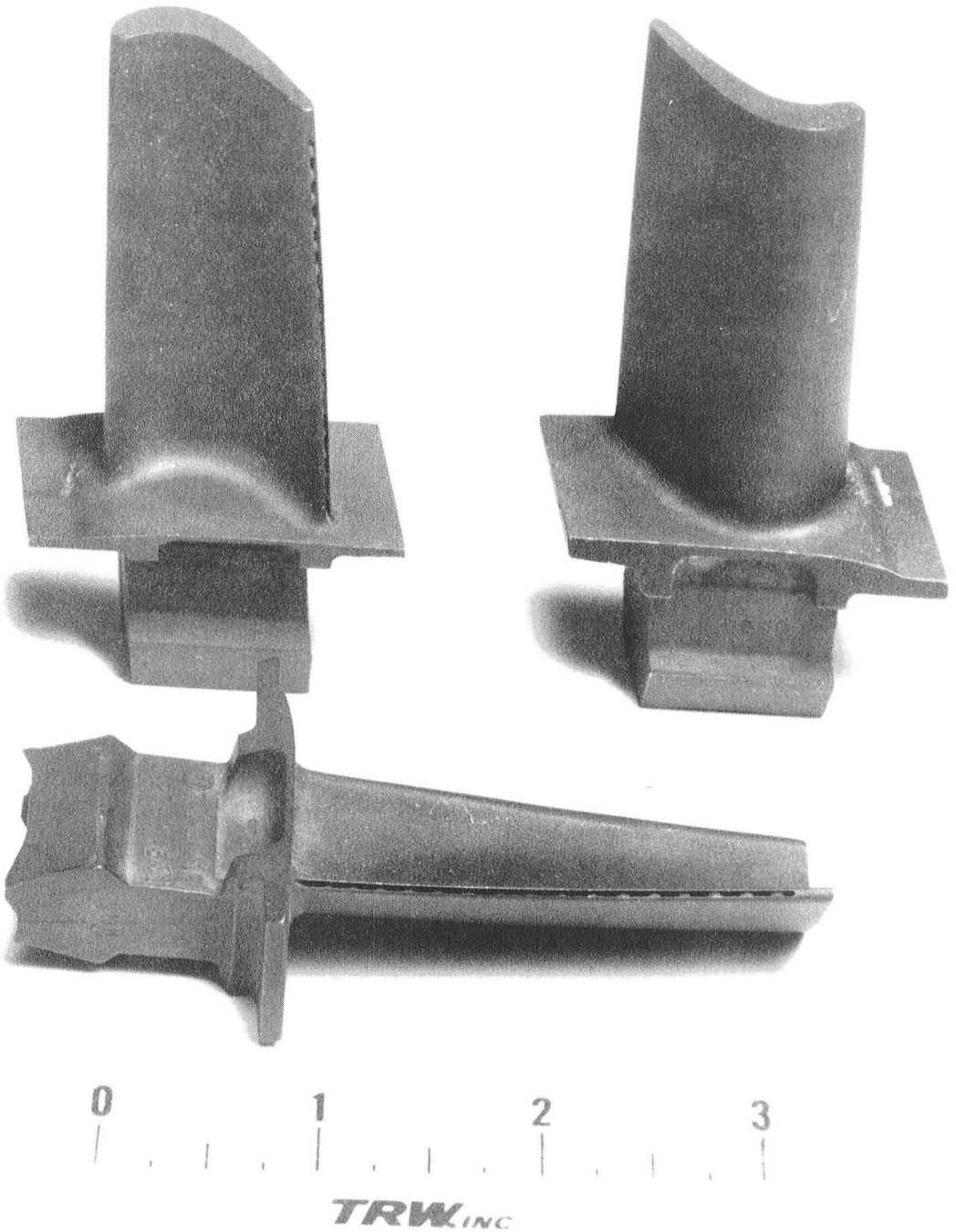

Figure 3-1. Three Views of JT9D-7F First Stage Turbine Blade.

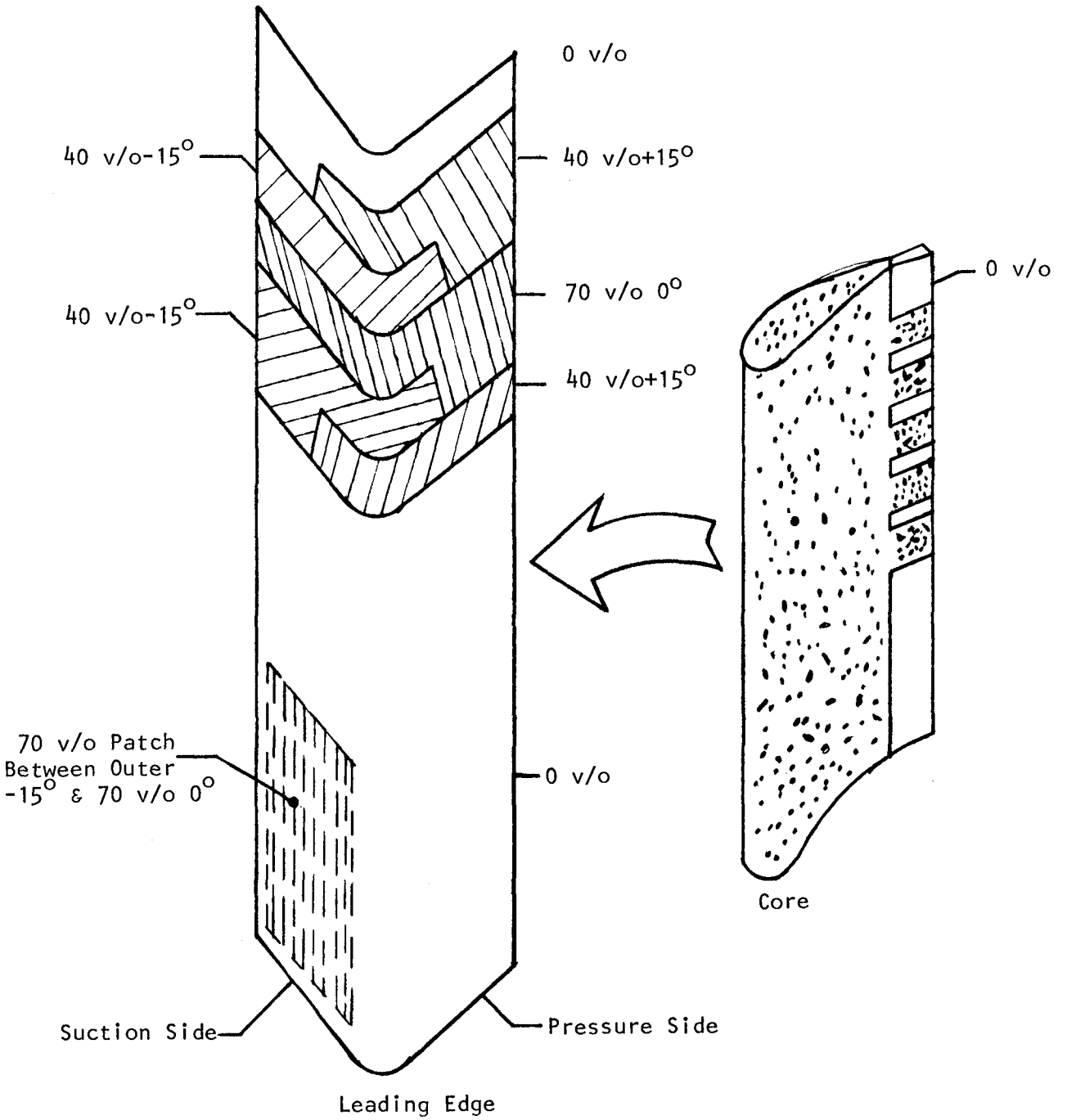

Figure 3-2. Reinforcement Pattern for Demonstration Blade.

3.3 Monotape Fabrication and Evaluation (Task II)

Monotapes, i.e., preconsolidated single-ply composites with the correct fiber spacing and volume fraction, have become the standard building blocks for complex shapes such as a cambered, twisted, and tapered airfoils. These monotapes are prepared by diffusion bonding sandwiches of matrix and collimated fibers. The matrix can be in the form of wrought foil or sheets of powder cloth. The latter was selected because FeCrAlY is not conveniently available in foil form.

3.3.1 Matrix Material Preparation

Powder cloth is made by a proprietary process involving the rolling of powder and a binder into sheets. Thin powder cloth requires very fine powders. However, even with -500 mesh powder, it was impractical to produce powder cloth of the nominal 0.05mm (0.002 inch) thickness required for 70v/o monotape containing 0.1mm (0.004 inch) fibers. Difficulties included, 1) excessive tearing of the sheets, 2) density uniformity could not be maintained, 3) thickness uniformity could not be controlled, 4) the process is susceptible to product contamination by extraneous materials, and 5) the process is costly and time consuming.

As an alternative, feasibility of spraying the FeCrAlY powder directly onto a steel foil substrate was investigated.

The particle size of the matrix powder was -500 mesh. A low ash cellulose nitrate solution was used as a carrier and binder. The substrate used was 0.1mm (0.004 in.) carbon steel shim stock cleaned in a four-step procedure. First, the as-received material was washed in an organic solvent (MEK) to remove any oil film and other surface deposits. The foil was then immersed for a few seconds in solution of nitric and hydrofluoric acids in water to dissolve the as-rolled surface layer. After rinsing in water, the material was wiped to remove surface smut. Finally, the material was immersed in hydrochloric acid to remove any rust film and wiped dry. The above, somewhat elaborate cleaning procedure was employed primarily to ensure that all organic and inorganic contaminants, the presence of which might otherwise interfere with the evaluation of the FeCrAlY matrix-steel interface bond zone, were removed from the substrate surface.

After drying, these sprayed foils were readily cut on paper shears.

As part of this overall task, an alternate method of powder cloth preparation was demonstrated. It consisted of spraying metal powder on a substrate with favorable release properties. Three different release substrates were used with about equally satisfactory results: teflon sheet, waxed paper and metal sheet spray-coated with a teflon-type release agent. To facilitate the release and to improve tape strength and handleability, a polystyrene solution in xylene was used as the carrier and binder. After drying, the material can be stored in large sheets for future use.

3.3.2 Fiber Preparation

The W-1ThO_2 fibers were converted into mats, i.e., sheets of collimated fiber held in place with a fugitive polystyrene binder. As is shown in Figure 3-3, the fibers are drum wound at the prescribed spacing and the binder is introduced. When the polystyrene solution has dried, the mat is cut along a generatrix of the drum, yielding a sheet the length of which equals the circumference of the drum and the width of which is controlled by the width of the band wound on the drum.

A typical segment from a W-1ThO_2 mat, together with two FeCrAlY sheets, is shown in Figure 3-4.

3.3.3 Monotape Assembly

Bonding of single sheets of monotape is not cost effective. Normally, a multiplicity of such monotapes are bonded in a single operation. This means that measures must be taken to preclude bonding the stack together. With powdered matrix alloys, precautions must also be taken to keep foreign material (such as parting compounds) from the porous powder layer. This is conveniently done by covering the FeCrAlY powder with a sacrificial mild steel shim. With the spray approach, the foil substrate serves this purpose. Of the three thicknesses of shim stock investigated 0.05, 0.075, and 0.1mm (2 mil, 3 mil and 4 mil) the four-mil material produced the best monotape surface finish with some improvement in thickness uniformity in the monotapes. From the standpoint of shim stock removal from the monotapes after diffusion bonding, starting thickness of shim stock material is of little consequence since it does not significantly effect the duration of the etching cycle.

The economies of monotape fabrication are influenced by the choice of the separator material. Two separator materials, unalloyed molybdenum and Mo/TZM sheets have been investigated in four thicknesses: 0.13, 0.25, 0.38, and 0.5mm (0.005, 0.010, 0.015, and 0.020 inch). Mo/TZM has higher elevated temperature strength than unalloyed molybdenum, but is objectionable because of reduced ductility. Unalloyed molybdenum was therefore selected.

The thinner 0.13mm (0.005 inch) separators of both types are undesirable from the standpoint of reusability. It was found that too frequently the thinner material would break during monotape batch disassembly after diffusion bonding. Instances of separator rupture during consolidation have also been encountered, although this is attributed in part to non-uniformity of the parting compound, such as running during spray application. The resulting "ridges" tend to act as stress raisers causing localized rupturing of the material.

Reusability yield is significantly higher with thicker separator material. Some improvement in the surface quality of the monotapes has also been observed.

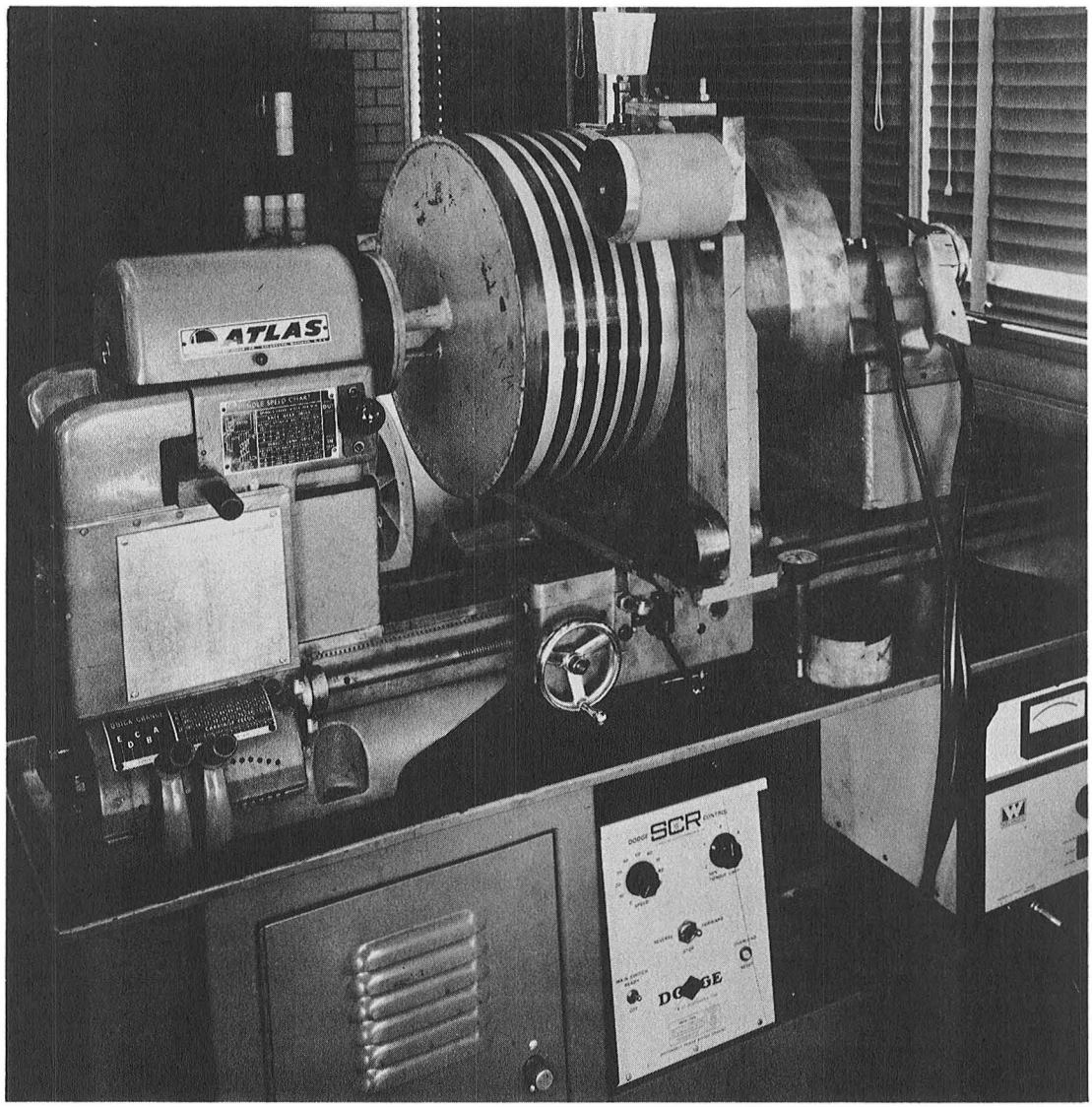

Figure 3-3. Filament Winding Machine and Several Fiber Mats.

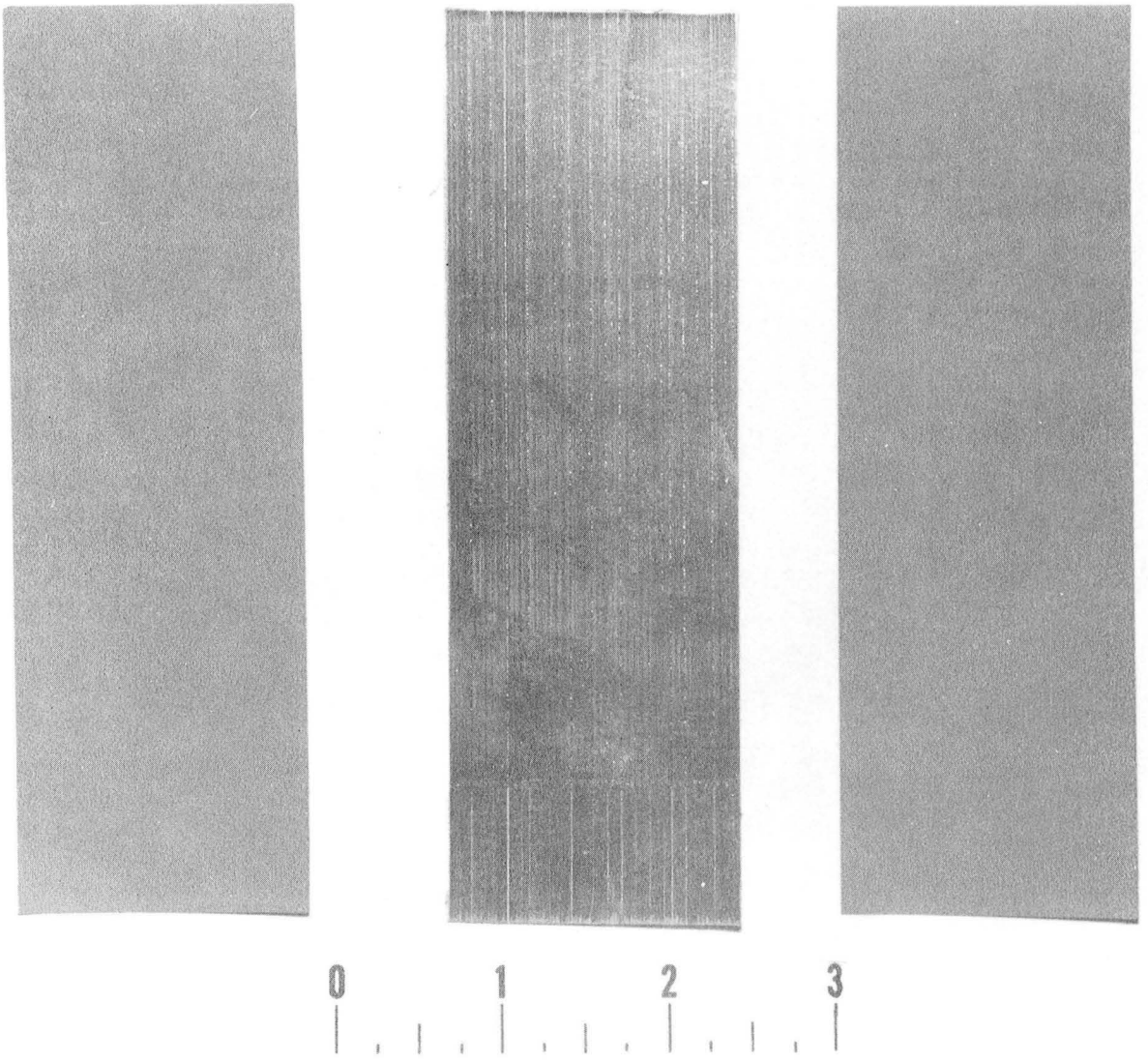

Figure 3-4. Elements of a "green" FeCrAlY-Tungsten wire monotape prepared by the spray method, including two pieces of powder sprayed steel substrate (side) and tungsten wire mat (center).

(Note: Dimensions in inches.)

Best results were obtained using 0.5mm (0.020 inch) thick molybdenum. Several monotape pressing runs in batches of 20 to 25 pieces per run were made with this material without loss of a single separator. It consequently was made the standard separator material in the fabrication of monotapes on this program.

The monotapes are bonded in TZM channel dies such as the one shown in Figure 3-5. All of the die parts, viz, the block, the two wedges, and the top and bottom punches must be coated with a parting compound. In addition, the molybdenum separators are also coated.

In prior work, the parting compound consisted of 30 weight percent zirconium oxide and 70 weight percent boron nitride. Xylene served as a vehicle, and a polystyrene solution in xylene was used as a fugitive binder. Because of difficulties encountered in the removal of the monotapes from the channel-shaped bonding die, the zirconium oxide content in the mixture was reduced to 20 weight percent and eventually eliminated entirely.

In addition, the xylene-polystyrene combination serving as a carrier and binder was replaced with a Cellulose Nitrate solution, a product of Pratt & Lambert Company. This product is widely used for application where low ash content is important. This change resulted in definite improvements in spray applications as well as better quality and uniformity of the applied coating. Improvements in ease of disassembly of the die components after monotape bonding, on the other hand, were effected by hand-stoning all working surfaces of the bonding dies after machining to remove the surface asperities.

3.3.4 Monotape Consolidation and Bonding

At the outset of this program, the "standard" bonding practice had been to introduce hydrogen into the bonding chamber at room temperature and to heat the monotape batch without a positive clamping load. Such practice resulted in a partial entrapment of the condensed moisture as well as of the decomposition product of the fugitive binder in the system.

The improved fabrication practice is as follows. The assembled monotape batch is placed into the vacuum retort shown in Figure 3-6 and a positive clamping load of about 7MPa (1 ksi) is applied. After chamber evacuation, the dies are heated by induction at a relatively low heating rate to about 400°C (750°F) to prevent a spontaneous evolution of gases resulting from the decomposition and/or vaporization of the polystyrene and cellulose nitrate binders. Heating rate is then increased and a dynamic vacuum is maintained until a temperature of about 650°C (1200°F) is reached. The vacuum valve is subsequently closed, the chamber is flushed with argon, and hydrogen is introduced into the system. At 1105°C (2025°F), a bonding load is applied gradually. Upon completion of the bonding cycle, heat and pressure are turned off and the assembly is cooled in flowing hydrogen to about 800°C (1500°F) or below. From this temperature, cooling is effected in argon. As part of the new practice, when not in use, the vacuum chamber is kept under dynamic vacuum to prevent condensation of moisture in the chamber.

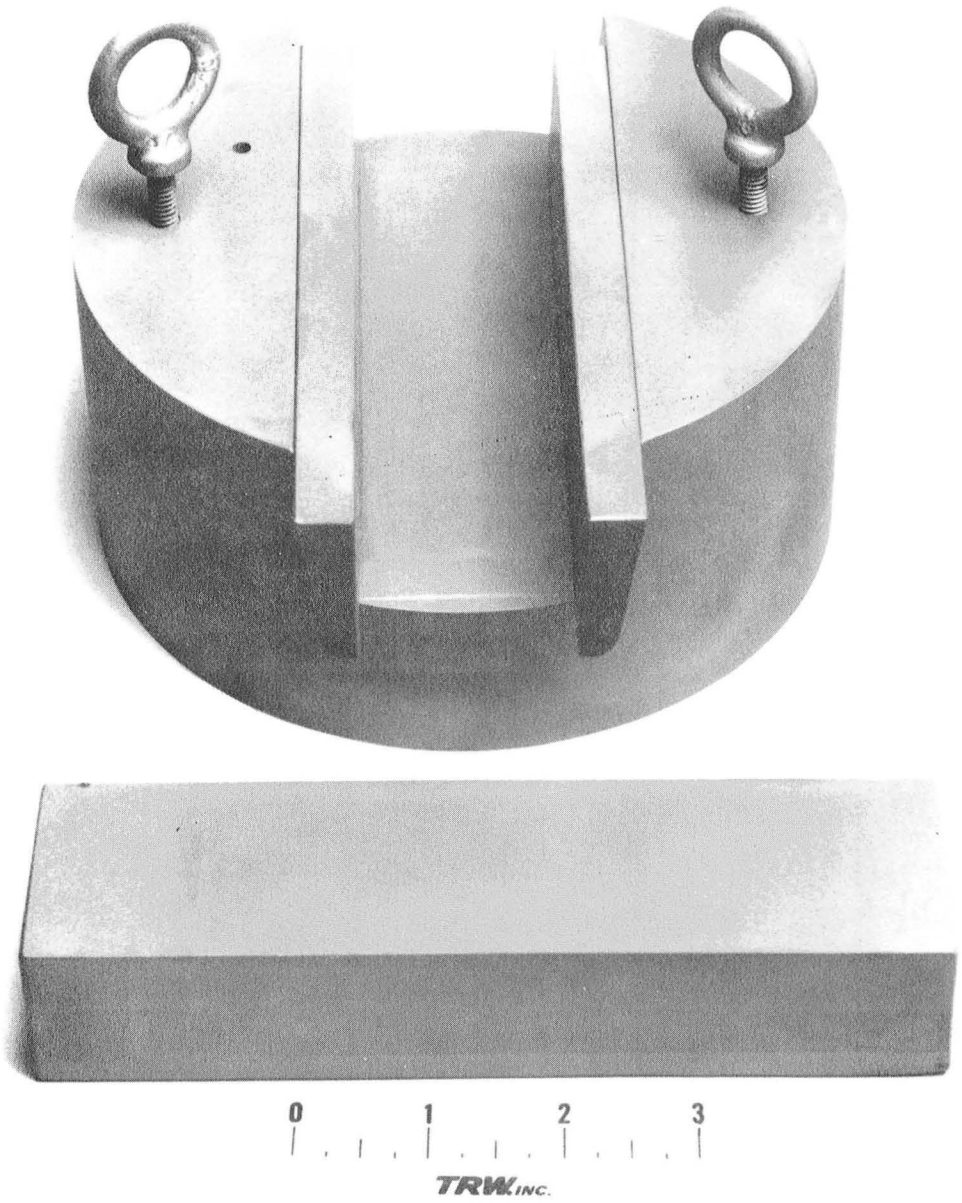

Figure 3-5. Mo/TZM Bonding Die Assembly Used in Fabrication of Monotapes.

(Note: Dimensions in inches.)

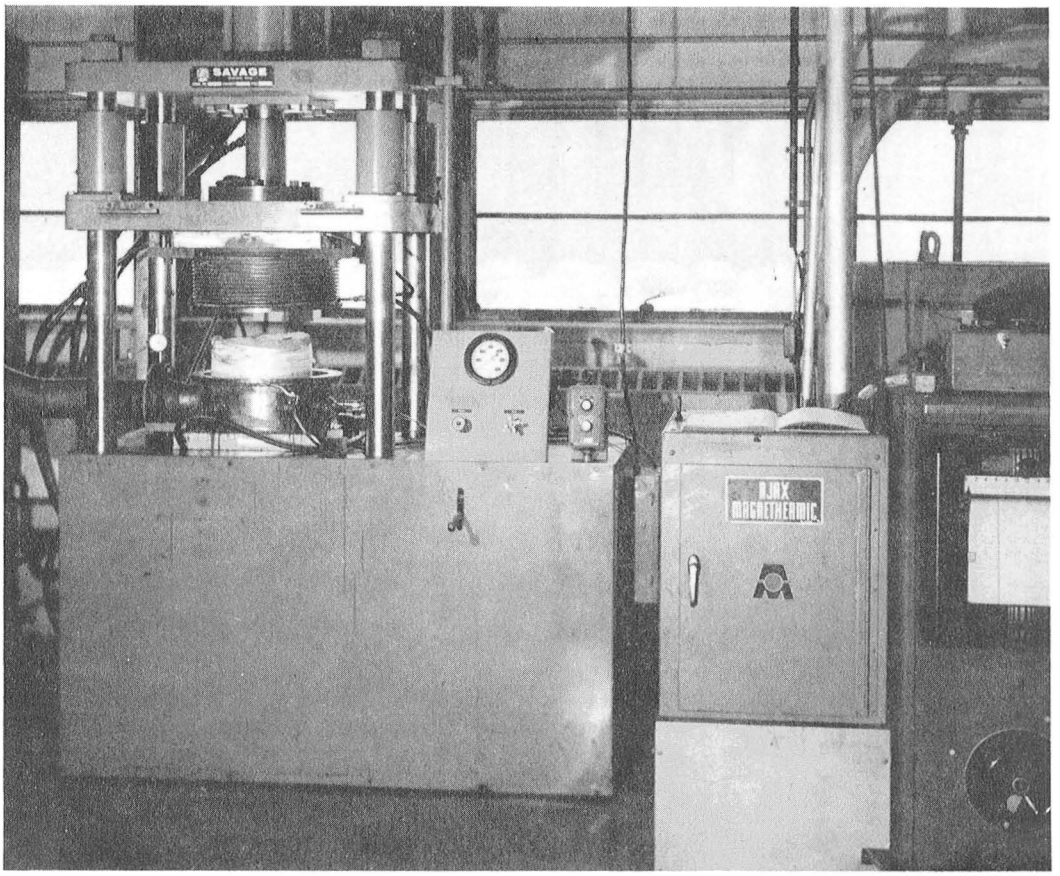

Figure 3-6. Vacuum Hot Press Used for FRS Specimens.

Additional work was also performed in the area of time, temperature, and pressure bonding parameter refinement (optimization). Initially, bonding pressures in the range of 174 to 210 MPa (25 to 30 ksi) for 30 minutes were deemed necessary to achieve full matrix consolidation at 1105°C (2025°C) using -500 mesh powder. Such bonding pressures have been found to be excessive. For example, 4.6 cm (1.8 inch) wide monotapes have been fully consolidated at bonding pressures as low as 105 MPa (15 ksi) at 1105°C (2025°F) for 35 minutes using the same (-500 mesh) powder particle size. It is conceivable that in the past, the presence of internal contamination and non-metallic inclusions in the rolled powder cloth matrix might have been interpreted (or misinterpreted) as lack of full matrix consolidation calling for higher bonding pressures.

Initially, monotapes were fabricated in lots of five(5), followed by lots of ten (10). Subsequently, monotapes fabricated in larger batches (30 monotapes)were evaluated for surface condition and fiber distribution and found to be comparable to the smaller batch (5-10 monotapes) material.

3.3.5 Monotape Evaluation

Photomicrographs of monotapes in the as-polished condition fabricated by the spray and powder cloth methods are shown in Figure 3-7. The photomicrograph on top (3-7a) illustrates the structure of the monotape obtained by the spray method; the one on the bottom (3-7b) represents the structure produced by the hand rolled powder cloth method. Photomicrographs of the samples after etching are shown in Figure 3-8.

The differences between the microstructure of the two monotapes are quite obvious. In the first place, the rolled powder cloth matrix shows numerous non-metallic inclusions which are not present in the sprayed matrix. Second, while the sprayed tape appears to be oxide free, the rolled tape shows a considerable degres of interparticle oxidation, even in specimens in the as-polished condition. The presence of internal oxidation is even more pronounced in the acid etched condition. Third, the matrix-steel bond zone is clean and well defined in the sprayed powder monotape (both as-polished and etched conditions), but oxidized and contaminated by non-metallic inclusions in the rolled powder cloth monotape. Fourth, the spray monotape shows uniform layers of matrix on each side of the fiber and is uniformly thin, while the rolled powder cloth monotape is oversize and non-uniform in thickness. In general, there is no pronounced interdiffusion band evident at the FeCrAlY matrix-steel interface.

Based on thickness measurements taken prior to and after diffusion bonding, the initial density of the sprayed powder layer is about 37% using -500 mesh powder particle size.

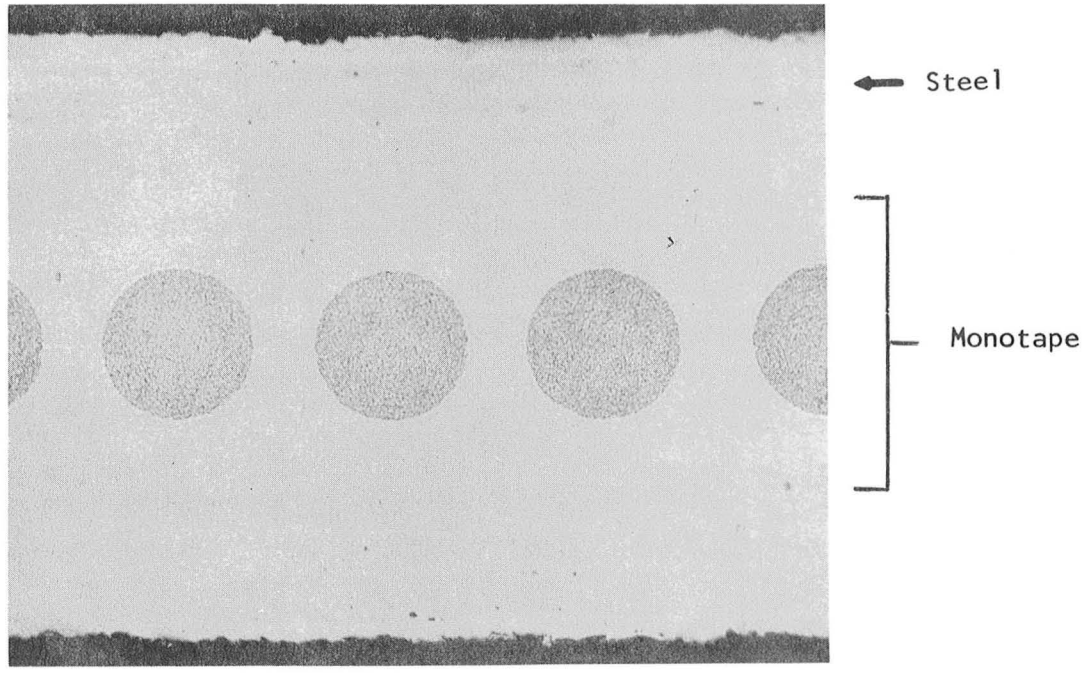

a) 200X

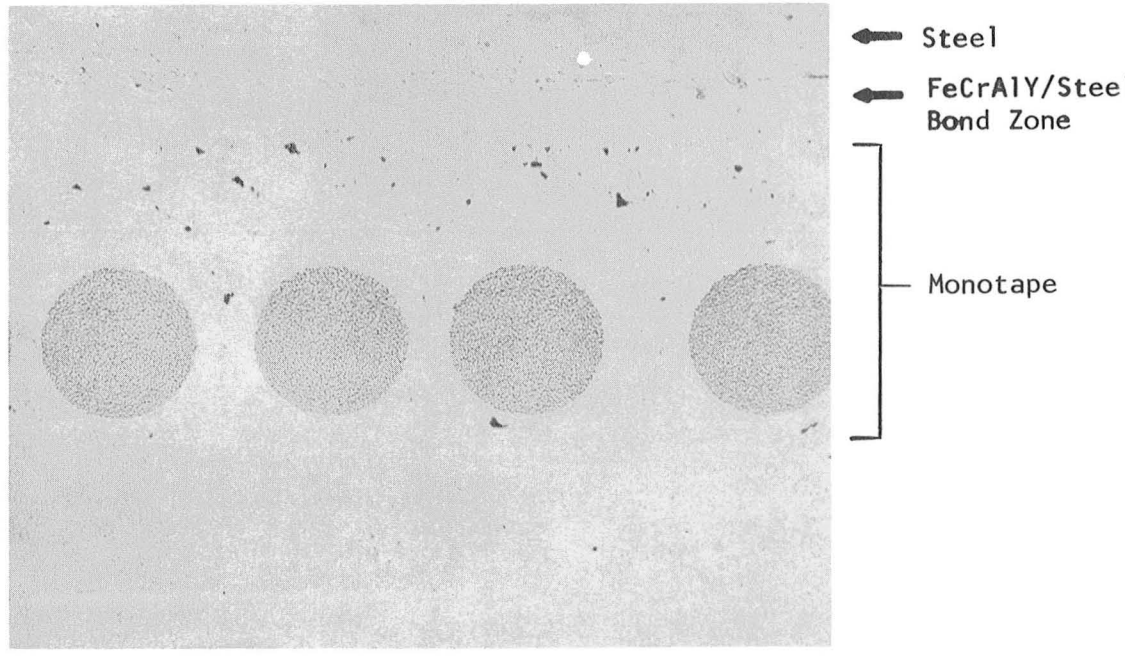

b) 200X

Figure 3-7. Microstructure of FeCrAlY-Tungsten wire monotapes in the as-polished condition fabricated by the powder spray (A) and the rolled powder cloth (B) methods. Note the overall cleanliness of the matrix in the powder spray monotape and the presence of nonmetallic inclusions and internal oxidation in the rolled powder cloth monotape.

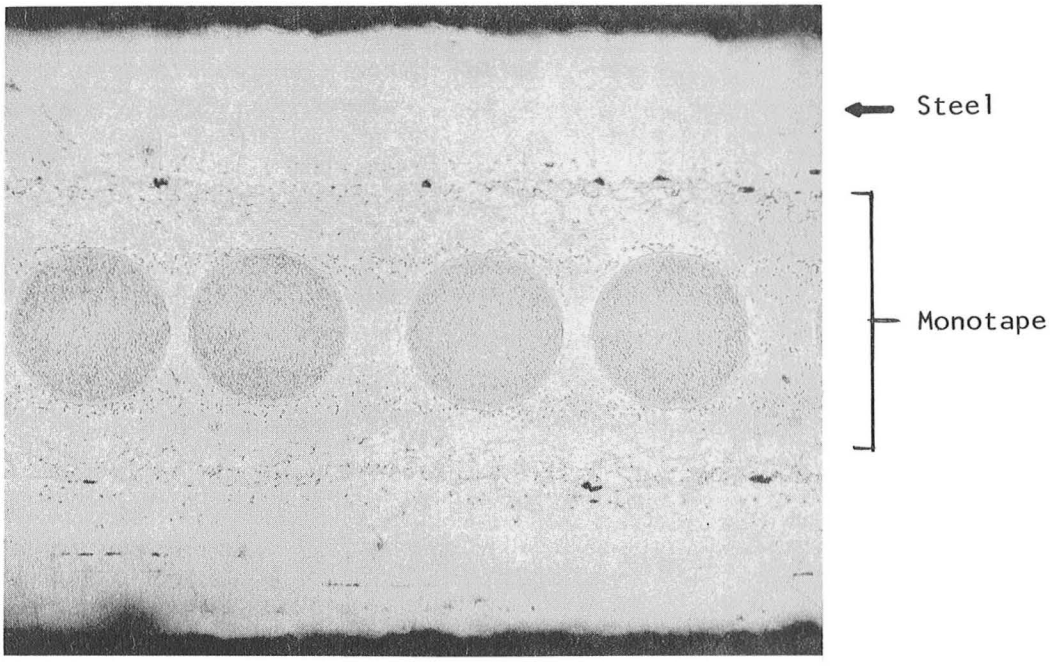

a) 200X

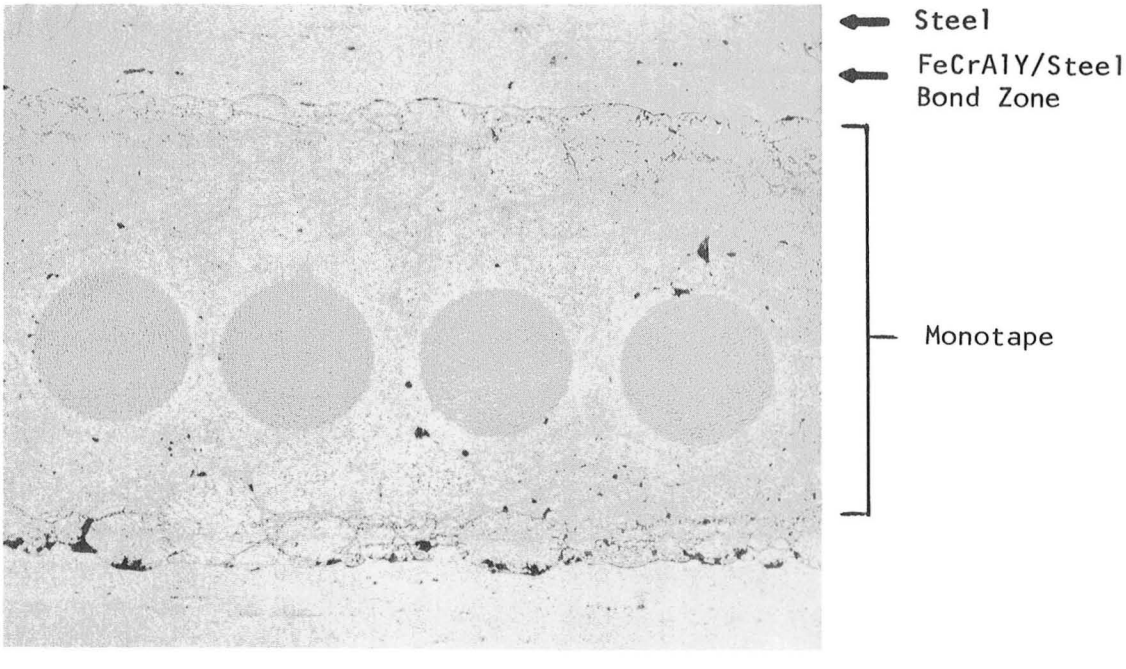

b) 200X

Figure 3-8. Microstructure of FeCrAlY-Tungsten wire monotapes after acid etching showing relative cleanliness of matrix and thickness uniformity of monotapes fabricated by the spray (A) and the rolled powder cloth (B) methods.

3.3.6 Chemical Milling and Cleaning

Chemical operations are used in the monotape fabrication process for two reasons, removal of the steel shim stock and final thickness adjustments on the monotape.

In the process of bringing the as-pressed monotapes into usable condition, they are first sandblasted to completely remove the parting compound and other surface impurities which otherwise would act as a stop-off causing non-uniform stock removal during acid etching.

A variety of acid combinations can potentially be used for the removal of the shim stock from the monotapes. Two acid combinations were evaluated under this program. The first was a solution of about 25% HNO_3 and 1% HCl in water. The second was a mixture of about 30% HNO_3 and 1% HF in water. Of the two, the latter was found preferable, primarily due to more efficient dissolution of the steel-FeCrAlY matrix interfacial diffusion zone without adverse effects on the matrix even after prolonged immersion periods. At room and moderately warm temperatures and low HF concentrations, this acid mixture is considered quite safe and reliable.

Three types of etchants were evaluated for chemical milling or sizing of FRS monotapes. The first was ferric chloride and the second included several modifications of the aqua regia reagent. Both types of etchants must be used at a temperature of 50°C (120°F) and above. The third, which could be used at room temperature, consisted of HCl and H_2O_2. This produces a reasonably smooth, clean surface. Ferric chloride produced a pitted surface; a similar surface condition was obtained with the standard aqua regia reagent consisting of about 25 ml HCl, 5 ml HNO_3 and 30 ml water. Surface finish improved with increasing HNO_3 content. The best surface finish was obtained using an acid mixture consisting of about 30 ml HNO_3, 35 ml HCl, 35 ml water. The choice of etchant is largely determined by the surface finish requirements. Regardless of the type of acid mixture used, chemical milling of superalloy materials is difficult and should be avoided whenever possible because of the problems associated with the control of the rate of reaction.

Because of the improvements made during this program in FRS monotape fabrication technology resulting in the production of monotapes to net thickness, chemical milling or sizing has become of lesser significance.

3.3.7 Monotape Cutting

A variety of monotape cutting techniques are potentially attractive; these include rule die cutting, laser cutting, and shearing.

Hardened steel rule dies were tried successfully. Not enough cuts were made to accurately forecast die life, but, intuitively, we expect life to decrease as wire diameter increases.

As part of a continuing IR&D effort to improve manufacturing techniques, some cursory laser cutting trials were performed by Sciacky. The principal of laser cutting is to melt a very localized area of the workpiece and then blow away the molten material with a gas jet. The first trials were run on monotapes. Some typical results are shown in Figure 3-9. The left side of Figure 3-9(A) illustrates insufficient power, i.e., the surface was melted but then resolidified with no material removed. The right side of Figure 3-9(A) shows the effect of more power. Here, the matrix was removed but the tungsten wires remain intact. When power is further increased so that the tungsten can be cut, the result is shown in the center of Figure 3-9 (A). A considerable amount of matrix material is lost on each side of the cut, and a zone of heavily oxidized material extends about 6 cm (1/4 inch) on either side of the cut.

On the back, or laser beam exit surface, the situation is even worse. The cut pictured on the right side of Figure 3-9 (B) is the same one shown in the center of Figure 3-9 (A). Note the presence of spatter, much like wild spatter, near the cut. Also note that on this surface, the oxidized zone is nearly 13 cm (1/2 inch) wide. Although not evident in these photographs, the tungsten wires are also heavily oxidized.

A final trial was made on a tungsten wire mat. A typical cut is shown in Figure 3-10. The polystyrene binder was removed near the cut to the points indicated by the small triangles. Note also the severe discoloration of the exposed tungsten wire.

Although we have determined that, at the current state of development, laser cutting of FRS material is not viable, we have included these observations for your information.

Conventional metal shears were used to cut both fiber mat and monotape without difficulty. This technique was used for the remainder of the program.

3.3.8 Monotape-to-Monotape Bonding

The quality of monotape-to-monotape bonds were evaluated by a tensile shear test at 538°C (1000°F). The specimen is shown schematically in Figure 3-11. The René 41 cover sheets were used to reduce the quantity of FRS needed without compromising test results.

All of the test panels were produced from monotape fabricated at 1107°C (2025°F), 96 MPa (14 ksi), and 30 minutes. The panels investigated were fabricated under the following conditions:

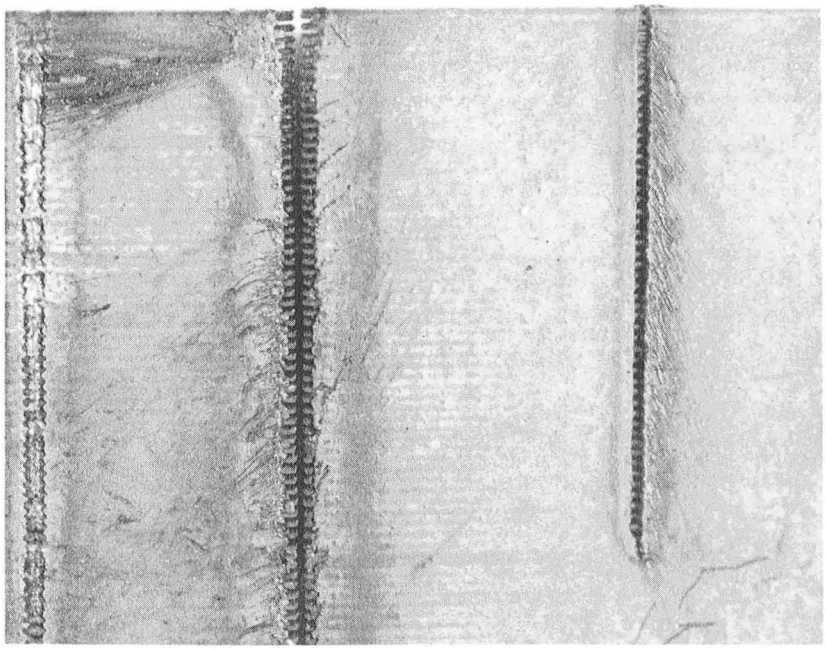

(a) Top
(Laser beam
entry side)

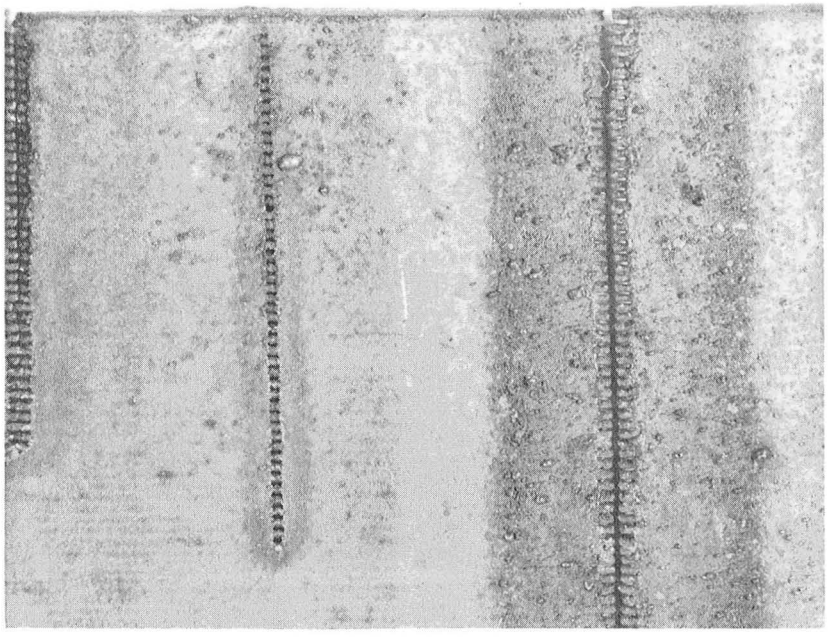

(b) Bottom
(Laser beam
exit side)

Figure 3-9. Laser Cutting Trials on W/FeCrAlY Monotape.

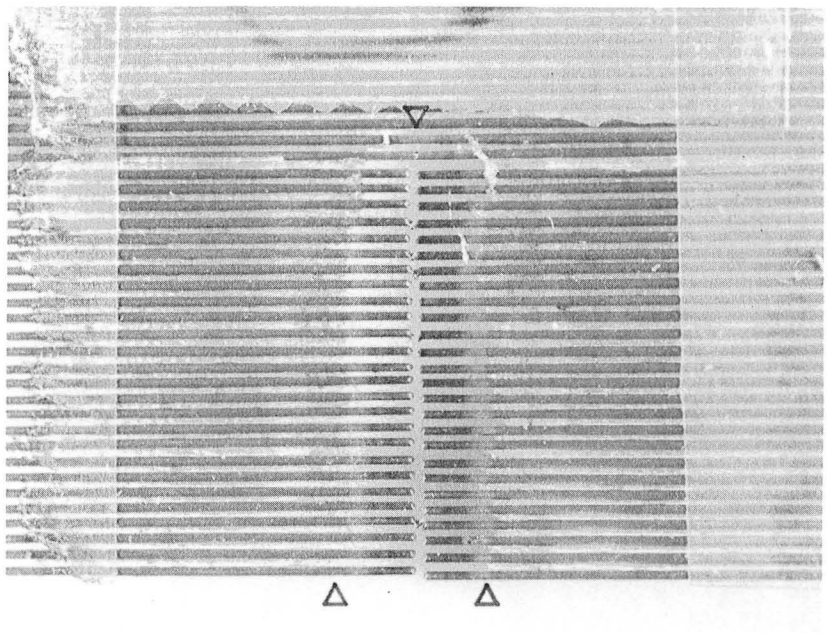

Figure 3-10. Laser Cut W Mat.

Note that the area bordering the cut was covered with transparent tape to facilitate handling prior to the cutting trials.

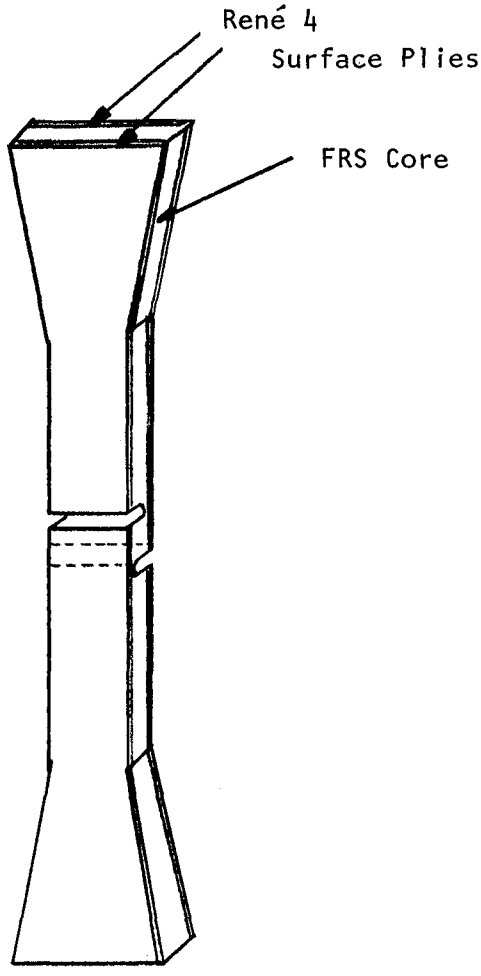

Figure 3-11. Schematic of Tensile-Shear Specimen.

two temperatures, 1024° and 1107°C (1875° and 2025°F)

two times, 15 and 30 minutes, and

two surface treatments.

The bonding pressure of 69 MPa (10 ksi) was constant.

Specimens were machined from these panels and tested on an Instron machine at a temperature of 538°C (1000°F) and in an air environment using a cross-head speed of 0.5 cm/min (0.02 in/min). Results are summarized in Table 3-III.

Visual examination of the fractured surfaces revealed a phenomenon which was not anticipated, that is, in all cases shear occurred at the fiber-matrix interface rather than at the matrix-matrix interface, the latter obviously being stronger. The main difference consisted in the mode of failure. The specimens fabricated at the highest time-temperature combination [1107°C (2025°F), 30 min] showed an irregular fracture path in the form of steps from layer to layer. The specimens fabricated at the lower time-temperature combinations failed predominantly along a single fiber-matrix interface plane. One explanation for this phenomenon is that prolonged exposure at higher bonding temperatures effected a stronger fiber-matrix bond. It should also be noted that roughening of the monotape surfaces prior to secondary bonding produced no measurable effect on the bond strength.

The obtained shear strength values should probably be treated as minimum values. In the single shear specimen design employed in these tests, a bending moment is imposed on the specimen shear gauge during testing, the effect of which is to introduce a transverse (peeling) force adjacent to the machine notch (slot). The resultant shear strength values would therefore be expected to be lower than those obtained in pure axial shear.

3.4 Blade Fabrication Development (Task III)

Metal composite blades are fabricated by bonding an assemblage of configured and, often, preformed plies of monotape in specially designed tooling. This section of the report deals with the development of the particular techniques and procedures required to make the candidate JT9D blade.

3.4.1 Tooling Development

The configured punch and die to bond the monotapes together into the blade shape must function at very high temperature. Therefore, Mo/TZM was selected as the tooling material. In addition, a twin set of punches and dies was produced in carbon steel; this was intended for use as an assembly fixture and possibly for ply forming.

TABLE 3-III

Summary of 538°C (1000°F) Tensile Shear Test Results

Panel No.	Bonding Conditions	Monotape Surface Preparation	Tensile Shear Strength MPa (ksi)
SNT2-1	1107°C, 30 min, 69 MPa (2025°F, 30 min, 10 ksi)	Acid Cleaned	76.9, 117.4, 117.8 (11.15, 17.03, 17.09)
SNT2-2	1107°C, 15 min, 69 MPa (2025°F, 15 min, 10 ksi)	Acid Cleaned	107.8, 109.1 (15.63, 15.83)
SNT2-4	1024°C, 30 min, 69 MPa (1875°F, 30 min, 10 ksi)	Acid Cleaned	70.1, 99.8, 104.7 (10.7, 14.47*, 15.18)
SNT2-5	1107°C, 15 min, 69 MPa (2025°F, 15 min, 10 ksi)	Acid Etch Pitted	119.5, 99.1, 106.4 (17.33, 14.37, 15.43)

* Specimen Failed at the René 41-FeCrAlY Interface.

The blade bonding die assembly is illustrated in Figure 3-12. It consists of one 16.44 cm (6.6 inch) diameter by 10.4 cm (4.1 inch) high channel-type die holder, one set of 16.44 cm (6.6 inch) long by 3.81 cm (1.5 inch) wide bonding die inserts and two 16.44 cm (6.6 inch) long by 4.77 cm (1.870 inch) wide wedges for easier disassembly after blade bonding.

The channel-type die holder and wedges were fabricated by conventional machining. The external blade configurations (I.D. and O.D. surfaces) were introduced into the bonding inserts by EDM. A cast JT9D-7F first stage blade was used as a master for the fabrication of the electrodes. In relation to the blade root, the tip of the blade at the trailing edge was twisted at about a 45 degree angle. This is shown schematically in Figure 3-13(a). If this orientation was used for bonding, the load would be applied at a steep angle over most of the airfoil surface. It is desirable to "rotate" the airfoil to create a flatter bonding plane, as is shown in Figure 3-13(b). However, if the rotation is excessive, reentrant or locking angles are created. These make it impossible to engage or disengage the tools (see Figure 3-13(c)). For this airfoil, it was determined that the line a-a' became vertical at about 13 degrees of rotation counterclockwise, as viewed in the sketch. Thus, a 10 degree rotation was selected for the bonding of the FRS airfoil. This rotation was simulated by regrinding the blade root flat and parallel at a 10 degree angle to the original base. These machined surfaces thus became planes of reference during electrode fabrication. Photographs of the blades in the as-cast condition and after root modification are shown in Figure 3-14.

The second item was the die split line and the configuration of the flash lands along the blade's leading and trailing edges. For the current cast blade, these details were not available. Instead of generating such information which would be both costly and time consuming, it was decided instead to EDM the airfoil configuration only, leaving excess material beyond the end points of the blade's leading and trailing edges. The die split line and the flash land configuration would then be put in separately.

The condition of the steel and Mo/TZM bonding inserts after EDM machining of the airfoil cavities is illustrated in Figure 3-15. In laying out the cavities, the as-cast blade, including the entire length of the blade root, was centered on the insert block, providing about a 3.3 cm (1.3 in.) extension past the root and tip ends of the blade. Only the actual airfoil bounded by the section at the tip and the section at the root radius was placed into the blocks, completely eliminating the blade root but extending the airfoil configuration at these sections to the ends of the block. Finishing of the EDM machined bonding inserts was carried out in conjunction with the development of a novel blade assembly method using the steel inserts as a ply assembly tool and bonding dies finishing model.

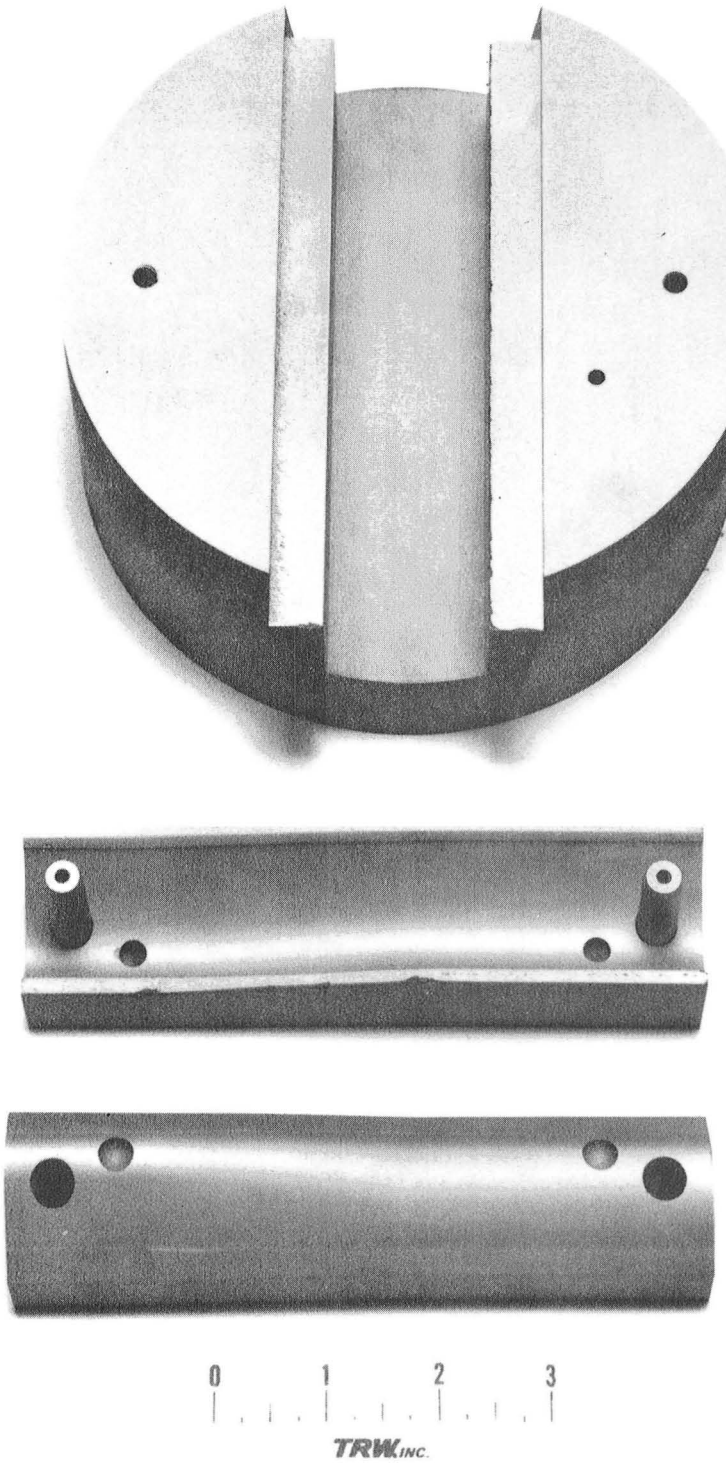

Figure 3-12. Bonding Die Assembly Used in the Diffusion Bonding of the JT9D-79 First Stage FRS Airfoil.

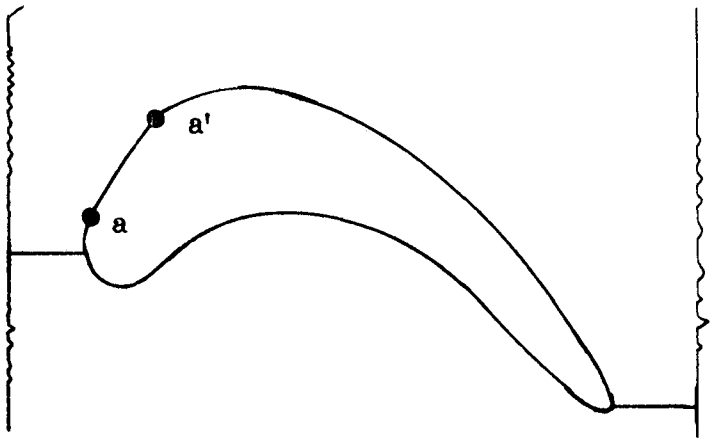

a) Actual Airfoil Orientation with Respect to Root

(Line a-a' at a positive angle)

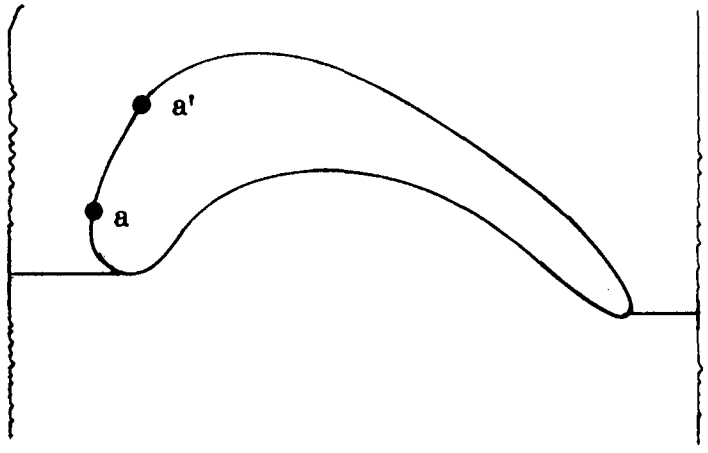

b) "Rotated" Airfoil Orientation with Respect to Root

(Line a-a' at a smaller but still positive angle)

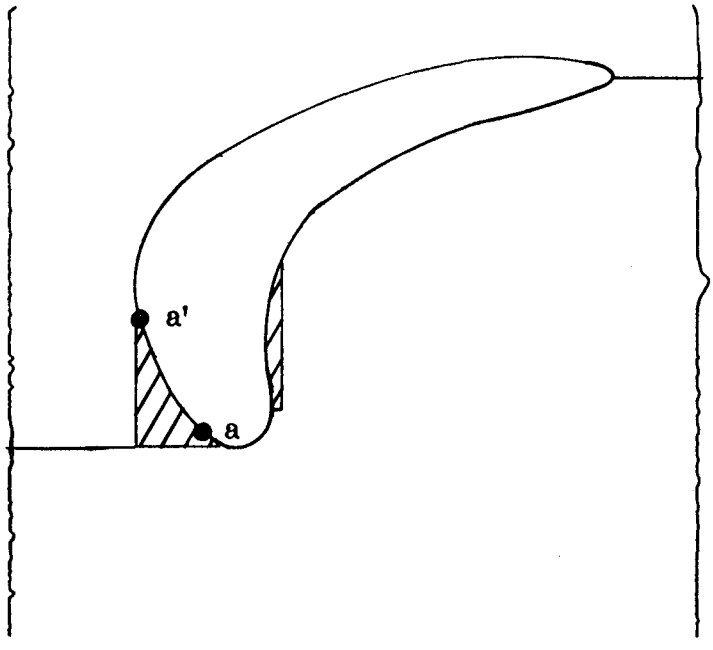

c) "Over-Rotated" Airfoil Creating Locking Angles (Shaded Areas)

(Line a-a' is now at a negative angle)

Figure 3-13 Blade Twist Considerations in Selecting a Bonding Plane

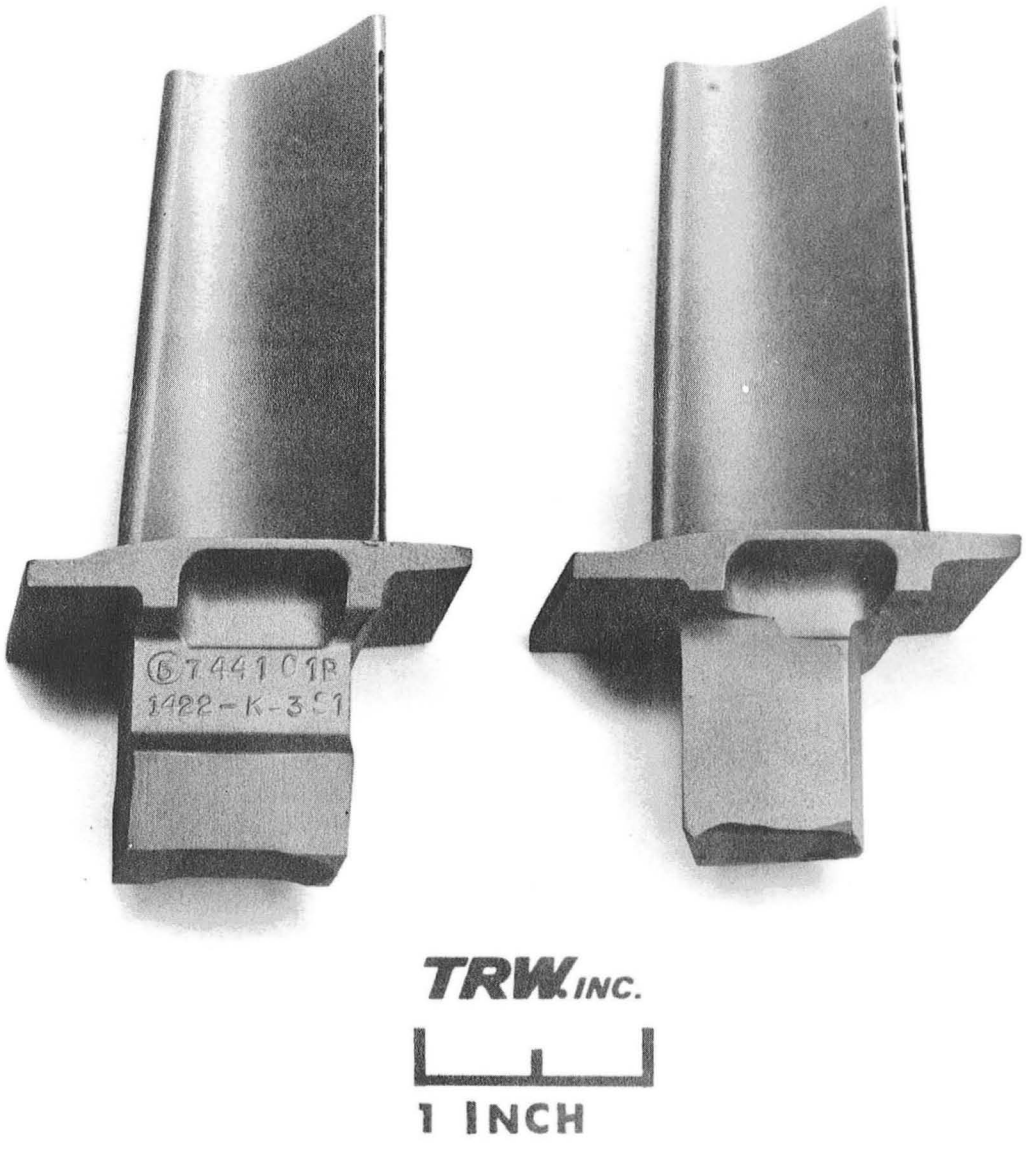

Figure 3-14. JT9D-7F First Stage Blade.

Left: As-Cast Condition.
Right: Modified Root for Airfoil Tracing During Electrode Fabrication.

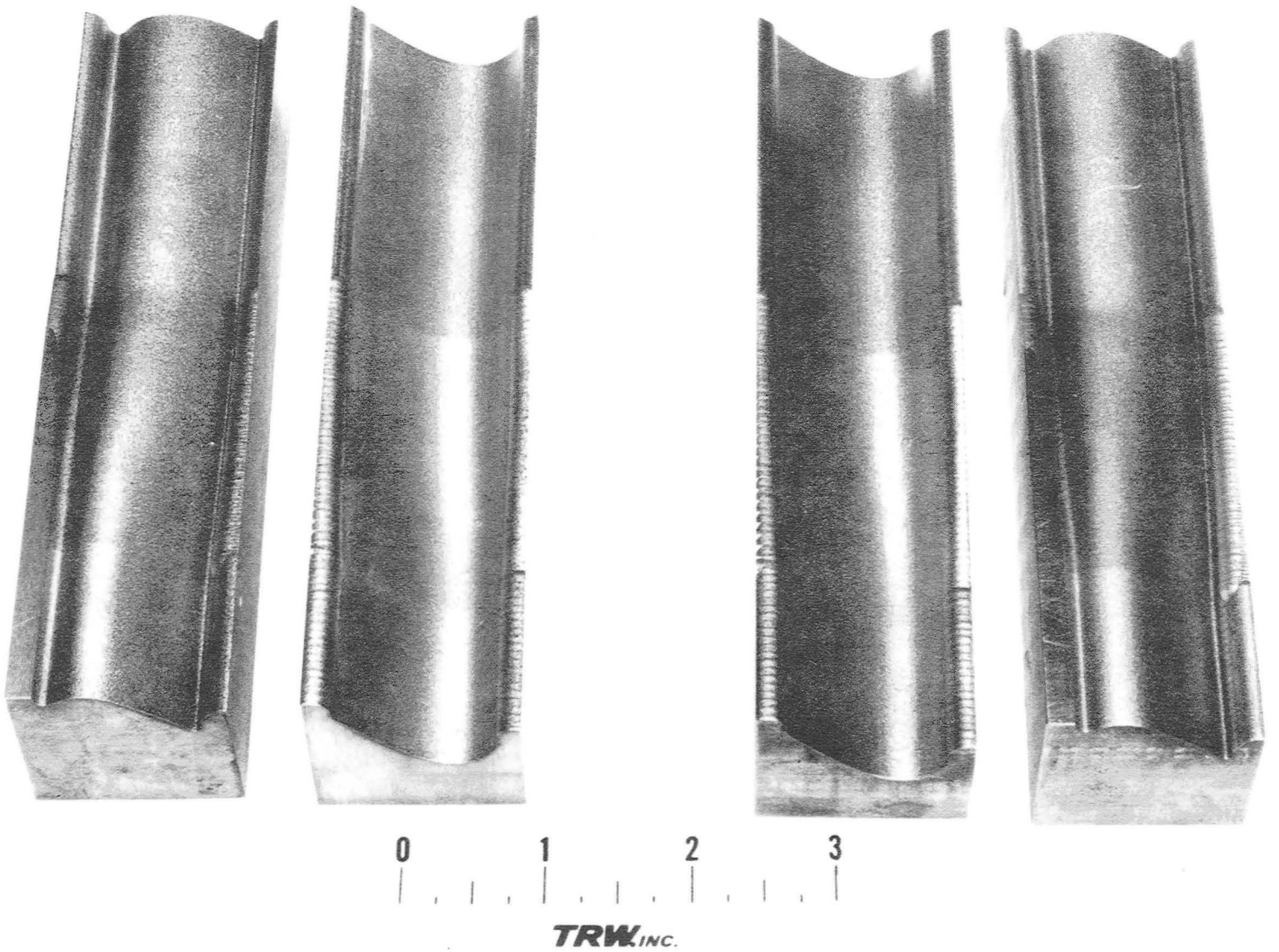

Figure 3-15. Overall Appearance of the JT9D-7F, Mo/TZM Airfoil Bonding Die Inserts (Left) and Steel Airfoil Assembly Fixture (Right) After EDM Cutting of Airfoil Cavities.

3.4.2 Ply Development

Ply shapes were developed graphically using 10x charts of blade sections. The techniques used in the development of airfoil ply shapes are illustrated in Figure 3-16. The process involved several steps as described below.

First, section split lines were established for six airfoil sections designated A-A, B-B, C-CD-D, E-E and F-F. This was accomplished by obtaining midpoint positions between the O.D. and I.D. contours at several locations of blade section charts and drawing a line through the midpoints, extending from the leading to the trailing edge of the chart.

Second, using a "peeling method", parallel lines of 1.54 cm (0.060 in)* were drawn on each section chart working from the O.D. and I.D. surfaces inward toward the split line. The points of intersections of these lines with the split line were then established and lines were drawn through such points normal to the chart surfaces.

Third, a new stacking axis was put in at 10 degrees to the original stacking axis to reflect the 10 degree rotation of the blade used in the machining of the electrodes, as described earlier. Using this new stacking axis as a reference, individual ply distances (widths) in each section chart, between the stacking axis and the intercepts with the split line to the left and right of the stacking axis, were measured and recorded. At this stage a double ply thickness step existed at each split line intercept, creating a void of a triangle base of 3.08 cm (0.012 in) and of varying height depending on the location in the section chart. To reduce such a sudden drop in thickness, a suitable stagger of the ply ends at the split line was necessary. Using a graphical layout it was found that the size of individual voids could be minimized, and the stagger between consecutive ply intercepts with the split line could be made consistently uniform by extending the O.D. ply by two-third distance and the matching I.D. ply by one-sixth distance between any set of preceding and succeeding plies. This ply stagger method was used throughout and the resulting ply width increments were reflected in the measured ply width values.

Fourth, using the recorded ply coordinates, individual ply shapes were drawn on plastic sheets (glassines). In doing this, a reference stacking axis was first put in, and the blade section heights were drawn perpendicular to the reference stacking axis. The distance to the left and right of the reference stacking axis was then marked on each section line for each ply and smooth lines were drawn through the points.

Fifth, the stacking axis was moved 0.38 cm (0.015 in) toward the leading edge to the maximum pitch thickness of the blade to enable one to place the locating notches and the blade bolting holes in the narrower plies. Because this also is the region of maximum horizontal position (flatness) in the airfoil, it became therefore the most desirable place for blade bolting and locating of the blade pack in the bonding dies.

---

* For a Ply Thickness of 0.154 cm (0.006 in).

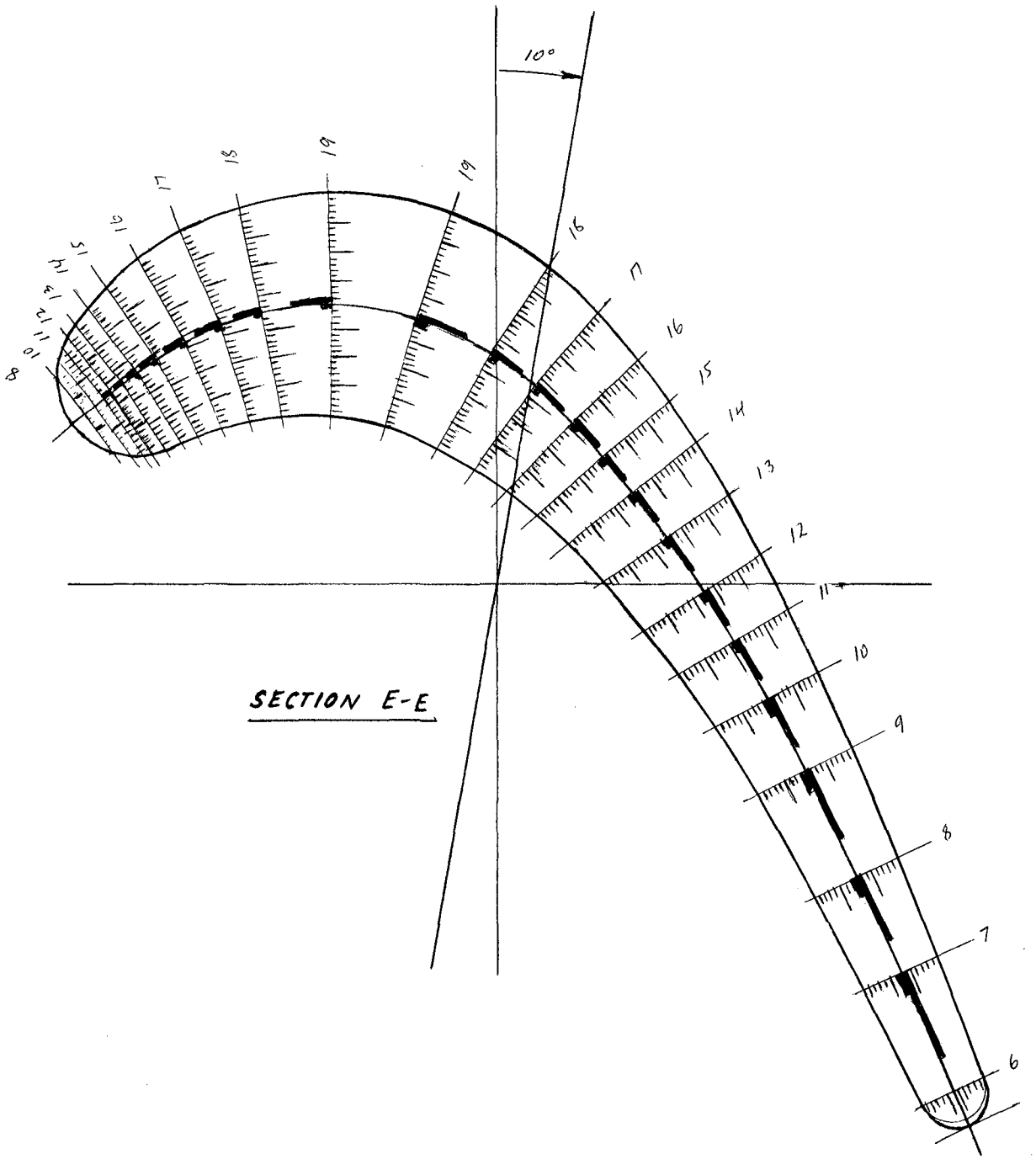

Figure 3-16. Typical Section Through Airfoil.

Finally, the individual plies were cut out with scissors and identified with a sequence number. A total of 48 plies, excluding the center buffer ply, are contained in Section A-A adjacent to the root radius. The ply trim templates are shown in Figure 3-17.

The graphic method of ply design proved to be fully satisfactory and, even if somewhat tedious and time consuming, is considered to be no less accurate and no more expensive than the computer method. One advantage of the graphic method consists in the ability to make on-the-spot adjustments without resort to costly computer iterations.

3.4.3 Ply Cutting and Assembly

It was determined that, since ply patterns were subject to change as the fabrication iterations proceeded, an investment in hard tooling for ply cutting would be premature. Therefore, all plies were hand cut with metal shears.

In the fabrication of metal matrix composite blades, the assembly of blade ply elements and the handling of the assembled blade pack has always been a problem of sorts, and for a variety of reasons. On the one hand, the methods employed are too frequently neither production oriented nor sufficiently reliable. For example, the assembly of aluminum matrix monotape plies by tack welding not only entails a great deal of manual input, but the strength of the tack weld is not adequate to prevent weld failure during the process of assembly or subsequent handling of the assembled pack during loading into the bonding press. Assembly methods involving transfer-type fixtures ("shuttle box") do not completely resolve the problem, although they contain some elements of mechanization and are useful in other ways, for example, serving as alignment fixtures during blade machining. However, the notches in the root area contain a degree of slack and the locking elements in the ply root area are very susceptible to splitting both during punching out of plies and during blade assembly. But even more important is the fact that the method is rather wasteful of material in the production of smaller (less than half length) plies since all plies have to be of the same width in the root locating area. Use of pins in blade assembly is not only time consuming, but also contains no provisions against shifting of plies in the assembled pack under press loading.

In an effort to improve on the blade assembly shortcomings described above, a novel ply assembly concept has been developed and tested. The new method can be described as a "bolting" method since it involves the use of small screws and nuts to firmly fasten the assembled blade pack at the blade's root and tip ends, and the bolt-nut arrangement is subsequently utilized as an effective means of locating and locking the assembled blade pack in the bonding dies. Although this method was initially conceived as a means of blade assembly and locating of the assembled blade pack in the bonding dies during air bonding of large boron-aluminum blades using unformed (flat) monotapes, this assembly method is also very suitable for the fabrication of FRS blades in a closed bonding chamber. The assembly fixture will vary depending upon whether flat or formed monotapes are used.

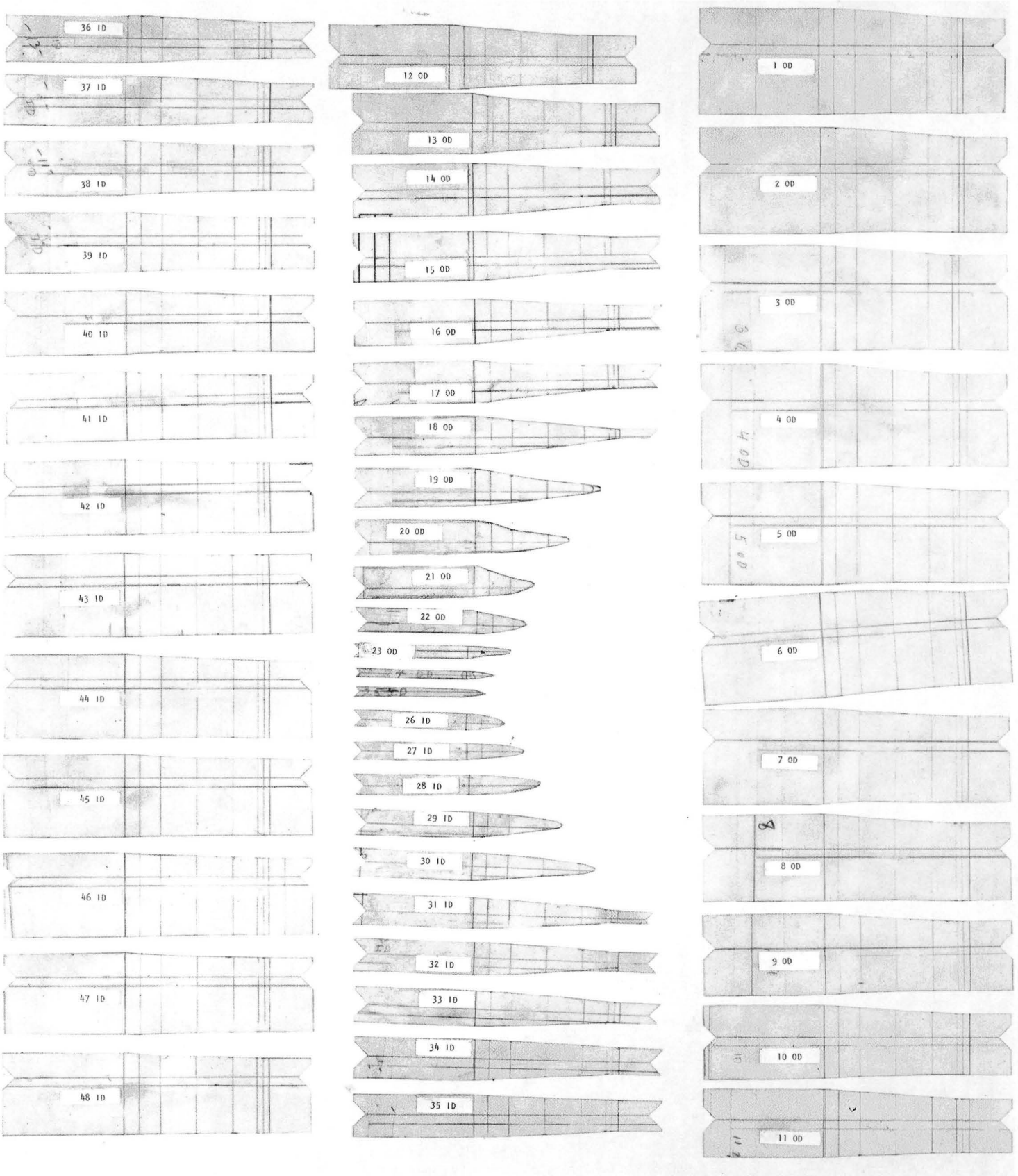

Figure 3-17. A Photograph of Ply Trim Templates for JT9D-7F Airfoil.

The airfoil assembly fixture along with the finished Mo/TZM airfoil bonding die inserts is shown in Figure 3-18. It consists of a punch and die of the blade including auxiliary features for ply assembly, as well as for bolting and locating the assembled blade pack in the bonding dies. The assembly fixture is made of steel and has the same configuration as the bonding dies. The larger holes at the extreme ends of the dies are for bolting the entire assembly fixture (containing the assembled blade pack) prior to drilling the screw fastening holes. The small holes contain ply alignment pins which are round at the base (die side) but contain a 90° angle in the position protruding above the die blade surface. The third set of holes serves as a receptacle for the guide bushing during drilling of smaller holes through the assembled blade pack as well as a clearance space for the screw head and screw nut in the fastening of the blade assembly into a well aligned and handleable blade pack. A step-by-step blade assembly procedure is described next.

The formed monotapes are scribed with the aid of ply trim templates, and V-shaped notches are punched at each end of the full length plies; a single notch is placed at the root end in the less-than-full-length plies. The distance between the base of the notches is the same as the distance between the tips of the 90° angle ply-locating pins. Starting with the O.D. surface ply as Ply No. 1, consecutive plies of diminishing size are stacked to the last and smallest ply of the O.D. half of the blade pack. The center buffer ply is placed next and the assembly is resumed starting with the smallest ply of the I.D. side of the blade pack.

Upon completion of the blade assembly, the punch half of the assembly fixture is placed on top of the blade assembly using the ply locating pins as guides, after which the entire fixture is tightly bolted together through the holes on the extreme ends of the assembly fixture. Guide bushings are next inserted into the large inside holes and smaller holes are drilled through the assembled pack at the root and tip ends of the blade pack. The guide bushings are then removed, both ends are tightly bolted together with screws and the blade pack is removed from the assembly fixture.

3.4.4 Consolidation and Bonding

Bonding of the blade is done in the Mo/TZM bonding dies illustrated in Figure 3-12. The dies contain holes for locating pins and recesses to accommodate the screw head and nut during bonding. Prior to diffusion bonding the assembled pack is located in the bonding dies, which then are placed into the Mo/TZM channel-type die holder.

Prior to the fabrication of an actual FRS airfoil, a trial run was made to check out tooling, ply assembly techniques and adequacy of the ply shapes. The entire airfoil except for the outer plies was made of 0.015 cm (0.006 in) thick 6061 aluminum foil. The outer plies were carbon steel shim stock to distinguish the flow pattern of aluminum relative to a non-deforming base (steel ply).

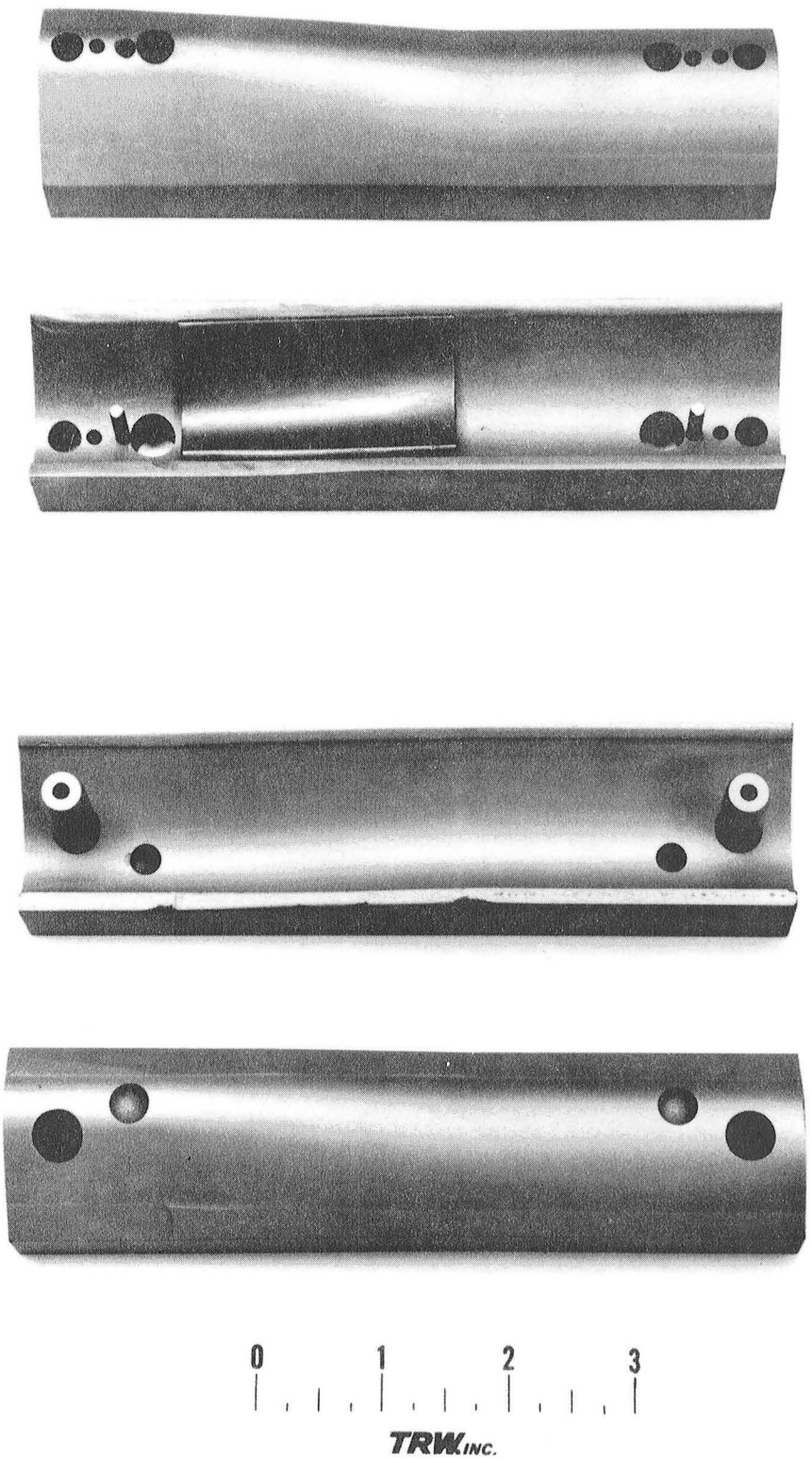

Figure 3-18. JT9D-7F Airfoil Assembly Fixture Showing the Location and the Length of Actual Airfoil (Top) and Finished Mo/TZM Airfoil Bonding Die Inserts (Bottom).

Blade assembly was effected using the assembly fixture described earlier. Because of the inherent softness of fully annealed aluminum, individual plies were formed to their proper configurations by hand in the process of blade assembly. After assembly, the blade was transferred from the assembly fixture to the molybdenum bonding dies and was diffusion bonded at 493°C (925°F) in vacuum.

The results were very satisfactory. The appearance of the airfoil after blending of the leading and trailing edges is illustrated in Figure 3-19. This trial run demonstrated the full effectiveness of the blade assembly concept and the adequacy of the blade ply shapes as evidenced by the uniform flashing of the material during bonding. No changes in ply patterns were deemed necessary prior to bonding the first FRS airfoil.

3.4.5 Forming

The preferred blade construction, shown earlier in Figure 3-2, involves wrapping the composite around the leading edge of the airfoil. A set of steel dies were machined by wire EDM for wraparound forming studies. These are shown in Figure 3-20. These were mounted in a simple four-column nest for alignment (see Figure 3-21) and installed in a hydraulic press.

Forming experiments were conducted using both single monotapes and seven-ply monotapes and seven-ply panels of the hollow blade design. Forming was conducted in the temperature range of 594° to 705°C (1100° to 1300°F). No problems were encountered during forming of monotapes of $\pm 15°$ configuration to the I.D. radius of the leading edge shell, which is the more critical radius. Cracking occurred on the o.D. surface during the first 7-ply panel forming experiment. With minor changes in setup, cracking of fibers was completely eliminated during forming of the second portion of the same panel, but localized shearing of the matrix ply on the O.D. side occurred. A second panel was then fabricated incorporating added compressive constraints on the O.D. side of the leading edge radius. One half of the panel was first formed into a V shape and then closed up to approximately the radius and configuration of a cross section of the airfoil without damage to the panel.

The first form is shown in Figure 3-22 and the second in Figure 3-23; the latter shows the steel backup material still in place. This has been removed in Figure 3-24. In Figure 3-25, some of the matrix has been etched away at the leading edge to reveal that the W-1ThO_2 fibers are 1) unbroken, 2) at the prescribed angle, and 3) still parallel and well-spaced.

3.4.6 Core Technology

The feasibility of creating controlled cavities in an FRS structure by use of selectively leachable carbon steel cores had to be demonstrated. This technology had to be extended to include fabricating a core having the required configuration and integrating same into the ply stackup prior to bonding.

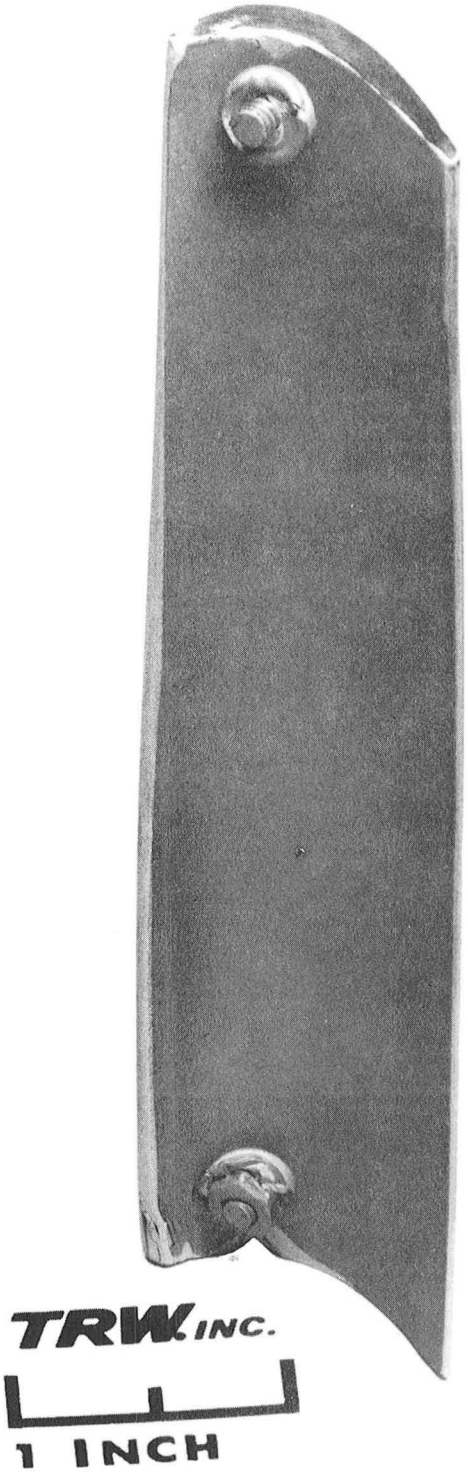

Figure 3-19. Overall Appearance of the Trial JT9D-7F Airfoil After Blending of Leading and Trailing Edges.

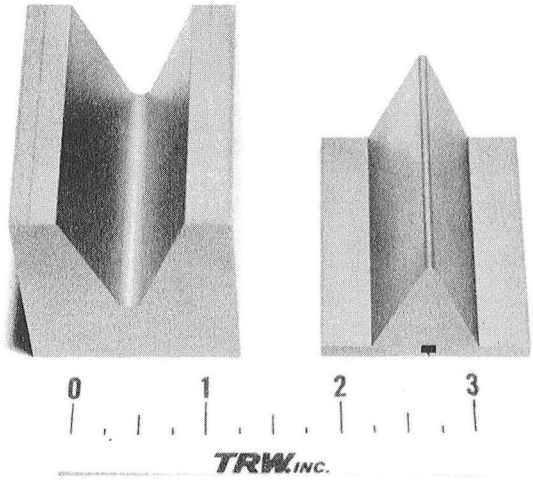

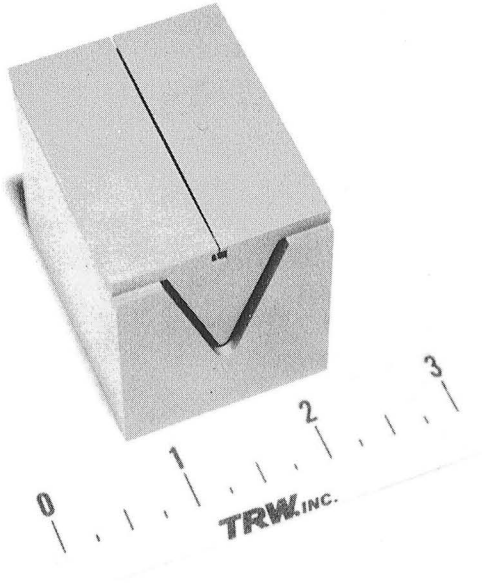

Figure 3-20. Forming Dies for Wrap-Around Trials.

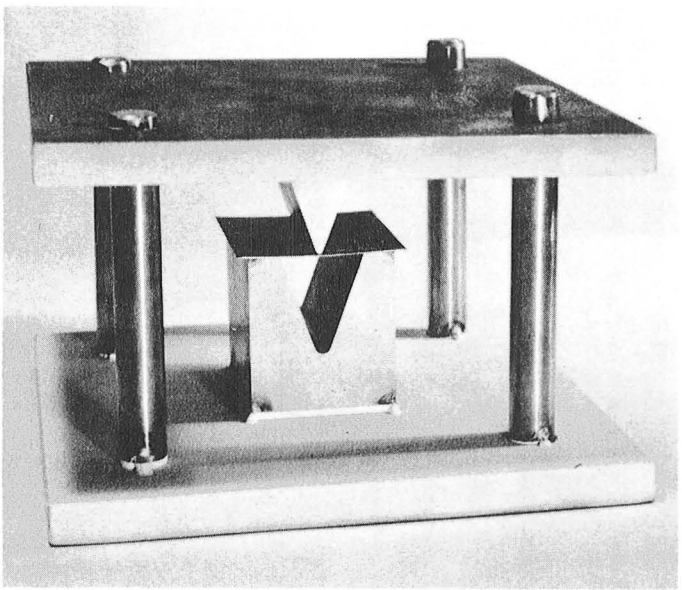

Figure 3-21. Forming Dies Installed in 4-Column Die Nest for Alignment.

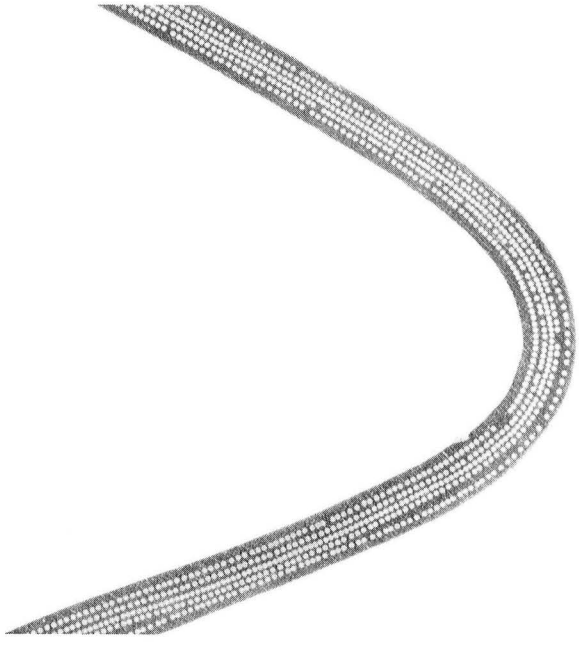

Figure 3-22. First Forming Operation on 5-Ply Panel.
Note that the steel back-up material has been removed.

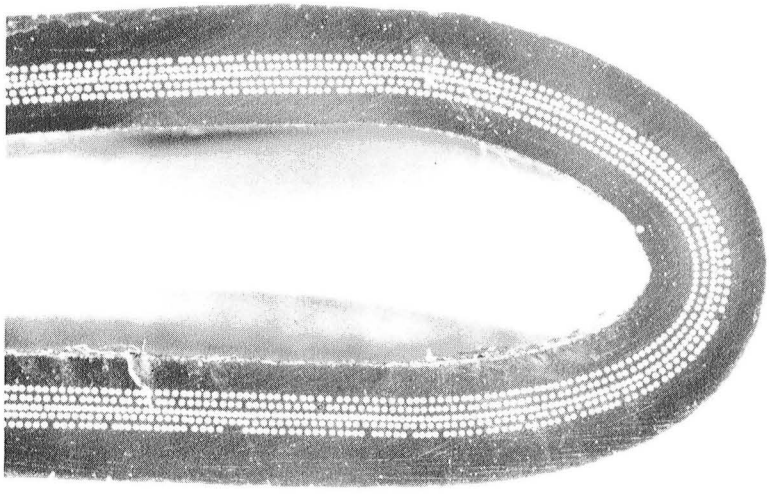

Figure 3-23. Second Forming Operation.
In this case, the steel back-up material is still in place.

Figure 3-24. Second Form after Removal of Steel Back-up Material.

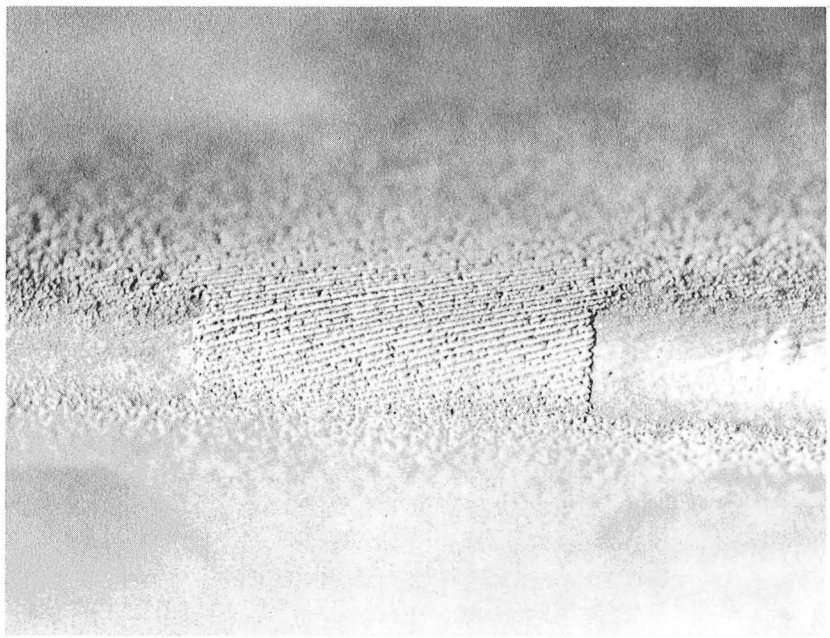

Figure 3-25. Leading Edge of Wrap-Around Panel after Etching to Expose Fibers.

In the absence of a suitable machining model, the leachable cores for the simple hollow FRS blades were produced using the existing blade bonding tooling. To accomplish this, solid blades were laid up with 0.15mm (6 mil) thick shim stock material. After diffusion bonding, ten layer thick skins were removed from the I.D. and O.D. surfaces of the blade at pretreated planes of separation and the remainder of the blade was available to be used for a leachable core insert.

Core removal was effected by selective leaching in a boiling solution consisting of 50 ml HNO_3, 1 ml HCl, and 50 ml H_2O. After leaching, the residual steel/FeCrAlY diffusion zone was removed in a mixture of HNO_3 and HF at room temperature.

3.4.7 Impingement Inserts

The finished hollow FRS blade was to contain a FeCrAlY impingement tube (insert). Sheets of FeCrAlY containing studs or "dimples" to provide the controlled separation between the insert and I.D. of the blades were vacuum hot-pressed from powder. A sheet of 0.05 cm (0.020 in) thick steel shim with 0.16 cm (0.0625 in) holes to form the "dimples" was placed over a sheet of powder cloth and pressed. After consolidation, the steel was leached away. These sheets were then hand-formed to fit the I.D. cavity of the blade.

3.4.8 Root Attachment

Two root-attachment concepts were considered, viz, a laminated root and a monolithic root block attached by brazing or diffusion bonding.

Design requirements are closely tied to material properties. The FeCrAlY system, attractive as it is from the standpoint of oxidation resistance, does not have sufficient strength at the operating temperature to qualify as a root material. If this material is to extend into the blade root, splaying of the composite in the root area or resorting to some other technique would be necessary. This, however, is in direct conflict with the economic objectives due to the technical complexity (involvement) of such an approach. A technologically simpler and economically more effective solution to the problem would be the use of bi-metallic material: FeCrAlY in the airfoil to provide the desirable oxidation resistance and a high-strength alloy in the root to ensure the required strength. Fabrication of bi-metallic monotapes by the spray method is not only technically feasible, but also acceptable from the standpoint of added fabrication cost. Pads, outserts, root blocks - or whatever we opt to call them-may be required in any case to fully develop the root dovetail area. The key to a cost-effective integration of the root attachments into the overall blade fabrication process will invariably rest in the ultimate simplicity of the basic design concepts and fabrication processes employed. For example, several viable options are available for the manufacture of root blocks; these include forging, casting, machining, laminated ply layups, etc. In the area of root bonding, alternate methods include high temperature brazing, diffusion bonding, or an integrated

single-step layup and diffusion bonding of the shell, core and laminated root components. The choice of any particular method of root attachment may well depend on the process employed in the manufacture of the shell and core blade components and the methods selected for blade assembly and bonding.

Two methods of attaching root blocks were investigated, viz. high temperature brazing and diffusion bonding. Two sets of root blocks were made from Hastelloy C material; the choice of the material was based strictly on availability. Three alternate methods of root block fabrication were considered: tracer milling, EDM using graphite electrodes and computer programmed wire EDM method. Tracer milling was abandoned primarily because of the severe curvature present in the blade cross-section which makes precision contour milling both difficult and unreliable. The other negative factor was the need for a master pattern. The graphite electrode EDM method was discarded because of the time and expense involved in preparation of the electrodes and the actual sinking of the airfoil cavities. Furthermore, new electrodes would be needed to produce additional sets of root blocks. The wire EDM method selection was based on attainable fabrication of subsequent parts at a nominal cost.

The contours of the airfoil I.D. and O.D. surfaces were digitized (in x, y coordinates) from the 10x airfoil section chart. The data were subsequently programmed on a computer and then used for the travelling wire EDM for the machining of root blocks. The high quality of the product obtained by this methods is illustrated in Figure 3-26. In designing the root block cavity, excess material was intentionally provided at the leading and trailing edge pads for the purpose of precision fitting prior to bonding.

These blocks were attached to FRS airfoils during the iterative block fabrication series discussed later.

The feasibility of a laminated root was also addressed. The confitured punch and die set shown in Figure 3-27 was designed to fit into the channel die shown earlier. The concept was to produce a double-ended specimen suitable for testing.

We found, however, that if moderately thick plies, i.e., on the order of $\sim$0.08 cm ($\sim$0.030 in) were used, the steps remaining after bonding were quite pronounced and there was considerable edge-effect (lack of bond to extreme edge of plies). A representative specimen is shown in Figure 3-28.

Use of thinner plies would improve the situation, but would not likely be cost-effective. Work on the laminated root was, therefore, suspended.

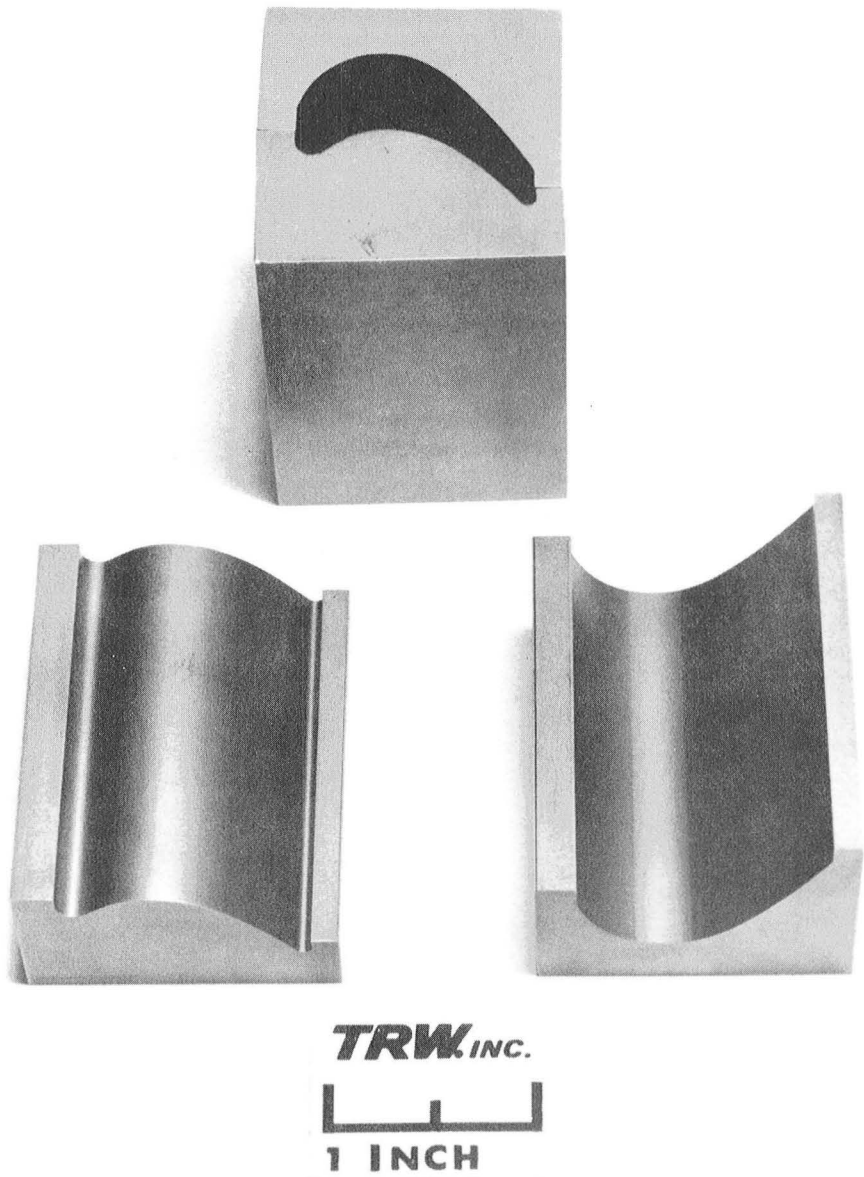

Figure 3-26. Overall Appearance of the Solid Root Blocks Fabricated by the Computer Programmed Wire EDM Method.

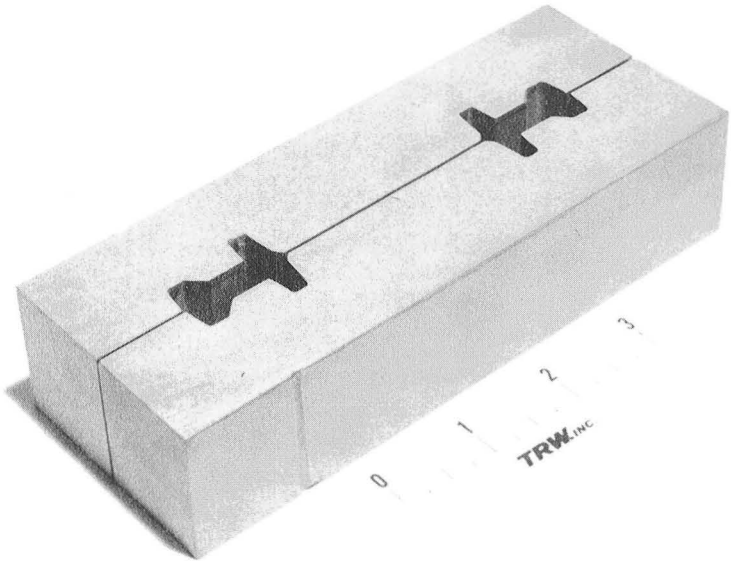

Figure 3-27. Punch and Die for Laminated Root Trials.

Figure 3-28. Typical Laminated Root Specimen.
(Note: Dimensions in inches.)

3.5 Blade Demonstration

During this portion of the program, all of the previously developed elements of the process were combined to produce a JT9D blade. Advances were made incrementally, starting with a solid airfoil and progressing to the hollow blade. Further refinements in procedures and technique accompanied each iteration.

3.5.1 Iteration No. 1, Solid Airfoil No. 1 (Unidirectional)

3.5.1.1 Monotape Fabrication

Powder cloth matrix/0.010 cm (4.0 mil) diameter tungsten wire monotapes for FRS Blade #1 were fabricated in 3.81 cm (1.5 in) and 4.57 cm (1.8 in) widths by diffusion bonding in a hydrogen atmosphere. The FeCrAlY powder cloth matrix was about 0.0154 cm (0.006 in) thick at nominal 50% density. Tungsten wire was in the form of a wire mat wound on 0.0132 cm (5.2 mil) centers to provide 40 volume percent reinforcement in 0.0154 cm (0.006 in) thick, fully densified monotape plies. The narrower monotapes were consolidated at 1105°C (2025°F) 174 MPa (25 ksi), 30 min. Because of a temporary press capacity limitation, somewhat longer bonding times at lower pressures were used in the consolidation of the wider monotapes. The monotape was fabricated in batches of 20 pieces. In laying up the monotapes for diffusion bonding, the tungsten/matrix-cloth assembly was encased between two pieces of 0.010 cm (0.004 in) thick carbon steel shim stock. The individual units were separated by 0.0127 cm (0.005 in) thick molybdenum sheets spray-coated with a boron nitride/zirconium oxide parting compound.

3.5.1.2 Monotape Forming

A decision was made to fabricate the initial batch of FRS airfoils using formed monotapes. Plies were preformed in the blade assembly fixture with a slight modification which consisted of a buildup of the center portion of the upper insert (punch) to provide the required clearances for the monotapes in the regions of steep curvatures in the bottom (die) insert, especially along the airfoil leading edge. Failure to do this would result in binding and tearing of the monotapes in these critical die regions. Forming was done in a hydraulic press in the temperature range of 480°-540°C (900°-1000°F), and the monotapes were used in the as-pressed condition with the steel outer layers intact to preclude monotape splitting. The sequence of steps involved in the monotape forming is described below.

To keep monotapes properly aligned in the forming fixture, shim stock was cut to the width of the die cavity and holes introduced on the ends to match the outer set of holes in the forming dies. A monotape was centered inside the shims and the package was securely aligned by interlocking with the guide in the forming die. The punch piece was placed on top and the assembly was then centered between preheated press platens. After temperature equalization, the press ram was allowed to creep downward until a load of 2,000 Kg (2 tons) was registered on the pressure gauge. The assembly was then removed from the press and immediately reloaded to minimize cooling of the forming die inserts. The overall appearance of the as-formed monotape is shown in Figure 3-29.

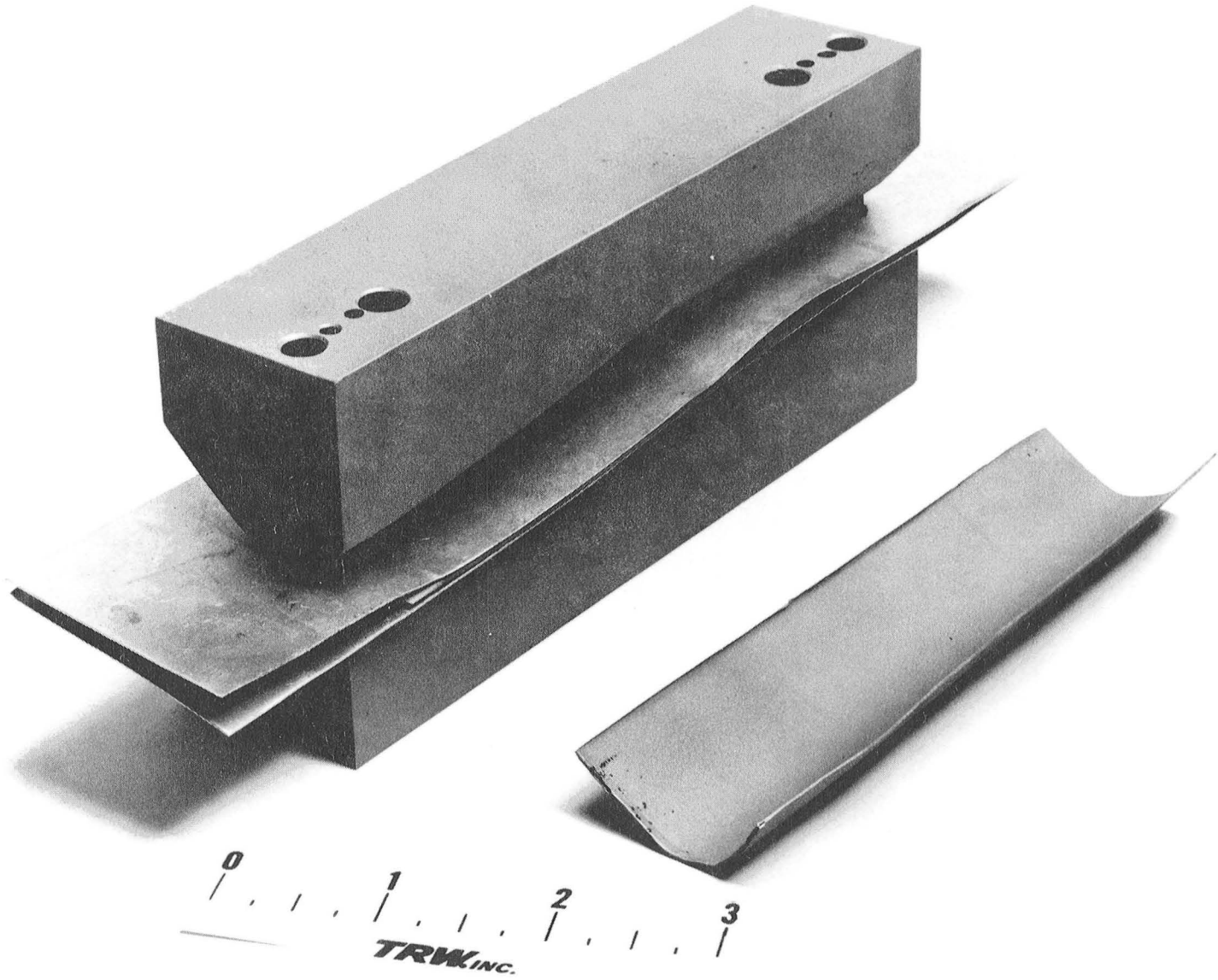

Figure 3-29. Tungsten-1% ThO_2-Wire/FeCrAlY Matrix Monotape Formed to the JT9D-7F Airfoil Configuration.

Only the full and intermediate width plies were preformed; the remainder of the plies were used flat.

3.5.1.3 Monotape Cleaning and Sizing

After forming, the monotapes were sandblasted to remove parting compound and the carbon steel shim covers were stripped (dissolved) in an acid mixture consisting of 100 parts of HNO_3, 100 parts of H_2O and 1 part of HCl.

After chemical stripping of the steel foil substrate, the monotapes were chem milled in an aqua regia type reagent to remove excess matrix. A problem developed at this point in that the ends of the monotapes were attacked by the acid more rapidly than the rest of the material. To prevent complete disintegration, the monotape ends had to be protected with a masking tape. Because of this, most of the etched monotapes were non-uniform in thickness and generally oversize. The problem had been traced to the use of tape adjacent to the matrix cloth during monotape layup. At the bonding temperature the tape charred and the residual free carbon depleted the matrix of chromium through the formation of chromium carbides.

3.5.1.4 Blade Assembly and Bonding

An additional complication was encountered after blade assembly. Because of the low monotape forming temperature and the inadequacy of the forming insert, much of the deformation occurred in the elastic range. After stripping the shim stock substrate, a partial unfolding of the plies occurred as the result of elastic springback, and the assembled blade became too wide to fit into the die holder. To correct this problem, the blade layup was placed back into the assembly fixture and post-formed in a hydrogen atmosphere under a moderate load. Ultimate diffusion bonding of the blade was carried out in the regular Mo/TZM bonding dies in a hydrogen environment, using bonding parameters of 1105°C (2025°F), 70 MPa (10 ksi), 30 minutes.

3.5.1.5 Evaluation

An overall appearance of the first solid FRS blade is shown in Figure 3-30. A photomacrograph of the airfoil section removed from the vicinity of blade root, illustrating ply layup and fiber distribution is shown in Figure 3-31. Center cushion ply was inadvertently omitted during blade layup. It is apparent from the photograph that, from the standpoint of consolidation, the use of an all matrix center ply is not required in the FRS composite system.

In spite of the initial problems during chem milling, assembly and post-forming, the overall pressing result was satisfactory. The blade was well bonded except for a small area along the trailing edge near blade tip which is attributed in most part to the oversized monotapes. Lack of thickness uniformity in the monotapes, particularly at monotape ends, and a partial contamination of plies during post-forming were also contributing factors. The problems associated with forming, sizing and assembly were resolved prior to the fabrication of the second solid FRS blade.

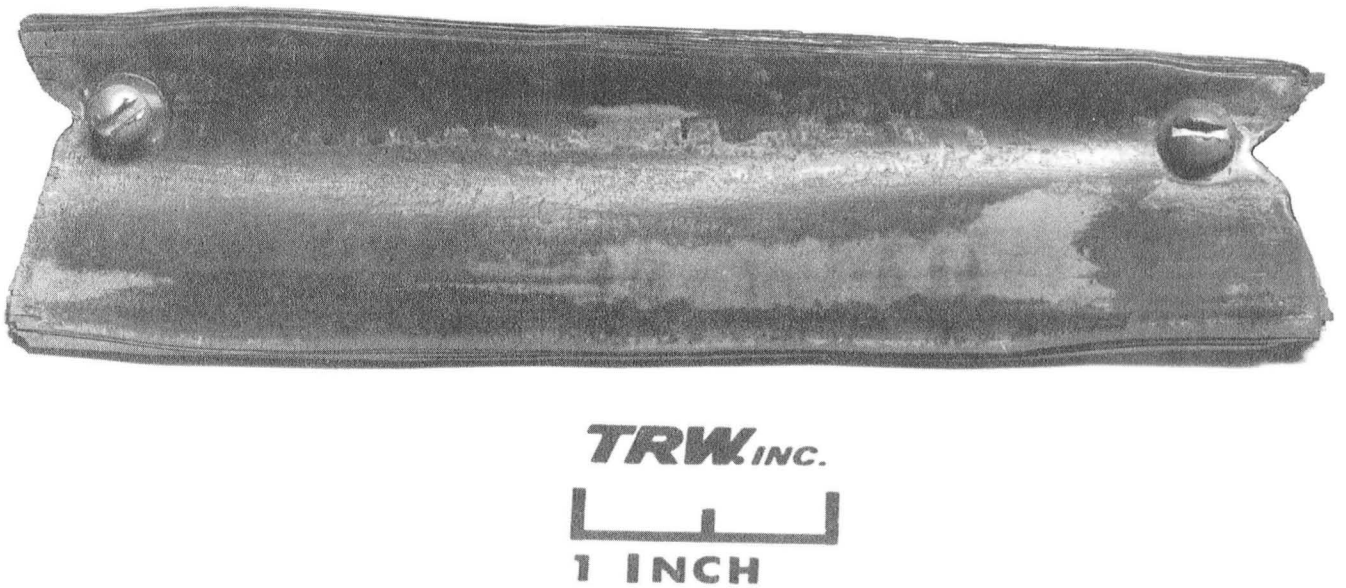

Figure 3-30. Overall Appearance of the Solid FRS Blade No. 1 in the As-pressed Condition.

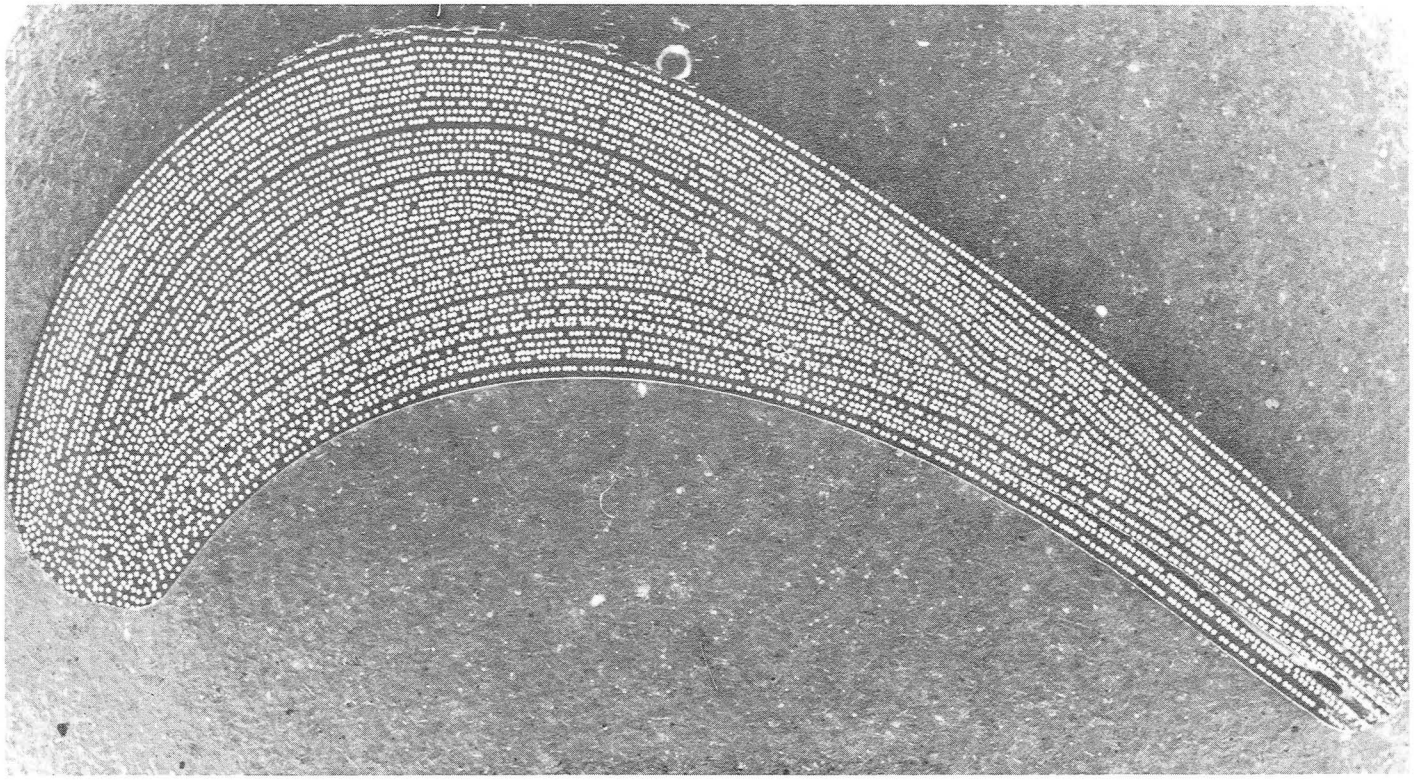

Figure 3-31. Photomacrograph of a cross-section of the solid FRS blade #1 illustrating good bond and the absence of the center cushion ply and the level of uniformity in monotape thickness and fiber distribution.

3.5.2 Iteration No. 2, Solid Airfoil No. 2 (Unidirectional)

3.5.2.1 Monotape Fabrication

Starting with the second solid FRS blade, all monotapes were fabricated using the spray method. The thickness of the sprayed matrix was adjusted to eliminate the need for chemical sizing after diffusion bonding. Using the 35 to 38 percent measured density of the sprayed matrix powder of minus 500 mesh size, a sprayed thickness of about 0.012 cm (5 mils) is required for a 40 volume percent using 0.01cm (4 mil) tungsten wire reinforcement with a 0.013 cm (5.2 mil) spacing in the wire mat. The procedures employed in the fabrication of monotapes by the spray method were described in detail earlier.

3.5.2.2 Monotape Forming

The problems associated with forming of monotapes for the first solid FRS blade were described previously. With a view to improving the monotape forming capability, forming inserts for the blade O.D. and I.D. surface configurations were fabricated from steel plies using the Mo/TZM bonding dies. After bonding, a ten-layer skin was removed from the O.D. side of one blade and the I.D. side of the other to serve as permanent forming inserts having necessary clearances. Mechanical removal of the outer skins was facilitated by the application of a parting compound at the skin-core interface. Using these forming inserts, monotapes were formed to the exact configurations of the I.D. and O.D. blade surfaces in the temperature range of 600°C (1100°F) to 700°C (1300°F) with no observable elastic springback after the removal of the steel substrate. The appearance of an actual monotape ply after forming and acid stripping of the steel substrate is illustrated in Figure 3-32.

3.5.2.3 Monotape Cleaning

After forming, the monotape steel substrate was dissolved in a nitrihydrofluoric acid solution in water of the composition described earlier. Practically all monotapes were used in the as-stripped condition without additional chemical sizing. Because of the fine tuning of the sprayed powder thickness performed in conjunction with this blade, the blade itself contains a mixture of standard size, slightly oversized and on the most part, slightly undersized plies.

3.5.2.4 Ply Cutting

Ply shapes were cut manually. Some of the plies were slightly corrected to reduce ply width at blade Section A-A which was extrapolated during the initial ply design using blade section charts. A trimmed full size ply was shown earlier in Figure 3-32.

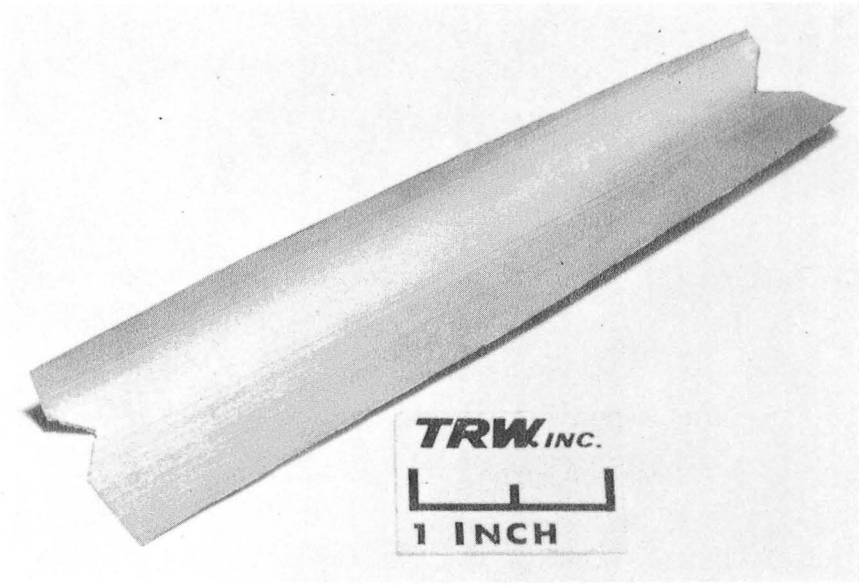

Figure 3-32. Overall Appearance of a Formed and Manually Cut Monotape Ply.

3.5.2.5 Blade Assembly

Because of the greater accuracy of the ply configuration made possible by the use of the improved forming techniques, the blade was assembled without difficulty using the assembly fixture and techniques described previously. The appearance of the assembled blade pack is illustrated in Figure 3-33.

3.5.2.6 Blade Bonding

After assembly, the blade pack was located in the bonding die insert and loaded into the die holder. The procedures employed in the bonding of the blade are described in detail below.

First, the entire assembly was placed into the chamber which was then evacuated to about 100 microns. The dies were then heated gradually to 400°C (750°F) under dynamic vacuum to remove stop-off binder and the condensed moisture. During this bake-out period, no positive load was maintained on the blade to guard against possible entrapment of air within the blade pack. While under dynamic vacuum and continuous heating, a load of 40 MPa (6 ksi) was gradually applied to the blade. When the temperature of 730°C (1350°F) was reached, the chamber was flushed with argon and backfilled with hydrogen. Heating rate was then increased and the load was raised to 50 MPa (7 ksi) and maintained during heating to the 1105°C (2025°F) bonding temperature. After temperature equalization, bonding load was raised to 70 MPa (10 ksi) and maintained for 30 minutes. Heat and pressure were then shut off and the system cooled first in hydrogen and then in flowing argon.

3.5.2.7 Blade Evaluation

The blade was evaluated by visual and dimensional inspection and metallography of cross-sections removed from the tip and root ends of the airfoil.

Visually the blade looked very good. The overall appearance of the blade after sandblasting, finishing of the leading and trailing edges and the removal of the metallography sections is illustrated in Figure 3-34. Dimensionally, blade pitch thickness was about 0.05 cm (0.020 in) undersize due to the mixture of variable thickness monotapes described earlier. Photomacrographs of blade cross-sections removed from the root and tip ends are shown in Figures 3-35 and 3-36, respectively. The dark band along the blade section split line represents a 0.012 cm (5 mil) thick matrix cushion ply. As noted earlier, the use of such ply is not necessary for a successful blade consolidation in the W-FeCrAlY system. The randomly distributed dark spots represent missing tungsten wires and are mostly attributed to poor splicing of the wires during winding of mats. Splicing of tungsten wire is somewhat difficult because of the residual cast in the wire. However, splicing techniques have been improved and splicing will not be a problem in the future. Otherwise, wire spacing in the individual monotapes is reasonably good. The matrix-matrix bond is sound throughout the entire cross-section, and the visual appearance of the remainder of the airfoil and of the as-pressed flash pattern shows no indication of possible bonding problems elsewhere.

Figure 3-33. Assembled Blade in the Assembly Fixture after Bolting of Blade Ply Ends.

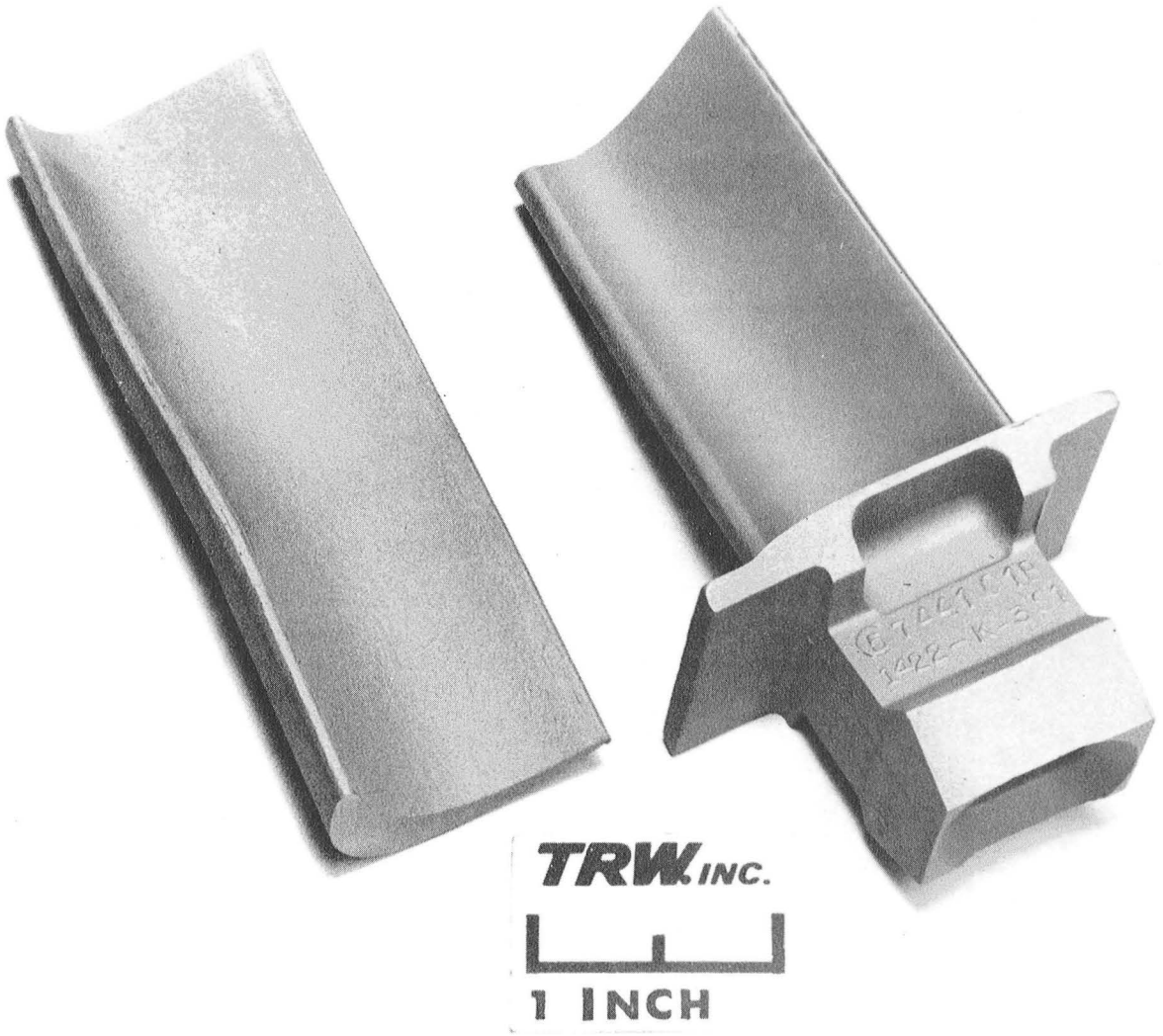

Figure 3-34. Appearance of the solid FRS Blade #2 after finishing of the leading and trailing edges and the removal of metallography samples from the root and tip ends.

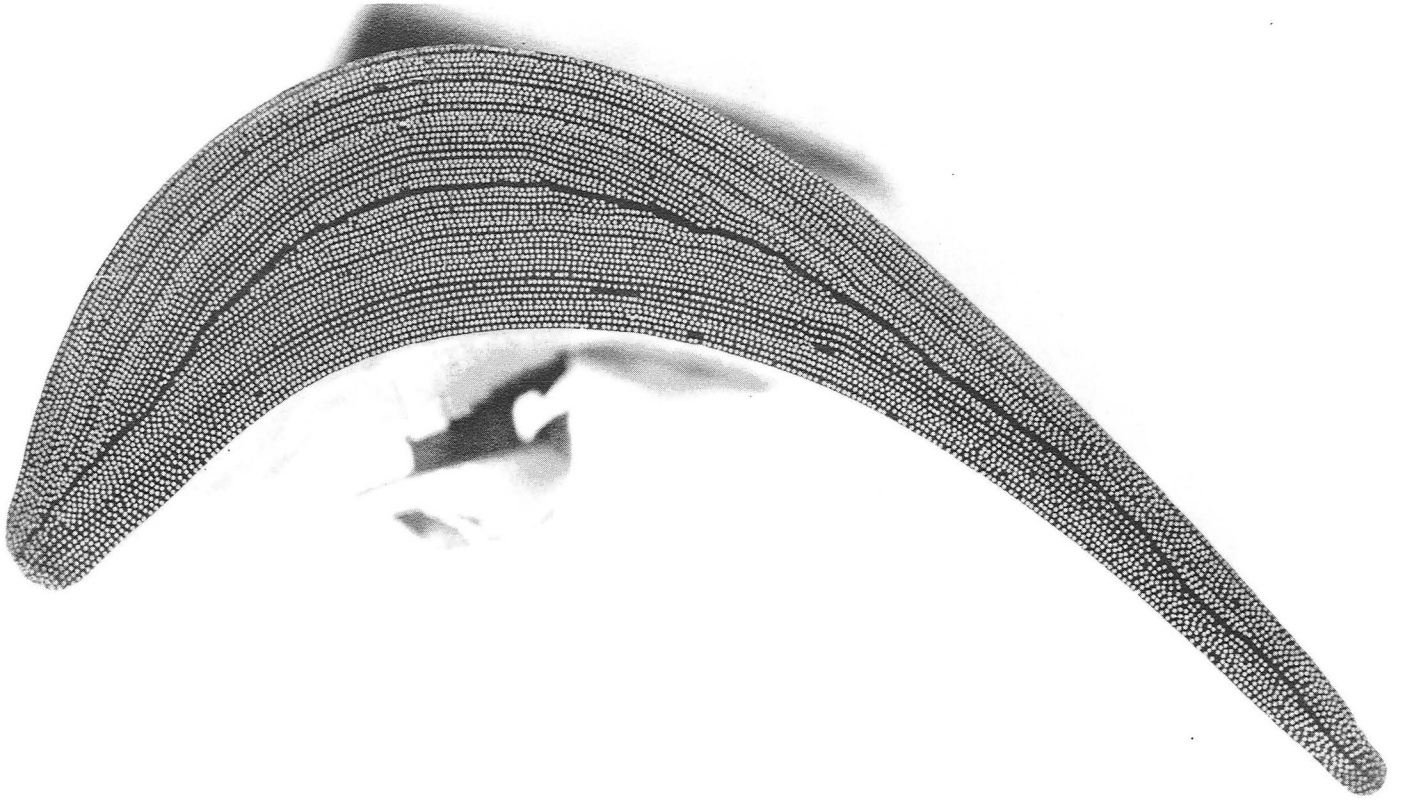

Figure 3-35. Photomacrograph of the solid FRS blade #2 cross section at the root end illustrating good bond and the uniformity of wire distribution in the monotapes.

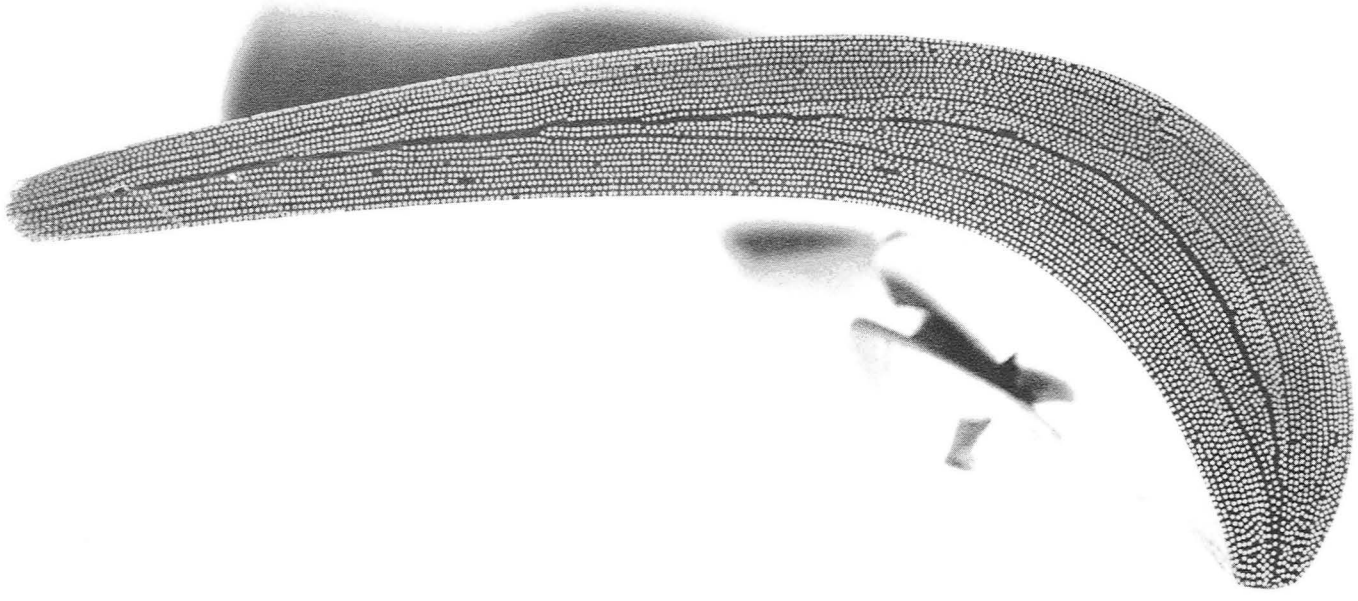

Figure 3-36. Photomacrograph of the solid FRS blade #2 cross section at the tip end illustrating good matrix bond and the uniformity of ply thickness and wire distribution in the monotapes.

3.5.3 Iteration No. 3, Solid Airfoil No. 3 (Cross-Plied)

This was superficially identical to the previous iteration except that the construction was changed to approach that to be used later in the hollow airfoils. The construction was as follows:

Ply	Material	Orientations
1	FeCrAlY	-
2	FRS, 40v/o	+15
3	FRS, 40v/o	-15
4	FRS, 65v/o	0
5	FRS, 40v/o	-15
6	FRS, 40v/o	+15
7	FeCrAlY	-
8-41	FRS, 40v/o	0°
42	FeCrAlY	-
43	FRS, 40v/o	+15
44	FRS, 40v/o	-15
45	FRS, 65v/o	0
46	FRS, 40v/o	-15
47	FRS, 40v/o	+15
48	FeCrAlY	-

In addition, since the pitch thickness of solid airfoil #2 was low, two additional 0° 40v/o plies, designated 17A and 37A were included.

Fabrication proceeded without incident. Root blocks were then attached to this airfoil by brazing.

The braze material was AMS 4778, Type NB-4 alloy containing 0.03C, 4.50 Si, 3.0 B, 1.0 Fe, balance Ni, and was procured from Vitta Corporation in the form of an adhesive-coated powder transfer tape. The recommended brazing temperature is 1052°-1177°C (1925°-2150°F). To check the braze characteristics of this material, a test run was made on a sample specimen consisting of INCO 718C root pads and FeCrAlY sheet insert. Brazing was performed in hydrogen gas flow at 1107°C (2025°F) for 15 minutes under a moderate press load. Because of the relatively high fluidity and the attendant running of the excess braze material from the brazing interfaces, the root blocks were subsequently brazed at 1066°C (1950°F). The blade is shown in Figure 3-37.

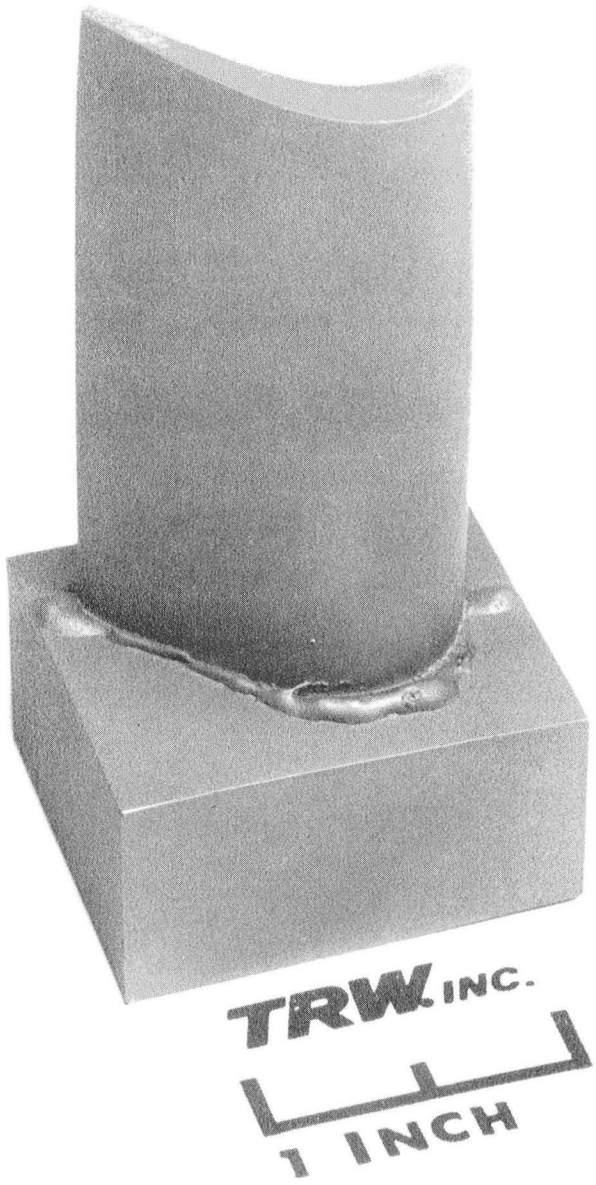

Figure 3-37. Solid, Cross-Plied FRS Airfoil with Brazed Root Blocks.

3.5.4 Iteration No. 4, Solid Airfoil No. 4, (Enclosed Leading and Trailing Edges)

3.5.4.1 Fabrication

This was identical to the previous iteration except that the plies were modified as shown in Figure 3-38 to provide total tip, leading-edge, and trailing-edge cladding with FeCrAlY.

Again, fabrication proceeded without difficulty.

Root blocks were attached to this airfoil by press diffusion bonding. This blade is shown in Figure 3-39.

3.5.4.2 Conclusions - Solid Airfoils

In conclusion, the experiments were very successful, demonstrating the feasibility of the fabrication method and the full adequacy of the fabrication techniques employed. As a result, no additional blade pressings of identical construction were deemed necessary, and effort would next be directed towards a hollow airfoil.

3.5.5 Iteration No. 5, Hollow Airfoil No. 1

In an effort to demonstrate the feasibility of a hollow FRS blade fabrication concept involving a minimal amount of initial engineering design input, the simplest hollow configuration was selected. The concept consists of the fabrication of a bi-metallic steel blade by the ply layup technique and the subsequent replacement of an arbitrary number of outer steel plies by FRS monotapes, with the remainder of the steel blade serving as a leachable core material. For the initial effort we selected a hollow construction consisting of a 12-ply thick outer shell, which is considerably higher than ultimately desired in a hollow blade. The choice was influenced almost exclusively by the blade's leading edge thickness (radius) considerations and the reluctance to undertake, at this stage, a major redesign of plies to ensure a full enclosure of the steel core at the leading edge by the FeCrAlY matrix. Such redesign would entail the narrowing of a number of plies at the leading edge and the replacement of the resultant void with a filler material. Furthermore, choosing the simplest route at the start would allow any subsequent changes in design and refinement of processes to evolve and progress in an orderly and systematic manner.

3.5.5.1 Core Fabrication

The blade containing a leachable steel core insert was fabricated by the ply layup method using both 300 series stainless steel and low carbon steel shim stock. The outer 12 plies were stainless steel and the core was carbon steel. The ultimate objective of this bimetallic blade layup was to achieve a nearly perfect fit between the die cavity and the blade pack consisting of the leachable core and the FRS shell, in order to eliminate plastic deformation in both the core and the shell during hollow blade diffusion bonding. It was felt that the above objective

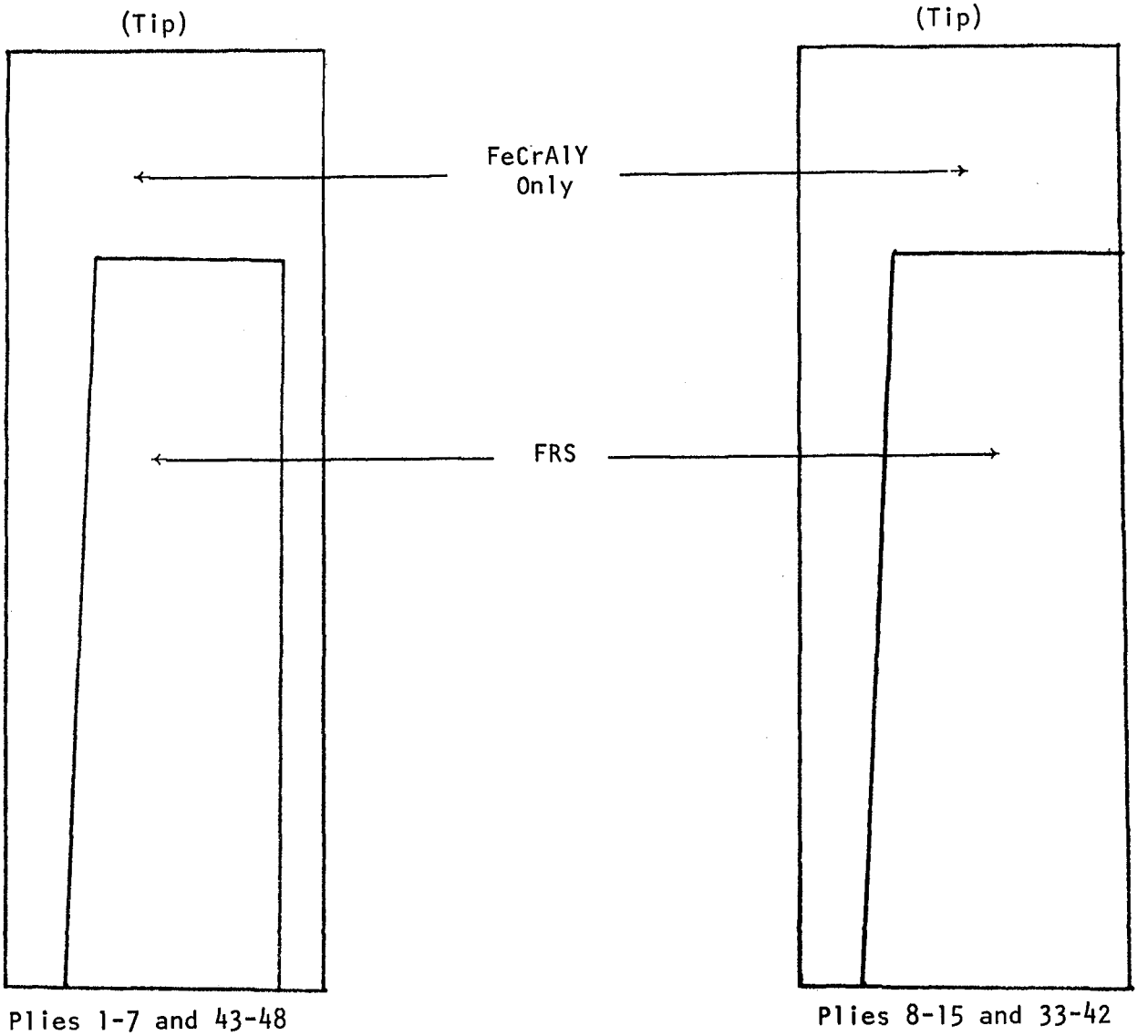

Figure 3-38. Special Monotape Configurations (Shown Actual Size).

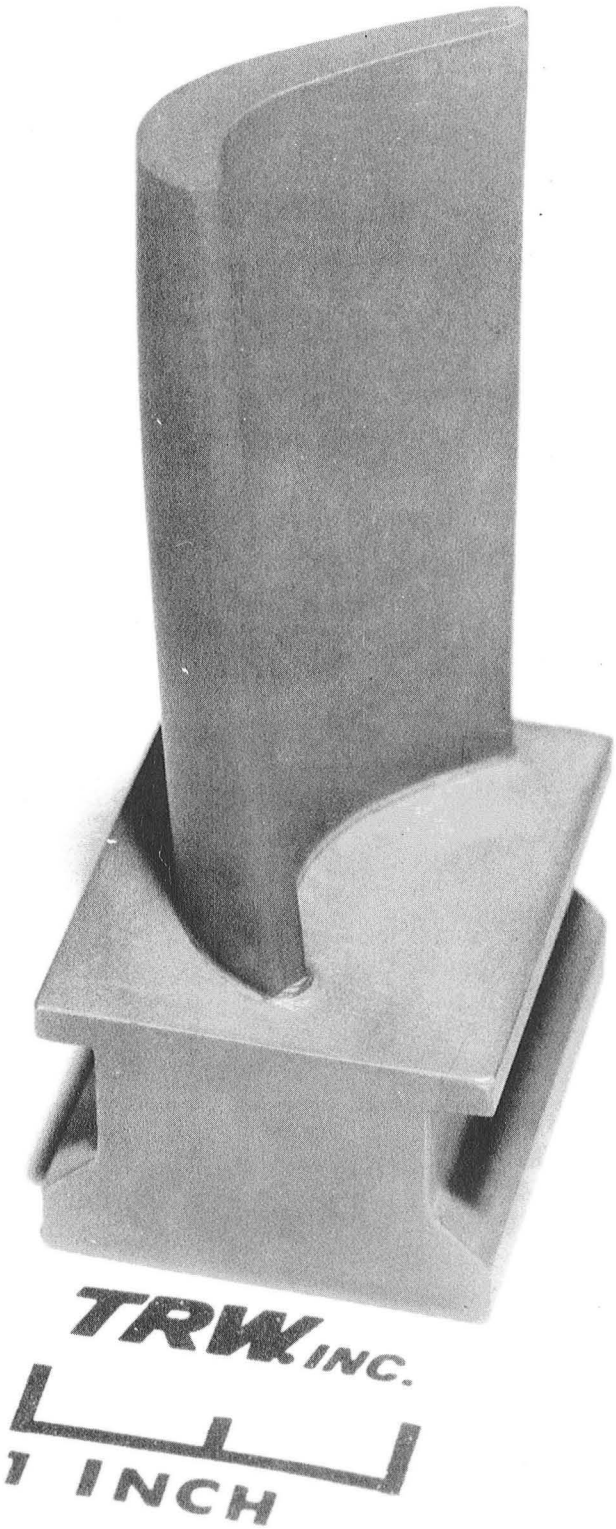

Figure 3-39. Solid FRS Airfoil with Diffusion-Bonded Root Blocks.

could best be attained by confining metal deformation, if any, to the relatively softer steel core.

The blade was fabricated in the regular Mo/TZM bonding dies under a moderate bonding pressure to guard against possible excessive flash formation. To facilitate the mechanical separation of the shell from the core, the interface was coated with a zirconia-boron nitride release agent. After bonding the blade was taken apart without difficulty. Finishing of the steel core consisted of trimming of the excess core width at the leading and trailing edges and smoothing out of the residual surface waviness at the trailing edge side by means of a non-metallic filler.

A typical steel core is shown in Figure 3-40.

3.5.5.2 Ply Preparation and Blade Assembly

Monotapes were produced using the updated fabrication practices and procedures described earlier. After forming, the steel substrate was dissolved in a nitric-hydrofluoric acid solution in water. Since the monotapes were fabricated to the finished thickness of 0.015 cm (6 mil) they were used in the as-stripped condition without any subsequent chemical sizing or cleaning. The monotapes and the steel core were assembled into a blade pack in the assembly fixture.

3.5.5.3 Blade Bonding

The procedures employed in the diffusion bonding of the first hollow FRS blade and the duration of the bonding cycle were the same as in bonding of the second solid FRS blade (see Section 3.5.2.6). No problems during the bonding cycle were encountered.

3.5.5.4 Blade Evaluation

The blade was evaluated by visual and dimensional inspection and metallography of blade sections. Visual inspection revealed no bonding problem areas. Dimensionally, the blade/pitch thickness was within the print tolerance band.

Photomacrographs of blade cross-sections with the steel core in place, and after chemical leaching of the core are shown in Figures 3-41 and 3-42, respectively. The extraneous material near the surface at the trailing edge side in the leached out section (Figure 3-42) is the residue of the non-metallic compound used for blending of the core prior to blade assembly. The full enclosure of the steel core at the leading and trailing edges is quite apparent in both cross-sections. The dark band at the leading edge is the FeCrAlY-matrix cladding of the inner shell surfaces. It was extended intentionally to the leading edge to provide additional material for the enclosure of the steel core. The improved quality of the monotapes used in this blade as judged by the uniformity of ply thickness and fiber spacing as well as the absence of missing wires (present in the previous solid blade) is also quite obvious in the photographs.

Figure 3-40. Typical As-Pressed Steel Core.

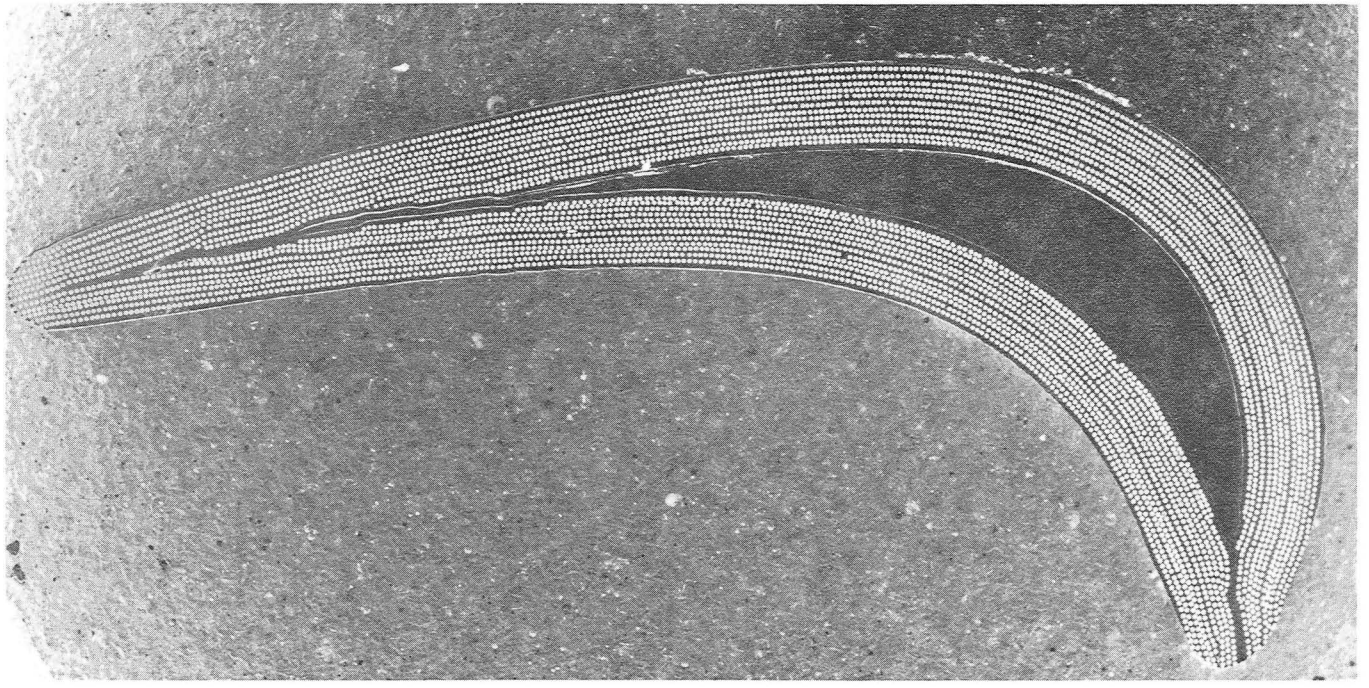

Figure 3-41. Photomacrograph of a cross section of a simple hollow FRS blade prior to leaching of the steel core.

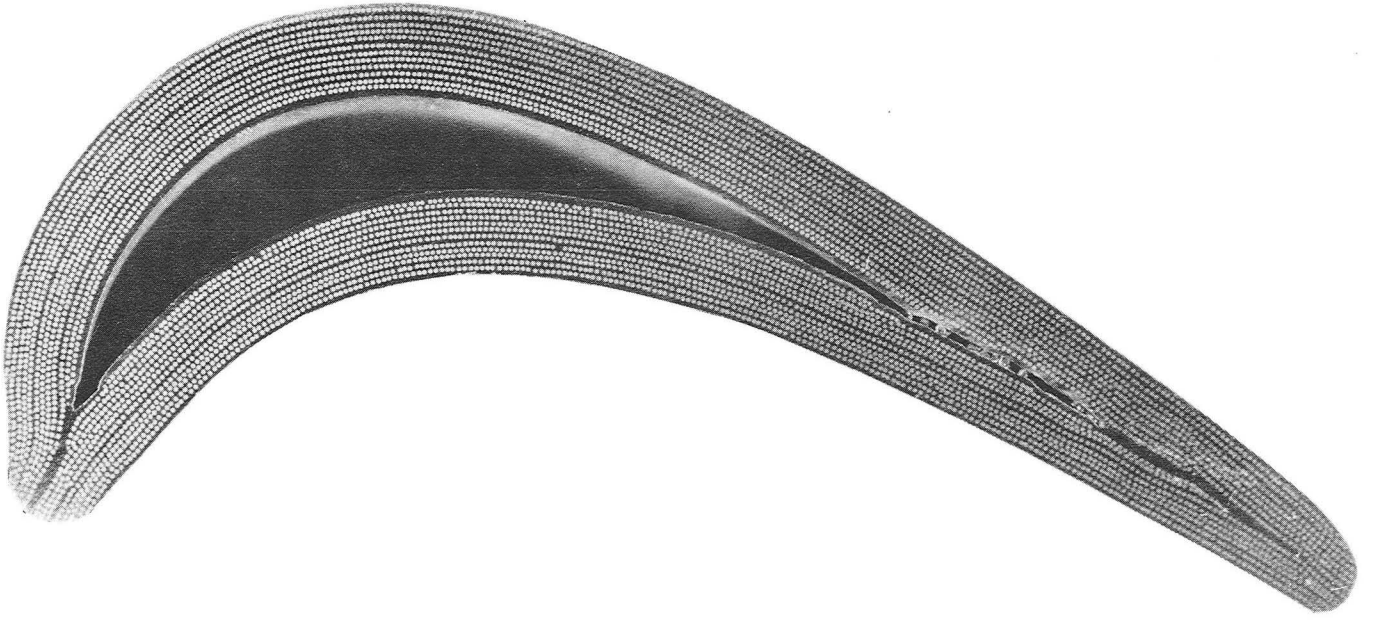

Figure 3-42. Photomacrograph of a cross section of a simple hollow FRS blade after core removal.

Typical microstructure of the FRS blade shell is illustrated in Figures 3-43 and 3-44. Figure 3-43 shows the uniformity of wire distribution over the entire thickness of the shell, including the FeCrAlY cladding on both surfaces of the shell at a high magnification level and with the wires etched as illustrated at the bottom. The cladding thickness was intentionally made twice as thick on the O.D. of the shell compared to the I.D. to comply with the requirements for the designed blade. Figure 3-44 further illustrates the general cleanliness of the sprayed powder matrix and the absence of reaction zone at the wire-matrix interface.

3.5.5.5 Core Leaching

Core leaching studies were performed using segments of the hollow blade. The leaching operation consisted of two steps involving two types of acid solutions. The basic core was dissolved in an acid solution consisting of about 30% HNO_3, 1.0% HCl and 69% water. To ensure a rapid core dissolution, the acid bath was maintained near boiling temperature. Hydrochloric acid was added to the solution to serve as a surface activator. After the removal of the steel core, the blade shell was immersed for about 5 minutes into an acid mixture consisting of about 30% HNO_3, 2% HF and 68% water to dissolve the steel core-FeCrAlY matrix bond zone. Both acid combinations are considered safe and reliable from the standpoint of attack on the matrix. No problems were encountered during the leaching operation. Because of the overall effectiveness and reliability of the above steel core leaching procedure, additional work in this area was considered unnecessary.

3.5.6 Iteration No. 6, Hollow Airfoil No. 2

This iteration was essentially a replication of the previous one. A second 12-ply shell hollow FRS airfoil was fabricated to verify the feasibility of the laminated steel core concept. The outer 7 plies of the shell had the same angle-ply construction as the hollow design blade; the remainder of the shell was made up of uniaxially (0^o) oriented plies including a FeCrAlY cladding ply adjacent to the laminated steel core. At this time, a process change was introduced. The use of bolts to hold the plies together was eliminated and vee-shaped pins were used instead, as can be seen in Figure 3-45. No problems in assembly or bonding were encountered. This pressing was also fully successful and the results confirmed the viability of the laminated, leachable core concept in hollow blade fabrication. The airfoil is shown in Figure 3-46.

A crack developed in the lower bonding insert during the fabrication of the first solid FRS airfoil had been gradually growing in the course of subsequent blade pressings. Although still usable at this time, we decided to machine a replacement using the available electrodes before the next pressing. In addition, a tooling change and process change was also made. Plies were directly assembled in the die without the use of bolts.

3.5.7 Iterations 7 and 8, Dummy Airfoils (Steel Sheet)

Upon receipt of the new bonding inserts, a dummy run was made using steel shim stock. Several high spots in the tooling were identified. These were eliminated by honing, and a re-run was successfully completed. Work has thereupon resumed on the hollow blade.

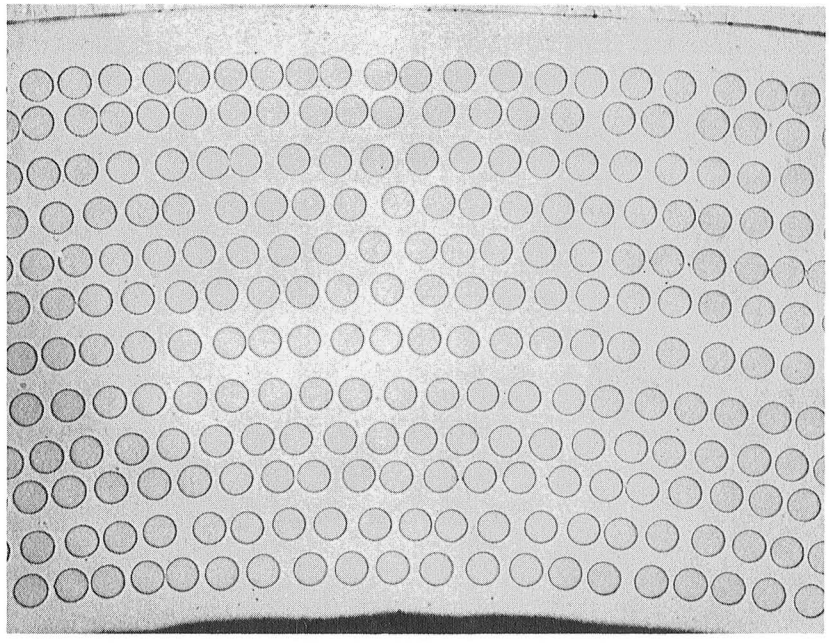

a) 40X

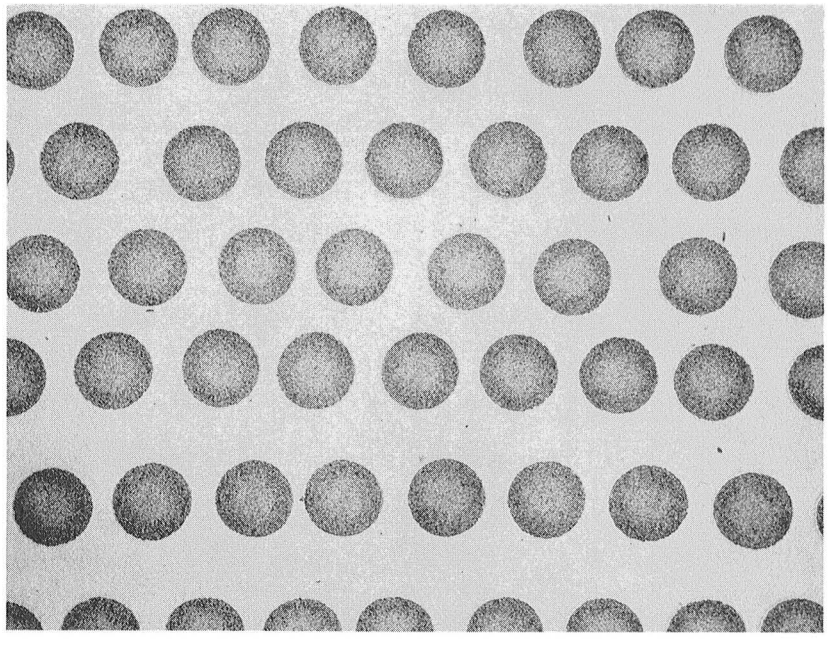

b) 100X

Figure 3-43. Photomicrographs of the shell in the simple FRS hollow blade illustrating good matrix bond, uniformity of wire distribution and cladding of the shell surfaces.

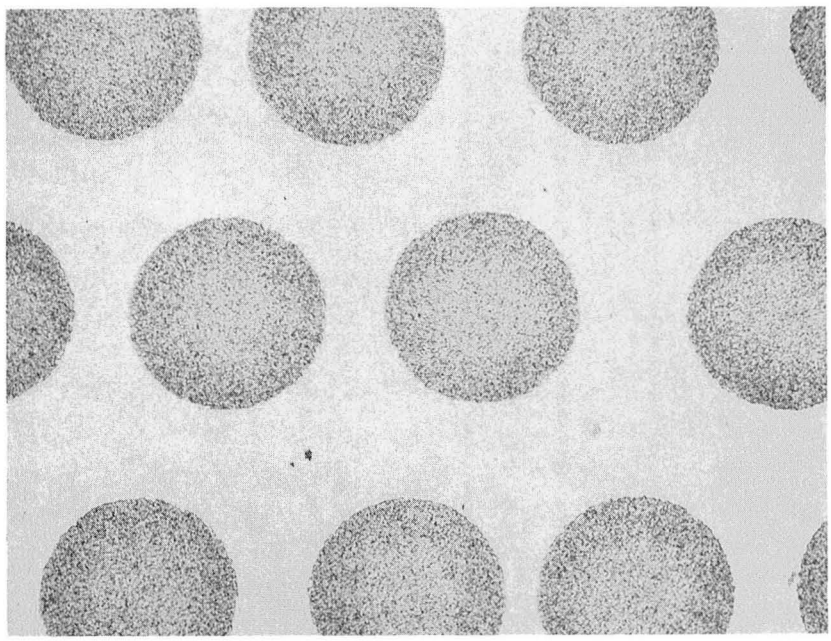

a) 250X

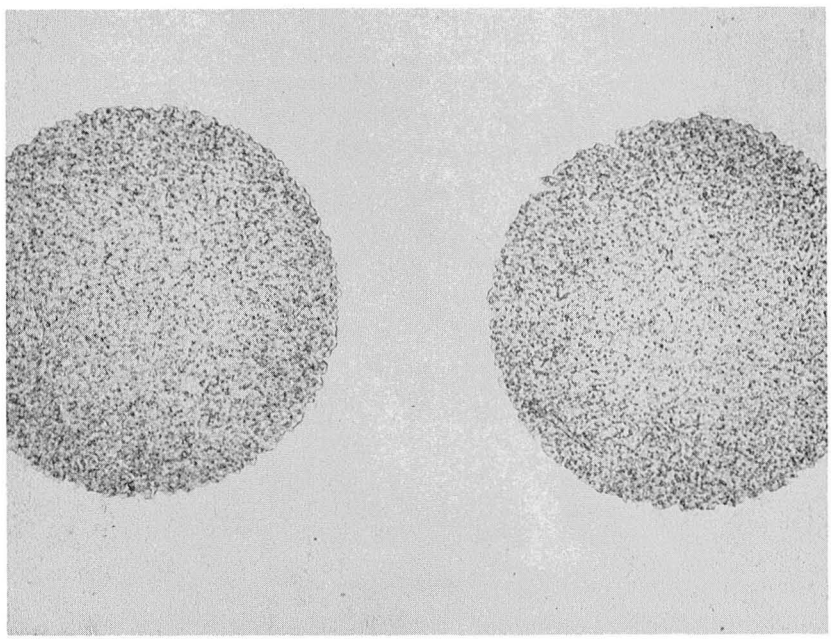

b) 500X

Figure 3-44. Photomicrographs of a section of the shell of the hollow FRS blade illustrating the high level of matrix cleanliness and the absence of matrix-wire reaction in the monotapes produced by the powder spray method.

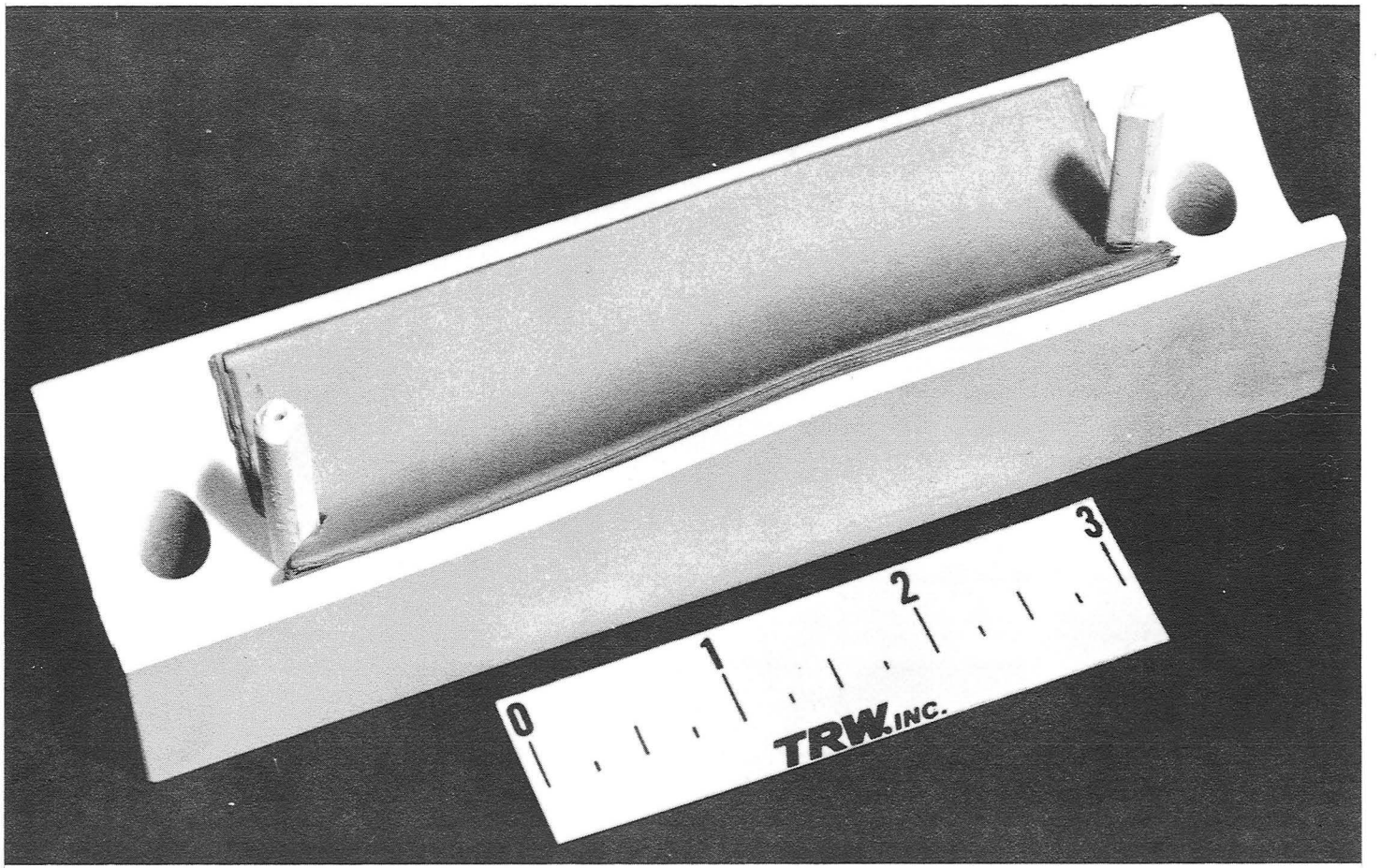

Figure 3-45. Assembly without Use of Bolts. (Note: Dimension in inches.)

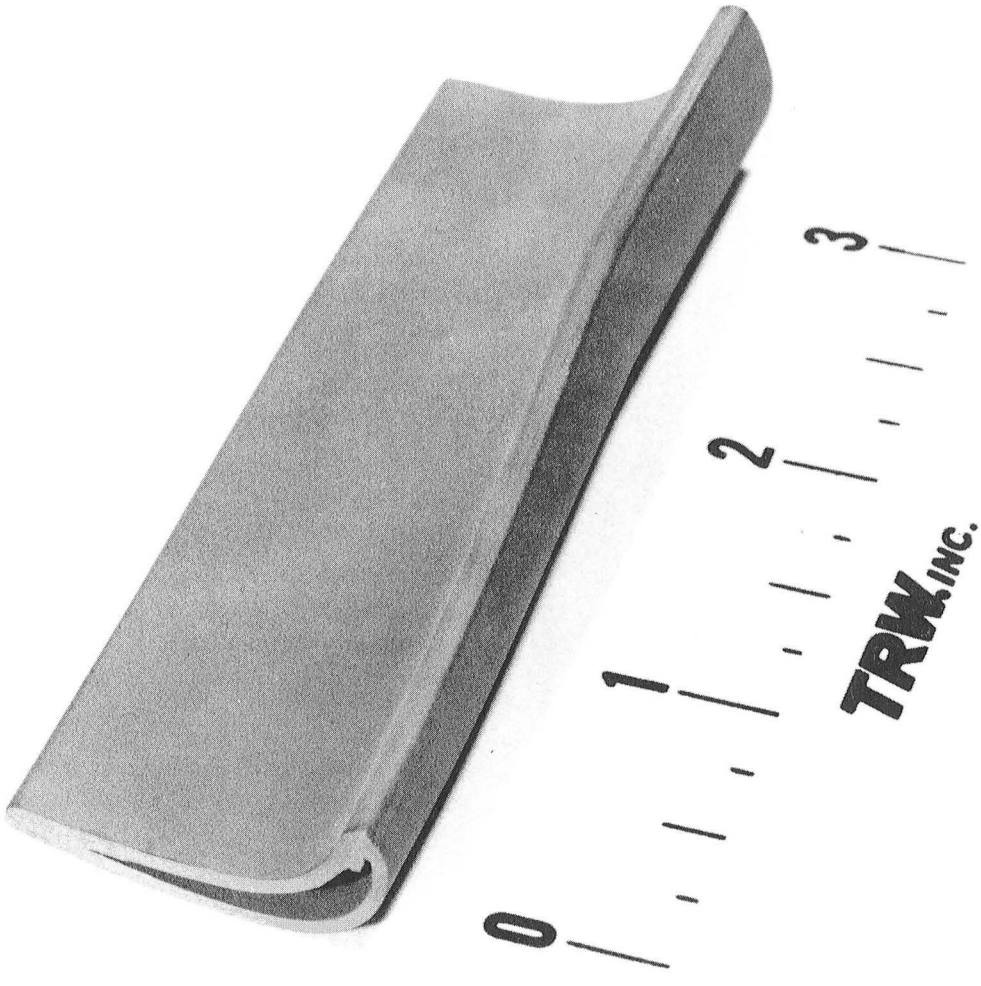

Figure 3-46. Second Hollow Airfoil. (Note: Dimensions in inches.)

3.5.8 Iteration 9, Hollow Airfoil No. 3

In preparation for the insertion of the tooling for the trailing edge slots, this airfoil included modifications to all but the outer 7 plies. Specifically, the leading edges of plies 8-15 and 34-41 were cut back by 0.25 cm (0.1 in) and that material replaced with FeCrAlY strips. Likewise, plies 8 and 41 were cut back 0.5 and 0.25 cm (0.2 and 0.1 in), respectively; this material was also replaced with FeCrAlY strips. The blade was successfully bonded.

3.5.9 Iteration 10, Hollow Airfoil No. 4 (T.E. Slots)

The objective of this iteration was to introduce the trailing edge (T.E.) slots. The relative locations of the hollow central cavity and T.E. slots are shown in Figure 3-47. The assembly shown in Figure 3-48, which consists of alternate "fingers" of leachable steel and FeCrAlY, is placed on the mid-plane of the blade and located from the two vee-notches shown. This insert was machined by wire EDM; the clearance between the steel and the FeCrAlY is controlled by the wire diameter.

The remainder of the blade was assembled as in the previous iterations and bonded. After bonding, both the core and steel "fingers" were selectively leached, resulting in the successful fabrication of the airfoil with trailing edge slots as shown in Figure 3-49.

3.5.10 Iteration, Bimetallic Hollow Airfoil No. 1

The major objective of this iteration was to fabricate a bimetallic hollow airfoil in which a high shear strength alloy (NiCrAl) would form the root end and conventional FeCrAlY the exposed airfoil end. Further, a solid FeCrAlY tip was needed to close the internal cavity.

Monotapes were prepared by selective masking and powder spraying of first one alloy and then the other onto the cleaned steel shims. These bi-alloy monotapes were consolidated and bonded as for the all-FeCrAlY monotapes.

These monotapes, however, were found deficient in quality due to an inadequate atmosphere during bonding. The problem was an acid attack on the nickel base alloy portion of the bimetallic monotape layup during stripping of the steel foil. This was attributed to the presence of oxygen and/or carbon in the chamber during bonding.

To correct this deficiency, additional improvements in atmosphere control were made. A gas purification tube furnace was built and installed to remove moisture from the cylinder gas (both hydrogen and argon) by means of titanium chips maintained at about 760°C (1400°F). In addition, a second cold trap for liquid nitrogen was installed between the drying furnace and the bonding chamber to remove residual moisture.

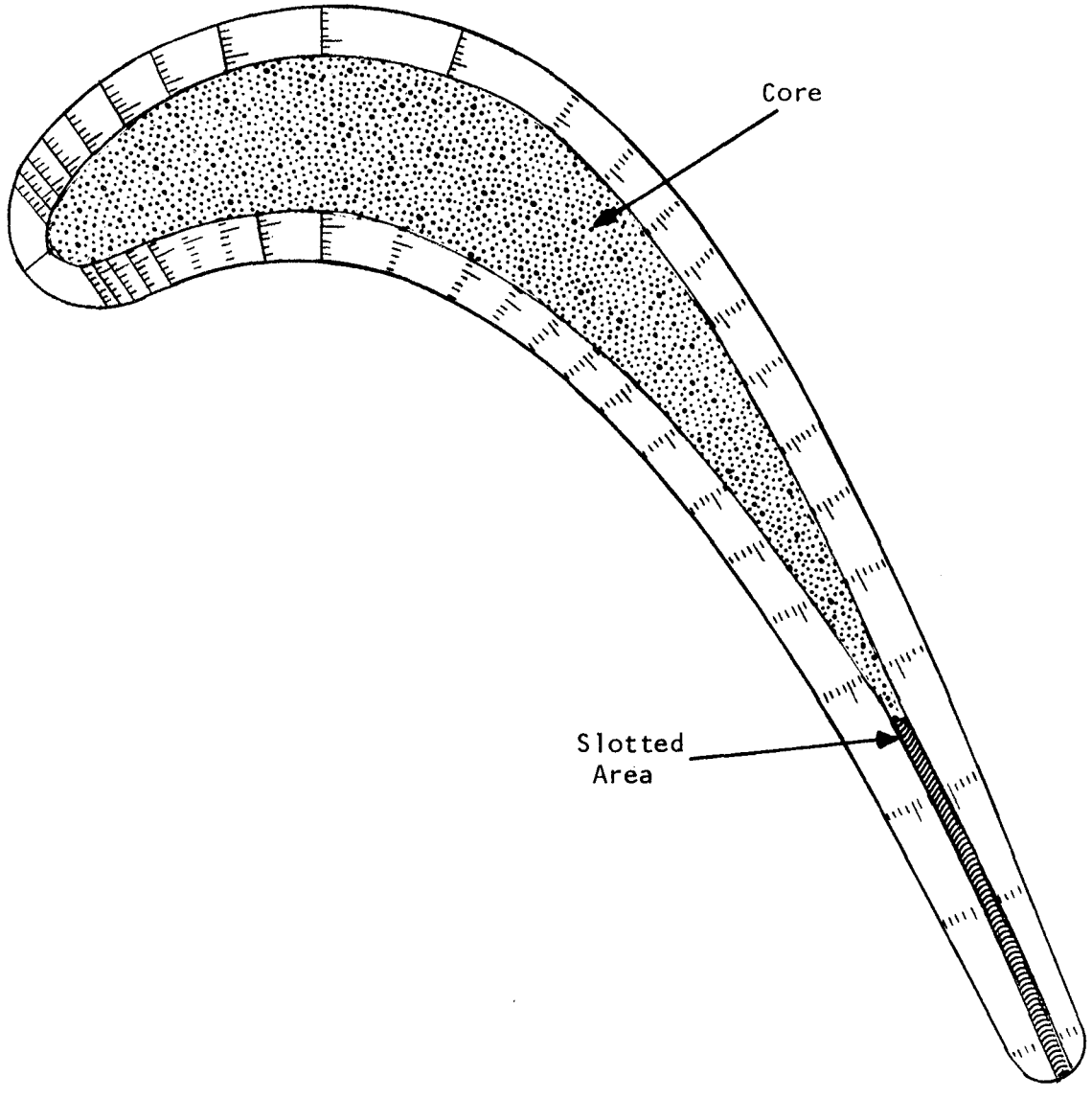

Figure 3-47. Relative Location of the Trailing Edge Slots.

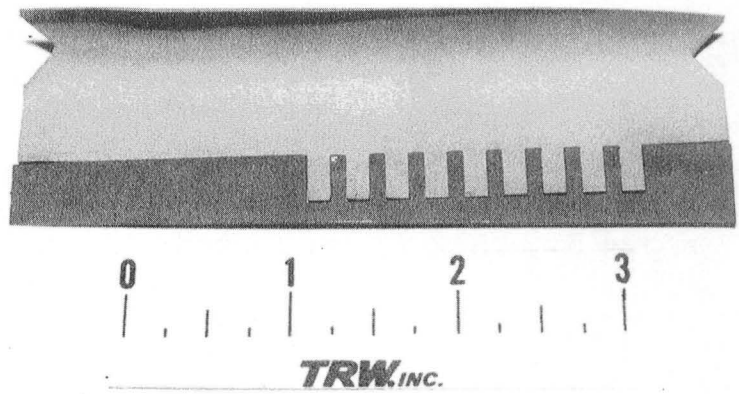

Figure 3-48. Tooling Concept for Trailing Edge Slots. The Lighter Material is the Leachable Steel Core and the Darker Material is Unreinforced FeCrAlY Matrix.

(Note: Dimensions in inches.)

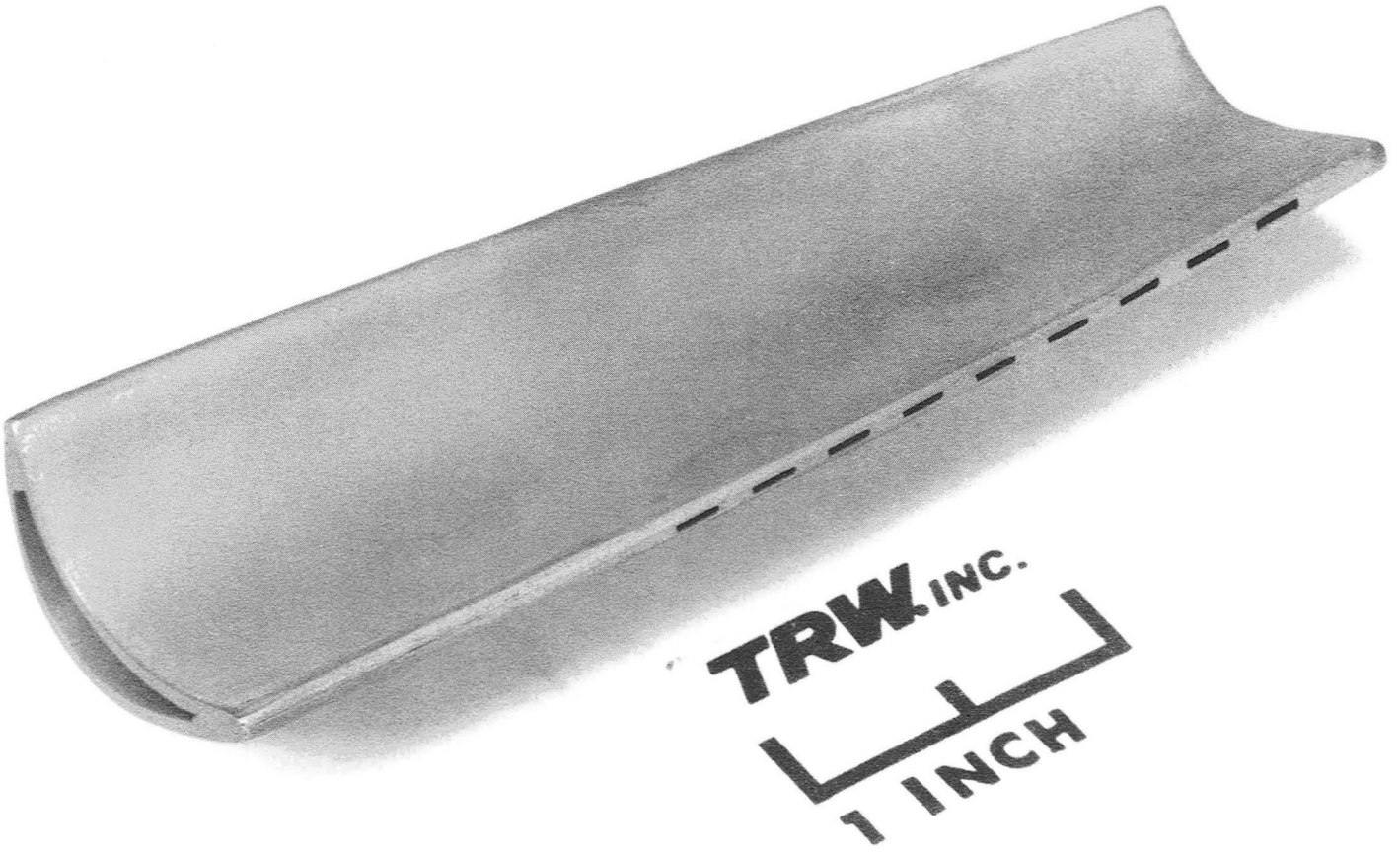

Figure 3-49. First Hollow Airfoil with Trailing Edge Slot.
(Note: Dimensions in inches.)

Using the improved atmosphere control system, a batch of bimetallic monotapes was fabricated with good results. The steel foil was removed by acid etching without detrimental effects on the matrix. A typical bi-alloy monotape, after cutting and forming, is shown in Figure 3-50.

Blade fabrication proceeded without incident. The steel tooling was leached out, and a solid FeCrAlY tip cap was welded onto the blade. It should be noted that the W-1ThO_2 fibers were terminated short of the airfoil tip to facilitate this operation.

The only problems encountered in this iteration were a slight core/ply shift and a slight surface attack at the FeCrAlY-NiCrAl junction. The effect of the former is manifest in Figure 3-51 as exposed fibers along the T.E. Also, this shift resulted in exposed core at the leading ledge. Since the blade was no longer suitable for use as a demonstration piece, it was used for welding repair experiments. The entire leading edge of the blade was ground open and then TIG welded without difficulty using Waspaloy wire as a filler material.

3.5.11 Iteration 12, Bimetallic Hollow Airfoil No. 2

The second hollow bimetallic blade was fabricated with a minor modification which consisted of adding thin FeCrAlY covers on the I.D. and O.D. sides of the composite shell. This action was taken to prevent erosion of the NiWCrAlY matrix during acid leaching of the steel core. The results were good in all respects. After leaching of the steel core, the airfoil tip was welded shut and an insert for impingement cooling was placed into the cavity.

This airfoil is shown in Figure 3-52. Note that the FeCrAlY surface plies prevented the localized attack encountered during the previous iteration.

3.5.12 Iteration 13; Hollow, Bimetallic, Wraparound Blade with Arc Root

The objective of this final iteration was to integrate all of the technologies demonstrated to date to produce a hollow, bi-alloy blade in which the composite plies wraparound the leading edge and which includes an arc-shaped root. The blade is shown schematically in Figure 3-53.

The approach selected was to prepare a 7-ply panel having the appropriate volume fractions and fiber orientation and to form same by wrapping around the core. Techniques demonstrated earlier on this program were to be used.

Fabrication of sufficiently large monotapes required a greater press capacity than the 68000 Kg (75 ton) unit used for all previous FRS work. TRW thereupon dedicated a second press, this a 136,000 KG (150 ton) with a large daylight, and a second induction power supply to FRS development. The press was fitted with a large retort, an appropriate vacuum system, all necessary plumbing and controls.

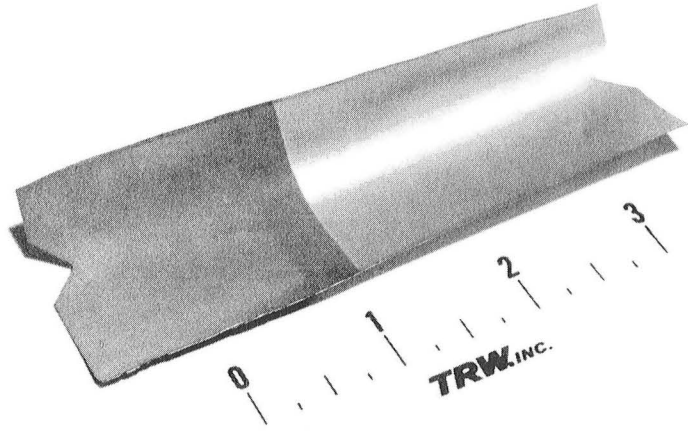

Figure 3-50. Bi-Alloy Monotape.
(Note: Dimensions in inches.)

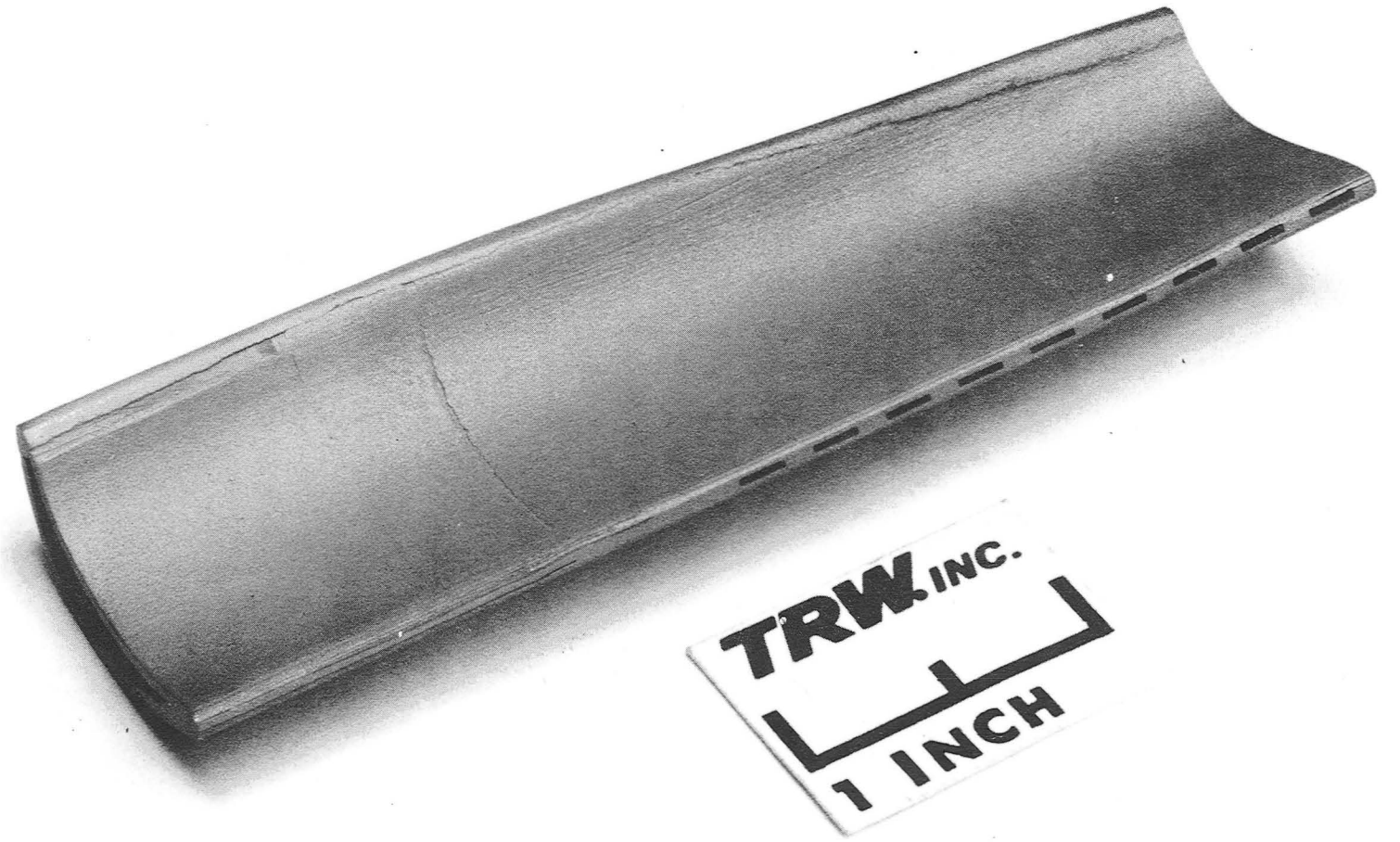

Figure 3-51. First Hollow, Bimetallic Airfoil. Note the slight surface attack at the alloy transition line.

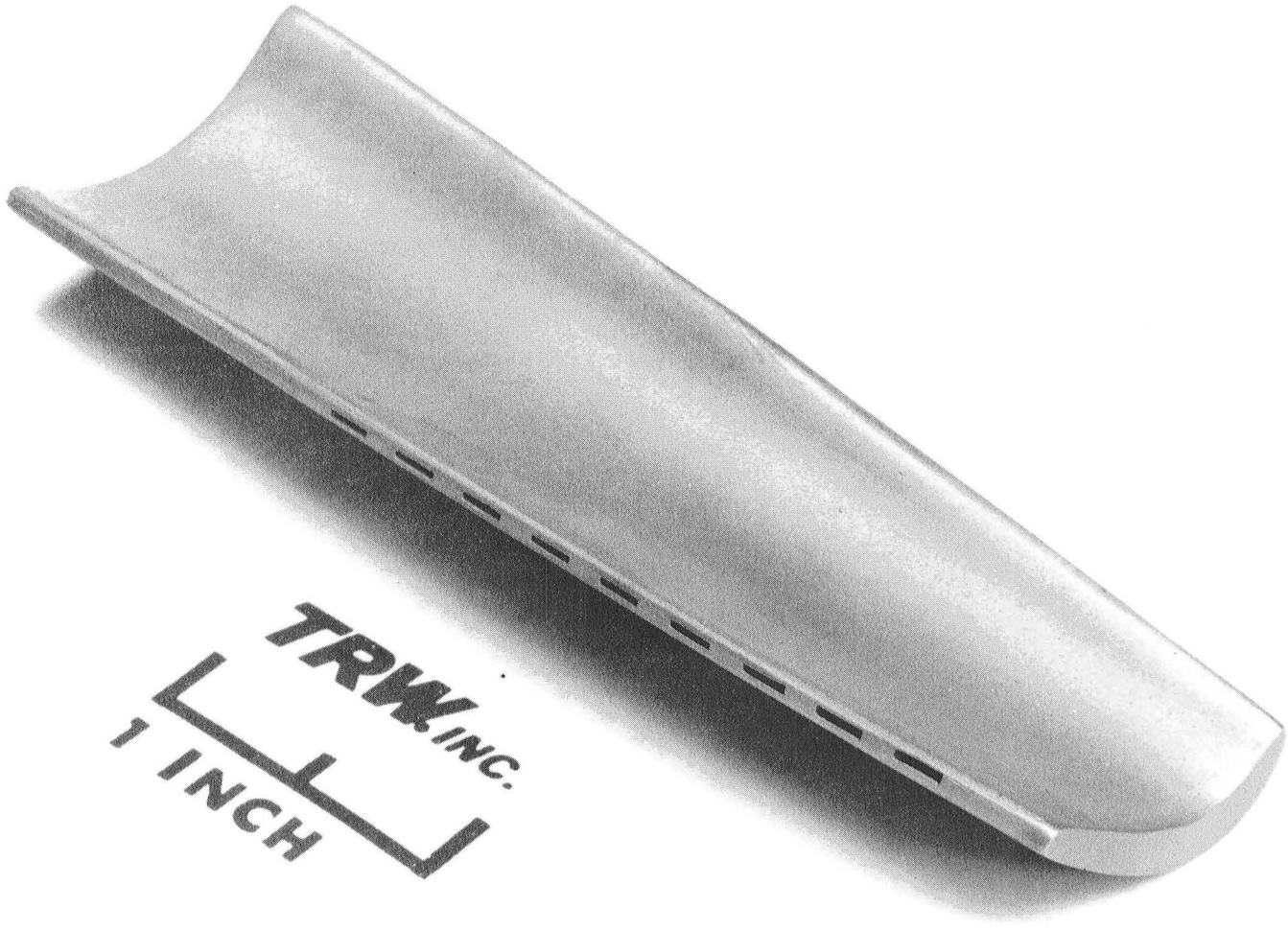

Figure 3-52. Second Bi-Alloy Hollow Airfoil.
(Note: Dimensions in inches.)

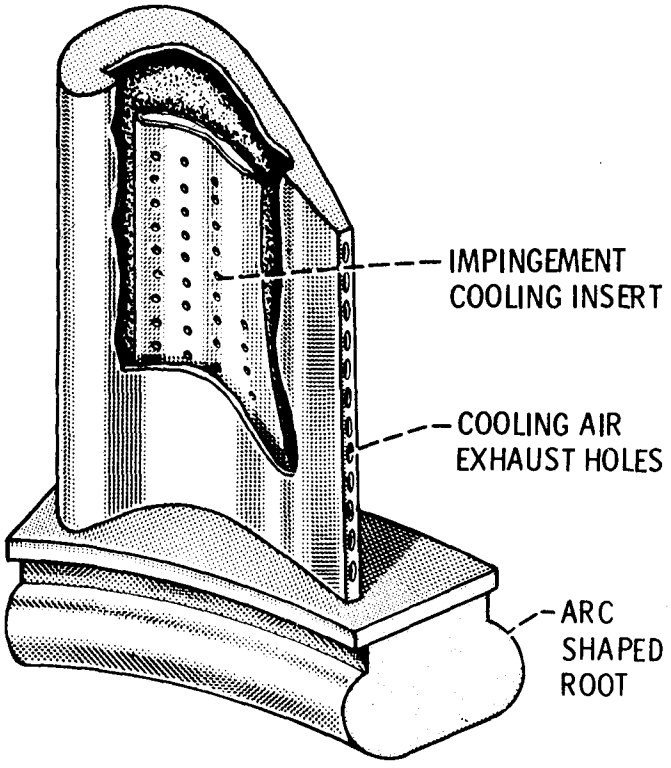

Figure 3-53. Schematic of Hollow FRS Blade with Impingement Insert, Tip Cap, and Arc-Root.

Because of the myriad of problems always encountered in the startup of new equipment, we experienced inumerable delays. Meanwhile, a large channel die, designed to accommodate 10x15 cm (4x6 in.) monotapes and panels, was machined from a TZM billet.

Steel cores were prepared for at least two more airfoils. Fiber mat was wound, and matrix alloy sprayed onto the steel shims.

Three attempts were made to bond these large monotapes, and each had to be aborted because of equipment problems.

An alternative concept was investigated. Narrow monotapes with fiber-free edges were prepared such that several sheets could be welded together. This proved impractical and was abandoned. The technical effort was suspended at this point.

4.0 SUMMARY AND CONCLUSIONS

This has truly been a milestone program. Prior to this study, there was serious doubt among the many non-believers that such a complex shape could be made from FRS. The parts made clearly dispel any such doubt.

Although it is unfortunate that the final demonstration blade was not completed, all of the necessary elements were conclusively demonstrated, viz the ability to wrap a 7-ply panel to the L.E. radius of the core, the trailing edge slots, the tip cap, the diffusion-bonded root blocks, and the impingement insert.

Parameters and procedures which consistently result in high-quality parts have been established. None require unusual processing, for example, bonding temperatures of 1107°C (2025°F) at loads of 69 to 103 MPa (10 to 15 ksi) for under 1 hour are considered very realistic. Most of the processing is still manual, and, eventually, automation will become necessary.

Certain of the innovations resulting from this program have much broader implications. These include the powder spray technology, the fabrication of cores from laminates, and the assembly techniques.

Major conclusions are summarized as follows:

A. Monotape Fabrication

1. A powder spray technique for these thin monotapes has been developed.

2. The powder spray approach was extended to include bi-alloy monotapes.

3. The recommended stop-off is boron nitride.

4. Molybdenum separators 0.05 cm (0.020 in.) thick are suggested.

5. Optimum monotape consolidation/bonding parameters are 1107°C (2025°F), 90 to 103 MPa (13 to 15 ksi), for 30 minutes.

6. The recommended agent for removal of the steel shim stock is 30% HNO_3 and 1% HF in water.

7. Monotape forming is readily accomplished at 594° to 705°C (1100° to 1300°F).

8. Recommended parameters for monotape-to-monotape bonding are 1107°C (2025°F), 69 MPa (10 ksi), for 30 minutes.

9. Bonding atmosphere must be very clean to preclude contamination which can lead to degraded corrosion resistance and loss in properties.

B. Blade Fabrication

1. Fabrication of FRS hardware from monotapes has been demonstrated.
2. Unlike, for example, B/Al, FRS needs no cushion ply to accommodate ply drops.
3. An innovative fixturing concept was reduced to practice.
4. Feasibility of laminated cores was demonstrated.
5. A unique tooling approach for trailing edge slots was developed.
6. Ability to form cross-plied FRS panels to small radii was demonstrated.
7. Techniques for selectively leaching steel tooling from both FeCrAlY and bi-alloy blades were established.
8. A fabrication concept for impingement inserts was demonstrated.
9. One approach to tip-cap and root attachment was successfully demonstrated.
10. The potential for weld repair was indicated by a feasibility trial.

5.0 RECOMMENDATIONS

As a result of this effort, FRS has cleared a major hurdle. Others remain however. The following, in particular, need to be addressed.

1. Develop a better understanding of basic process fundamentals.

2. Consider more sophisticated root attachment schemes.

3. Develop an NDE capability and couple same with a "significance of defects" study.

4. Upscale and begin to automate the various aspects of FRS manufacture.

6.0 REFERENCES

1. Petrasek, D. W., Signorelli, R. A. and Weeton, J. W., "Refractory Metal Fiber Nickel Alloy Composites for Use at High Temperatures," NASA TN D4787, 1968.

2. Petrasek, D. W. and Signorelli, R. A., "Preliminary Evaluation of Tungsten Alloy Fiber-Nickel Base Alloy Composites for Turbojet Engine Applications," NASA TN D-5575, February 1970.

3. Winsa, E. A. and Petrasek, D. W., "Factors Affecting Miniature Izod Strength of Tungsten-Fiber-Metal-Matrix Composites," NASA TN D-7393, October 1973.

4. Petrasek, D. W. and Signorelli, R. A., "Stress-Rupture Strength and Microstructural Stability of Tungsten-Hafnium-Carbon-Wire Reinforced Superalloy Composites," NASA TN D-7773, October 1974.

5. Brentnall, W. D. and Toth, I. J., "Fabrication of Tungsten Wire-Reinforced Nickel-Base Alloy Composites," NASA CR-134664, October 1974.

6. Brentnall, W. D. and Moracz, D. J., "Tungsten Wire Nickel-Base Alloy Composite Development," NASA CR-135021, March 1976.

7. Friedman, G. I. and Fleck, J. N., "Tungsten Wire-Reinforced Superalloys for 1093°C (2000°F) Turbine Blade Applications," NASA CR-159720.

8. Brentnall, W. D., "Metal Matrix Composites for High Temperature Turbine Blades," Final Report, Contract N62269-75-C-0119, April 1976.

9. Winsa, E. A., Westfall, L. J., Petrasek, D. W., and Signorelli, R. A., "Predicted Inlet Gas Temperatures for Tungsten Fiber Reinforced Superalloy Turbine Blades," NASA TM-73842, April 1978.

10. Petrasek, D. W., Winsa, E. A., Westfall, L. J., and Signorelli, R. A., "Tungsten Fiber Reinforced FeCrAlY - A First Generation Composite Turbine Blade Material," NASA TM-79094, February 1979.